日本地震工学会

土構造物におけるライフサイクルコスト戦略の研究委員会　最終報告書

2009 年 3 月

土構造物におけるライフサイクルコスト戦略の研究委員会

Contents

Outline of the project results (in English)

The demand for safety during earthquakes is increasing everywhere in the world nowadays. Safety means that of not only life but also properties and social activities. On the other hand, requirement for relevant cost is desired by people as well. To cope with this, engineers have to think about the essential meaning of safety.

In the past times, safety in design of constructed structures meant that no damage should occur during a design earthquake. This meant that the factor of safety during earthquakes should be greater than unity. Although this design principle achieved a significant safety during earthquakes, as compared with pre-modern times, the above-mentioned desire for safety has made it very difficult. One of the main reasons for this is the increasing intensity of design earthquakes, which makes it nearly impossible for geotechnical structures to be designed against it. The major problem lying behind this is that geotechnical materials such as sand and gravel have limited material strength as compared with steel and concrete. To cope with the increasing intensity of design earthquakes, therefore, there are only two ways to go, which are either the use of cement mixing, soil reinforcement, and concrete retaining structures, or increasing the slope angle of embankment etc. Both ideas increase the construction cost, which is against the people's attitude toward cost reduction.

In this situation, the idea of performance-based design has been developed and is going to be introduced in practice of design. This design principle assesses the performance of a concerned structure under a given design earthquake and examines it in the light of allowable seismic performance. For example, the residual deformation of extremely important geotechnical structures has to be less than a serviceability limit so that the emergency action immediately after a quake may be conducted. Also, most important structures have to be repaired within a limited period and with reasonable cost, and therefore their seismic deformation has to be within restoration limit. From these remarks, it is understood that the performance-based design consists of two important components that are good prediction of performance and reasonable decision on limit values.

The latest design codes such as EURO Code or ISO stress the importance of prediction methods. Numerical and analytical methods are therein addressed in order to predict the deformation and stress states of concerned structures during earthquakes. It is frequently asked, however, how practical and how reliable those predictions are. The reliability of prediction is governed by the accuracy of mathematical modeling, which is otherwise called understanding of soil/earth behavior, and the accuracy of input soil/earth parameters that is put in calculation.

From the viewpoint of business, the progress of performance-based design is advantageous to capable geotechnical engineers. First, prediction of performance is possible only by engineers who have good knowledge of both real ground behavior and analysis. In the case of earthquake

performance, which is the chief theme of the present project, engineers of seismic countries and regions have more advantage than those from other regions because they have more opportunities to experience seismic events and to learn from reality.

Although the performance-based design is pushed in many regions and codes in the world, it is not clear yet whether or not it satisfies the demand of people for cost effectiveness. For example, the performance-based design refers to serviceability, easy restoration, avoidance of total collapse, etc., which are the concepts of limit state design. These concepts do not explicitly exhibit the financial aspects. Therefore, it seems difficult for non-engineering people, such as financial officers, business clients, and tax payers, to understand and accept the importance of performance-based design. This means that advanced analyses for prediction of seismic performance may not be accepted generally, certainly except extremely important cases, because of the cost problems. It is therefore necessary to convert the idea of seismic performance to monetary issues for better understanding of people.

The idea of life cycle cost is a solution to this situation. It is attempted therein to convert all the issues into monetary units and to achieve the minimum cost during the service time (life cycle) of a facility. What is converted is, for example, the initial design and construction, possible reinforcement against earthquake risk, maintenance cost, damage caused by natural or artificial hazards, restoration of damage, and final demolition. It is supposed in this idea that good quality of initial construction reduces the maintenance cost and damage due to hazards, and thus minimizes possibly the total cost (life cycle cost).

The above-mentioned relationship between initial construction cost and maintenance as well as damage costs hold true in those structures that are made of steel and concrete. The deterioration of materials due to adverse environments may be mitigated by good construction provisions, and maintenance and risk during natural disasters are thereby reduced. Moreover, the number of victims (killed people) during natural disasters is reduced by good initial construction. The life cycle of structures is clearly related with the deterioration of materials. Moreover, recent unfortunate experiences of earthquakes in Kobe in Japan, Turkey, Bam in Iran, and Suchuan Province in China strongly support this relation. Note that the loss of human life forms a tremendous damage cost in life cycle cost calculations because human life in most countries is considered expensive after conversion to monetary units.

In contrast, the calculation of life cycle cost for geotechnical structures has different features. First, the materials that compose structures are mostly soil and stones which are not likely to deteriorate with time. This implies that life cycle of geotechnical structures is not clearly defined. For example, there are very old irrigation facilities in the world that have been in service for hundreds of years. Second, geotechnical seismic hazards such as failure of embankments, harbor quay walls, and subsoil liquefaction have hardly killed people. The essence of damage has been the induced inconvenience to people’s life and pending of operation that caused negative effects to the

public and economic activities. For example, since quay walls in Kobe Harbor collapsed in 1995 due to backfill liquefaction, the harbor service was significantly affected for two years and a large amount of harbor business was permanently lost; customers went to other harbors without coming back. Also damage to lifelines stops supply of water, electricity, communication, and sewage, causing fundamental problems to both people's life and industrial activities. Since most of these damages are related to economic issues, conversion of damage to monetary values appears important. Although a failure of a natural slope may kill hundreds of people, such a slope is not a product of design and construction, and hence will be removed from further consideration. With these issues in mind, the present project conducted a variety of activities. They are going to be addressed in what follows.

(1) Shaking model tests and analytical issues

The aim of this activity was to assess and validate the reliability of analysis that plays key roles in prediction of seismic performance and evaluation of damage-induced cost in life cycle cost calculation. The concerned types of structures were pile foundation, embankment, quay wall in harbor, and earth dam.

(1-1) Shaking model tests

There are two kinds of shaking model tests. They are namely shaking in 1-G gravity field and centrifugal model tests. The former is relatively easy and less expensive in spite of the greater size of tested models. The latter is characterized by the increased magnitude of gravity force by using centrifugal effects. Hence, the level of stress induced by the weight of soil in a small model is made similar to the one in the prototype (full scale). Since the stress-strain behavior of soil is substantially affected by the stress level, this feature has been considered important. This does not mean, however, that centrifugal model behavior is a perfect reproduction of the prototype behavior. This is because centrifugal models are generally small, being smaller in most cases than the models in 1-G shaking tests, and the size of monitoring instruments and the size of soil grains are relatively large. It is often said, therefore, that sand in centrifugal model is equivalent to gravels / stones in reality. Moreover, whether 1-G or centrifuge, all the model ground misses effects of geological history and ageing.

1-G model tests on pile foundation focused on liquefaction and induced lateral flow. A particular interest lay on the distribution of lateral earth pressure among individual member piles in the group pile. Important findings are the rate-dependent (viscous) behavior of liquefied sand that flows around a pile, and the varying magnitude of lateral earth pressure on individual piles. To make these findings more reliable, results of E-Defense full-scale tests on pile foundation were analyzed. The said rate-dependency was found as well. The pressure distribution among piles was not studied because the number of piles was small and those piles buckled or failed during shaking in E-Defense

tests.

1-G tests on dam models were conducted by reproducing a reservoir lake model as is the case in reality. The subsidence in the upstream side of the dam model was significant when the dam body was less compacted, because excess pore water pressure developed, effective stress was reduced, and shear strength became low therein. It is important that a large step occurred between the upstream shell and the central core, which is similar to the observed behavior of Sam Fernando Dam in California.

Another shaking test on a dam with surface lining (pavement) demonstrated a remarkable behavior of the dam embankment. Since the reservoir water pressure is converted to effective stress by an impervious lining, the dam body gains significant shear resistance and therefore the earthquake-induced damage is drastically reduced. Although possible cracking in the lining has been feared during earthquakes, the recent seismic event in China showed that the lining and the underlying dam body behave satisfactorily due to the increased effective stress level.

Harbor quay wall models were tested in both centrifugal and 1-G gravity environments. The centrifugal tests studied the effects of long duration of shaking with reference to the expected gigantic earthquakes in the Tokai-Nankai subduction zone. It was shown that the elongated duration time of gigantic earthquakes induces greater deformation owing to the longer lasting time of high excess pore water pressure. Since the traditional design principle of factor of safety > unity is difficult to maintain under such gigantic earthquakes, this finding supports the development of performance (deformation) prediction by using equivalent-static (reduced modulus as will be stated later on) or viscous-liquid methods.

The 1-G tests on a quay wall investigated the possibility of soft cushion materials behind a quay wall body. This material was expected to absorb the displacement of backfill soil and thereby to reduce the dynamic earth pressure, leading to mitigated quay wall displacement. Test results showed that the dynamic earth pressure was reduced by a cushion as expected. Conversely, the residual deformation of a quay wall showed less effects of a cushion. Although the earth pressure from the backfill to the wall was reduced, the inertia force of the quay wall itself was not mitigated. Hence, the wall translated along the foundation and the consequent displacement was not much reduced. This implies that a quay wall of a gravity type is a less advantageous structure.

Centrifugal model tests on embankment concerned the choice of subsoil improvement. When the natural subsoil is prone to liquefaction, some soil improvement is needed. The present tests were conducted on different topographies and different extents of compaction so that the variation of seismic performance due to different specification of soil improvement might be demonstrated. The observed seismic performance herein was made use of in the later calculation of life cycle cost for different types of soil improvement.

(1-2) Numerical analysis on seismic performance

The aforementioned model tests supported the modeling of liquefied sand as viscous liquid. With a reasonable simplification of the mode of ground deformation, this idea leads to very quick calculation of ground deformation (seismic performance). For the case of a group pile, however, a numerical problem has made the calculation difficult. Being basically similar to the conventional FE analyses on a solid medium, large deformation of softened ground around rigid pile bodies is still difficult. Hence, the viscous calculation is given to river dikes and shallow foundations, which are out of scope of the present project, and the analysis on piled foundation is left for a future study.

In contrast, deformation analysis on modern earth dams is easier because, being different from early dams made by hydraulic filling without compaction, the deformation of modern dams is less significant and is easier for analysis. By considering application to practice, the present project examined the method of strain potential in which laboratory tests on deformation characteristics of soil play major roles. It was revealed that a compacted dam body develops very limited deformation in the upper surface of the upstream slope. Moreover, the direction of plastic strain vectors suggests the existence of a plastic potential function for a dam body, suggesting future possibility of developing a very simplified plasticity approach for a dam body.

A criterion on good and poor predictions is always an important point of discussion. The quality of prediction relies not only the quality of numerical technique but also on the accuracy of stress-strain modeling and reliability of field investigation. Since very good quality of field investigation is not expected in most practices, the present project proposed a less strict (probably reasonable) criterion. It seems that most analyses in both the present study and those in recent well-organized projects satisfy this criterion.

Analyses on harbor quay wall were initiated by an advanced nonlinear dynamic effective-stress computation. Although such an advanced analysis is a powerful tool to predict the earthquake performance of a given structure, its application to a design procedure is not very easy. This is because the high computation cost and difficulty in determination of many soil parameters make its trial-and-error use difficult. This point is significantly important in design procedures in which many calculations are needed on different design options. Hence, the advanced analyses are employed to date for only confirmation of the safety of the finally-decided version of a structure. This point is fatal, furthermore, in the life cycle cost calculation in which earthquake events are treated in a probabilistic manner and many analyses have to be repeated as a Monte Carlo approach.

To overcome this difficulty, the present project proposes to, first, run many advanced analyses on different cross sections of a quay wall, and to make a regression formula on the ultimate deformation. Other projects can simply use the regression equation for design and can save time significantly. This idea made it possible to calculate life cycle cost in a probabilistic manner.

Independent analyses were carried out on the cushion effect as well. The effects of cushion

material on mitigation of seismic damage were reproduced.

Embankments were analyzed as well by advanced numerical tools. The results were used in life cycle cost calculations later on.

(2) Discussion on Performance-Based Design and Calculation of Life Cycle Cost

(2-1) Discussion of Seismic Performance

Discussion was made of the future design principle for geotechnical structures undergoing earthquake actions. First, it was stated that the performance-based design requires a good quality of performance prediction and a reasonable decision on allowable performance. Since the former issue was dealt with in the previous section, the latter is addressed herein.

Recent developments in performance-based design quote different kinds of performance to be achieved by structures. Similar to those in limit state design principles, they are serviceability, quick restoration, and others. The problem is that those names are merely qualitative and there is no clearly-defined methodology to work out quantitatively the performance targets. Hence, different fields and industries determine the target deformation empirically and any method in one field cannot be directly applied to other fields. It should be noted in this regard that decision of the allowable deformation is very difficult or unclear; for example, when subsidence of 30 cm is allowed, why 35 cm is not?

In view of this, the present project introduced a past attempt by JSCE (Japan Society of Civil Engineers) which was made by the present author. Interviews were made of engineers and officers who experienced a hard time in restoration of seismically-damaged geotechnical structures. They were asked about their opinion about the magnitude of allowable deformation, allowable restoration time, and factors that govern the magnitude of allowable damage. It was found that the negative effects to the public are very important in decision of the allowable damage. This point implies the importance of life cycle cost in a design procedure. Moreover, it was proposed that the allowable damage (deformation) can be determined in a systematic manner by first determining the size of affected area (or population or economy) and then the allowable restoration time, followed by the allowable deformation. The restoration time means the length of period in which the expected service of a structure stops, causing negative effects to the affected area. Note that determination of the size of area and decision of allowable restoration time are easier than direct decision of allowable “deformation.”

(2-2) Example Calculation of Life Cycle Cost

Trial calculation was made of life cycle cost of three kinds of structures. All of them were subject to seismic damage and subsoil improvement was required. It was attempted to determine the best

specification of subsoil improvement by calculating the life cycle cost and selecting the option of the minimum cost. For simplicity, the present study defines the life cycle cost as the summation of soil improvement cost and earthquake-induced damage cost. This is reasonable because other types of cost such as construction of the main body of the structures, purchase of land, and maintenance expenditures are independent of the soil improvement and do not affect the conclusion.

The calculation of the life cycle cost of an express motorway was intended to be a model of such a work. Hence, fundamental principles of life cycle cost analysis were followed as much as possible. However, several geotechnically specific problems were encountered and solved. For example, the life cycle of a geotechnical structures were determined to be 80 years. This number was decided not because of the deterioration of composing soil materials but because of the fact that, in the recent era, functions of any structure become unnecessary after service for three generations or 80 years, and new construction becomes necessary. Another problem was the conversion of human life to monetary units. Although this was not an enjoyable work, the present project referred to the international situations and finally decided on 200 Million Japanese Yen for one life. This amount of money somehow reflects the GDP (Gross Domestic Product) per capita multiplied by mean remaining life time or WTP (willing-to-pay) evaluation.

Another and most difficult problem was the evaluation of economic (indirect) loss caused by seismic damage. Although there are evaluations on the total economic damage caused by a single earthquake, it is difficult to determine the damage that is related with an individual damaged structure. For an express motorway, the present study finally decided that the economic loss is given by the elongated travel time that is converted to money. The elongated travel time is a reasonable index of economic damage because people use an expressway in order to save their travel time. Hence, the benefit of an expressway is equivalent with the saved time.

With these decisions, life cycle costs were calculated for different options of soil improvement. It was found that one option with deep mixing of soft soil with cement can achieve the minimum (optimum) life cycle cost.

Similar attempts were made of a harbor quay wall. For this structure, the economic damage was simply evaluated as five times the cost of reconstruction. Another attempt on a river dike employed the significant damage by flooding as the indirect economic cost. It was found that the life cycle cost principle works only when such a significant economic indirect loss is taken into account.

To introduce a new perspective, a study was made of life cycle energy consumption. This idea implies that a construction option that spends the least amount of energy is the best option. From this viewpoint, cement mixing is less favorable than sand compaction piles because production of cement needs more fuel and energy.

(3) International Survey on Soil Investigation

As stated before, the reliability of investigation on site of construction is extremely important in successful prediction of seismic performance and calculation of seismic damage cost. Hence, the present study sent inquiries to engineers in many countries in the world. The answers revealed that most countries consider SPT (standard penetration test) as the first priority because many design codes suppose SPT to be used for determination of soil parameters. It is widely understood that SPT procedure is not actually standardized and has many local differences. This makes the use of empirical formulae inappropriate.

Another issue is that CPT (cone penetration test) is considered to be more reliable. However, it cannot identify soil type directly. Also, CPT machine may not be able to penetrate into liquefaction-prone sandy ground. In this situation, therefore, it is necessary for design and site engineers to understand the limitation of SPT during field operation. It should be appealed that site engineers pay more attention to details of SPT procedure and maintenance of equipments.

(4) International Workshops

Workshops were organized at five places in the world in order to promote and familiarize the importance of performance-based design and life cycle cost principle in the field of geotechnical earthquake engineering. The sites of the workshops were London in UK, Nantes in France, Tehran in Iran, Nanjing (南京) in China, and Sacrament in California, USA. These occasions were made successful through collaboration with many Japanese and international organizations. Those organizations are Institution of Civil Engineers of UK, Japan Society of Civil Engineers, Japanese Geotechnical Society, International Society for Soil Mechanics and Geotechnical Engineering, Laboratoire Central des Ponts et Chaussées of France, Tehran University of Iran, Hohai (河海) University of China, and American Society of Civil Engineers.

(5) Conclusions

The conclusions of the present project are described in what follows.

- Shaking model tests under 1-G gravity or centrifugal environments were conducted in order to show the capability of numerical analyses
- The structures concerned in model tests and numerical analyses were pile foundation, embankment, quay wall in harbor, and earth dam.
- Numerical analyses have a reasonable, although not perfect, capability to reproduce the real seismic performance of geotechnical structures.

- Very advanced numerical analyses require expensive computation time and cost as well as determination of advanced soil parameters.
- To save the computation load, a method of regression analyses as combined with EXCEL calculation was proposed.
- Methodologies for calculation of life cycle cost which considers specific nature of geotechnical structures were constructed and practiced.
- International workshops were held at five cities in the world for familiarization of the importance of performance-based design and life-cycle-cost concepts.
- The seismic performance-based design and life cycle cost principle are the direction of future design of geotechnical structures in seismic countries because they help avoid unnecessarily conservatism and achieve the optimum choice of design.
- It is very important for engineers to improve the quality of field soil investigation by paying attention to details of procedures and maintenance of equipments.

: 3896 words

Outline of the project results (in Japanese)

地盤構造物の耐震設計は、静的な地震力の下で安全率 1 以上を確保する、という伝統的な考え方を保っている。他の構造物の分野と比べて地盤の分野ではどちらかというと古い考え方が残った理由として、地盤が品質管理されて製造されたものではないので、力学的性状が複雑かつ不均質で、地盤の調査も完璧は期しがたいことが考えられる。近年、社会において安全への希求が高まり、地震災害の分野でも設計用の想定地震が強まる一方である。これに対して安全率＞１を維持しようとしても、材料強度が鋼やコンクリートに劣る土材料では、困難が大きい。そこで従来法から脱却して地震時の性能評価（変形評価）を取り入れる気運となった（ＩＳＯやＥＵＲＯ ＣＯＤＥ）。すなわち、たとえ安全率が一時的に 1 を下回っても、地震後に起こっている変形量が基準値以内にあれば、これを許容するものである。

もとより性能評価は容易でなく、地震動や土の力学的性質に関する知識が必要である。しかし他方、そのような知識を持つ優れたエンジニアには、ビジネスチャンスでもある。また、性能評価の意義は技術の世界では理解されやすいものの、財政担当者、事業の施主、一般市民にはなじみにくい。これらの人々の理解を得るためには、さらに進んだ概念であるライフサイクルコストＬＣＣの手法を推進して経済的なメリットを訴えることが、意義深い。

性能設計やＬＣＣでは、構造物の地震時挙動の予測技術が重要である。予測技術の良否とは、単に数値解析技術の精緻だけでなく、妥当な計算コストおよび、入力データの信頼性すなわち地盤調査技術の裏づけが必要である。これらの諸点を調査して新しい時代の耐震設計手法を推進することが、本プロジェクトの目的であった。例となる構造物として、杭基礎、アースダム、港湾岸壁、道路盛土を取り上げている。

まず地盤構造物の模型振動実験を行ない、設計法推進に有意義な知見の取得に努めた。液状化地盤流動が群杭基礎に及ぼす横荷重の実験では従来の均一荷重分担とは異なり、上下流端の杭に荷重が集まることを見出した。これにより既存杭基礎の耐震補強のために上下流端に捨て杭を打設する手法が提案できた。アースダムの実験では実破壊例と同じ破壊パターンが再現できた他、表面遮水型ダムの耐震性が高いことが示され、本年の四川省の地震でもそのことが実証された。港湾岸壁の実験では巨大地震の長時間震動の影響や護岸裏の衝撃吸収材の性能が示された。道路盛土実験では、地盤改良タイプの違いによる性能の差異が比較検討された。これらを承けて数値解析が行なわれたが、特に港湾岸壁を取り上げて、精緻な解析を多数行なって岸壁諸元と耐震性能の間に回帰式を作り、実設計ではこれをもって精緻な解析に代える方法が、推奨された。

ＬＣＣの計算事例では、地盤構造物特有の問題の取り扱いを提案した。たとえば土材料には材料劣化が起こらないため、従来の考え方では構造物の寿命の算定が出来なかった。そこで材料劣化ではなく用途劣化すなわち社会の変化によって施設の使命が完了するまでの年限を 80 年と見積もり、これを寿命と見なした。また地震時の間接経済被害の算定においても、高速道路では旅行時間の増大値によって被害と見なして間接被害額を評価した。これらによりＬＣＣに基づく設計諸元の決定例を示すことが出来た。

地盤調査技術の現況の国際アンケート調査では、各国とも標準貫入試験が第一であるが、技術的問題点は意識されていることがわかり、その解消に努めることを個々の技術者に求めることを提案した。

これらの成果をまとめ、最終年度に海外五箇所で巡回ワークショップを開催した。また、国内でも２００９年3月１１日に「地盤構造物におけるライフサイクルコスト戦略」セミナーを開催した。 : 1498 **文字**

Results of the project

1. Introduction

Natural disaster is one of the significant threats that tremendously affect the life of people, properties, and activities in communities. In some situations, thousands of, or tens of thousands of people are instantaneously killed by a single disaster. It is also possible that an economic and industrial prosperity is destroyed by a natural disaster, and that afterwards people have to suffer from adversities.

Mankind has been trying to mitigate the effects of natural disasters in different ways throughout its history. Today, the desire for more safety is stronger than in the past all over the world. Since the extent of natural disasters differs from country to country, depending upon geological, climatic, and other situations, people in some countries know more about disaster mitigation technologies, whether being traditional or modern, while people in other countries know less. Hence, technology transfer for disaster mitigation is considered very important.

Technology transfer is not necessarily a voluntary or non-profitable activity as may often be thought. There are industrial or governmental needs for disaster-mitigation technologies to be introduced on a commercial basis so that the local economy is protected from negative and possibly fatal effects of natural disasters. This is one of the directions to which the experiences and advanced engineering for disaster mitigation should head for.

Japan, being one of those countries, has many types of natural disasters such as heavy rains, flooding, consequent slope failures, strong winds, and earthquakes among others. The present project has focused on earthquakes, aiming to support international export of technologies that can reduce earthquake-induced damages in geotechnical structures. This aim is important because many earthquake-prone countries do not have their own engineering tradition in spite of their present demand for safety. Moreover, validity of many earthquake-resistant technologies in Japan has been examined during past earthquakes. Even if not yet thus examined, many other technologies have been validated by shaking model tests or field shaking tests. In this regard, it has been supposed that more international markets should be developed more substantially for good disaster mitigation technologies. This is particularly important because engineers who have advanced capability but lacks business at the present time due to shrinking size of domestic construction business.

To achieve this goal, it is important to show internationally the value of earthquake engineering which advanced engineers can do but others cannot. The recent ISO code on earthquake-resistant design of geotechnical structures and such other codes as EURO Code strongly emphasize the importance of performance-based design. This is because the performance-based design allows more economical design by allowing for a limited extent of damage to structures, thus avoiding

unnecessarily high extent of safety. Since this design principle requires quantitative prediction of seismic performance, which is the residual deformation of structures undergoing strong earthquake shaking, engineers need to have good knowledge of earthquake action and reaction of composing materials. This situation favors advanced engineers.

One possible problem of seismic performance concept is that financial officers, business clients and ordinary people may not easily understand this concept. To cope with this situation, the idea of life cycle cost has been proposed. Although its essence is similar to that of performance-based design, life cycle cost converts every thing to monetary units, and hence non-engineering people can understand the validity of performance prediction more clearly.

The present project considers that promotion of performance-based design and life cycle cost principle in geotechnical earthquake engineering requires following issues. First, reliability of performance prediction has to be validated, because it is generally imagined that soil and earth materials behave in an unpredictable manner. The prediction of these geomaterials is made difficult not only by their granular (discrete) mature but also by the fact that they are produced by natural procedure (not produced in a factory under strict quality control). Hence, the quality of prediction depends on the capability of field investigation on the mechanical properties of ground. It is thus noteworthy that advanced computational technology is far less enough for satisfactory prediction. Prediction should be examined as much as possible against real behavior or results of model tests. Or studies on reality and model tests should be carried out in order to get more knowledge about behavior of geotechnical structures undergoing strong earthquake motion. Moreover, structures made of geomaterials are different from other types of structures, which are made of steel and concrete, in the sense that geomaterials do not decay with time and life time (life cycle) could be much longer than that of other structures. It is therefore necessary to show a geotechnical-specific example of life-cycle-cost analysis in which the nature of geomaterials is considered.

The present project concerns the realization and international familiarization of performance-based seismic design of geotechnical structures. It consists of (1) shaking model tests for verification and examination of the reliability of numerical prediction of seismic performance, (2) trial design based on seismic performance principle and minimization of life cycle cost (LCC), (3) international study on significance and reliability of geotechnical site investigations, and (4) international seminars / workshops for the above-mentioned familiarization. The final outcomes from these activities are addressed in what follows.

2. Shaking Model Tests and Associating Numerical Analyses

2.1 Shaking Model Tests on Behavior of Pile Foundation in Liquefied Ground

2.1.1 Tests on Small Pile Model

Shaking tests on group pile subjected to lateral flow of liquefied ground were conducted focusing on different mechanisms of soil flow and mitigation. The concerned flow mechanisms were the surface slope and the movement of a nearby unstable quay wall. The latter is a reproduction of damage in building foundation in water front areas. For both mechanisms, the employed pile foundation consisted of 3×3 nine group piles. Fig. 2.1 illustrates models of a group pile embedded in a sloping liquefiable ground or behind an unstable quay wall. Lateral flow of liquefied ground was generated by the static gravity force in a slope or tilting of a quay wall.

(a) Model of gentle slope (b) Model of unstable quay wall

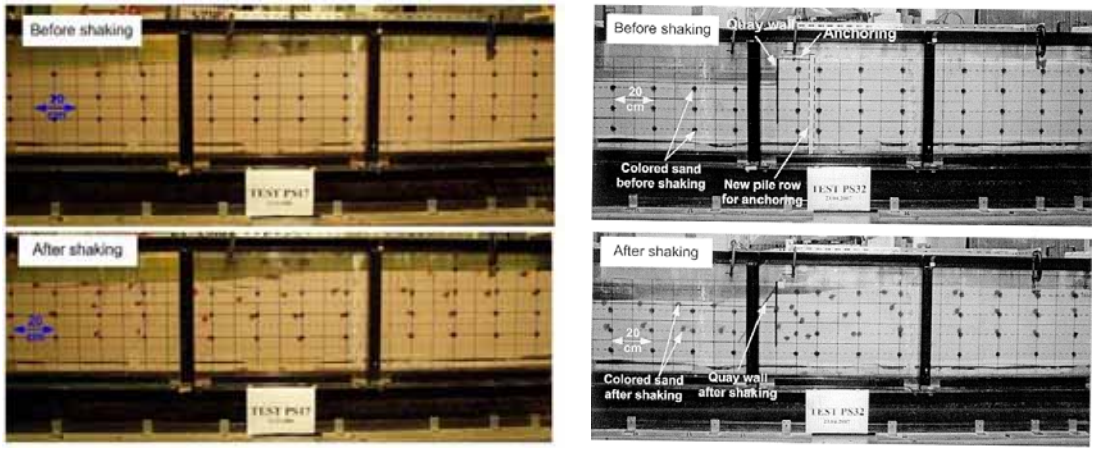

Fig. 2.1 1-G shaking model of group pile foundation in unstable liquefiable ground (top: before shaking, and bottom: after shaking)

The effect of lateral soil flow during shaking and liquefaction is illustrated by the bending moment in individual piles. Fig. 2.2 shows the magnitude of bending moment in individual piles. It is seen therein that the bending moment was the greatest on the downstream side of the group pile, and the lowest on the upstream side. It is interesting to compare this finding with the bending moment that occurred in piles embedded in a sloping ground (Fig. 2.3). The sloping ground model revealed that bending moment was greatest on both upstream and downstream sides, being lower in the middle.

The different features in bending moment distribution thus found are attributed to different distribution of soil velocity (or displacement). In the quay wall model, the lateral displacement was triggered by the failure of a nearby quay wall. Therefore, the soil velocity and displacement were

greater near the wall. The more significant soil motion generated the greater lateral earth pressure on piles and caused the greater bending moment. On the contrary, the sloping ground model generated approximately uniform displacement of soil in the central part of the container where the pile model was located. In such a situation, the middle piles were protected by the upstream piles from the effect of soil flow (shadow effect). Therefore, the middle piles had the lowest bending moment. The upstream piles, conversely, were directly pushed by the significant soil flow and their bending moment was substantial.

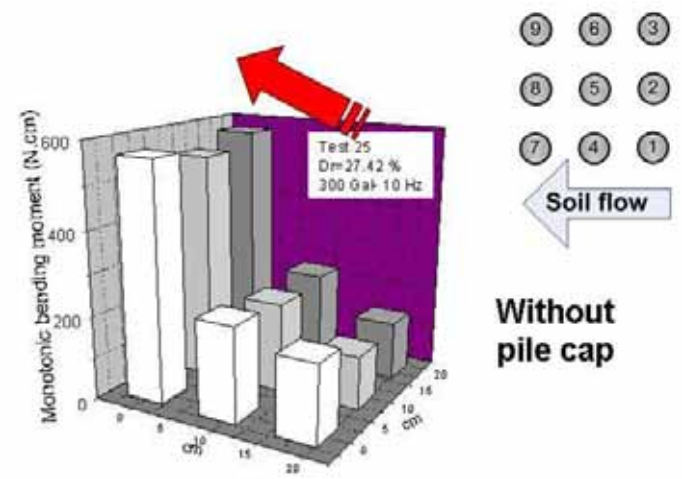

Fig. 2.2 Variation of maximum bending moment in group pile behind unstable quay wall

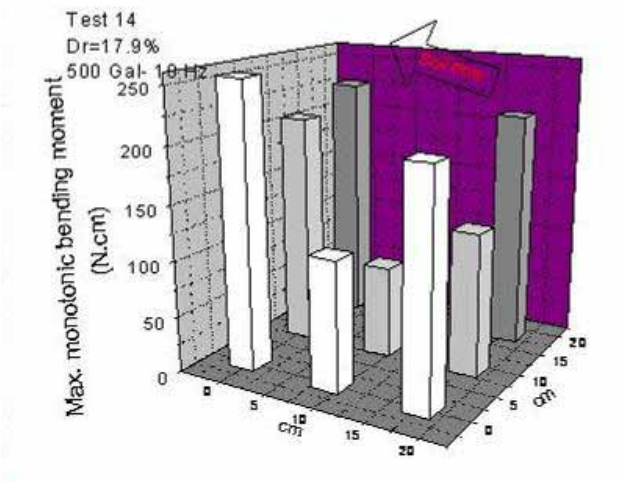

Fig. 2.3 Variation of maximum bending moment in group pile embedded in sloping ground

What appeared peculiar was the greater bending moment in the downstream piles in Fig. 2.3, which should have been protected by other piles. This point was understood by referring to the subsidence of ground surface on the downstream side of the group pile. Since the soil outside the group pile (downstream side) was free to flow away laterally, lateral expansion occurred in the

ground, resulting in surface subsidence (Fig. 2.4). This is in contrast with the ground surface inside the group pile where strain was not tensile or even compressive due to constraint by piles and the ground surface did not subside. Consequently, the different surface elevation around the downstream piles resulted in differential earth pressures from upstream and downstream sides of piles, which generated significant bending moment.

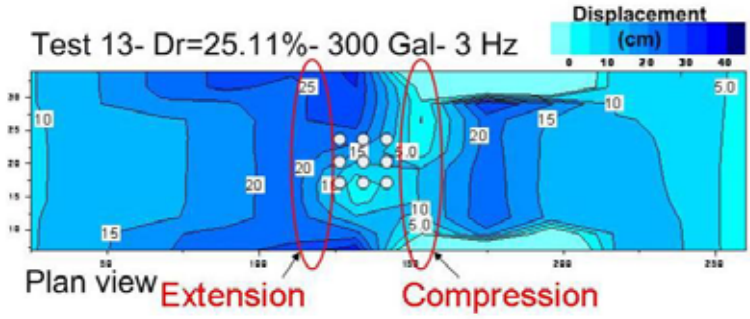

Fig. 2.4 Lateral strain in ground surface around pile foundation embedded in sloping ground model

2.1.2 Interpretation of E-Defense Full-Scale Test

The data of an E-Defense full-scale shaking model test, which was conducted during the first year, was analyzed during the second year of the project. Fig. 2.5 shows a tilted structure model which was placed behind a quay wall model and was supported by a 2×3 group pile. A major finding in this test is the verification of the mechanism by which flow of liquefied sand generates lateral pressure on piles. Fig. 2.6 indicates time histories of bending moment and soil velocity. It is clearly seen that the magnitude of bending moment is correlated with the velocity, suggesting the rate-dependent (viscous) nature of liquefied sand. An opposing opinion against this idea is that different excess pore water pressures in front of and behind a pile generates net lateral pressure, and that this differential pore pressure is the consequence of compressive and tensile stress conditions on respective side. This idea does not hold true, however, because the test result in Figs. 2.7 and 2.8 indicate that the pressure difference is negligible as compared with the extent of lateral earth pressure.

Fig. 2.5 E-Defense quay wall model after shaking

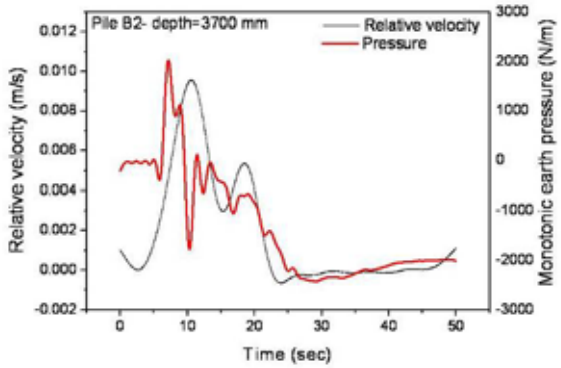

Fig. 2.6 Relationship between soil velocity and earth pressure in pile obtained by E-Defense full-scale test

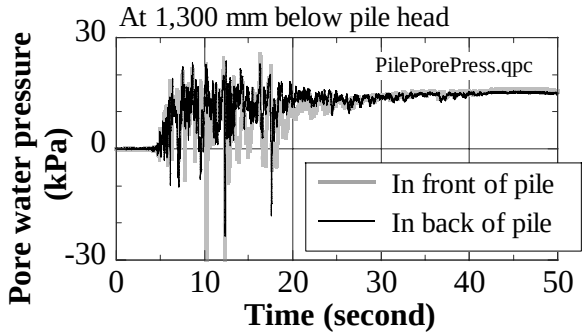

Fig. 2.7 Variation of excess pore water pressure in front of and behind pile obtained by E-Defense full-scale test

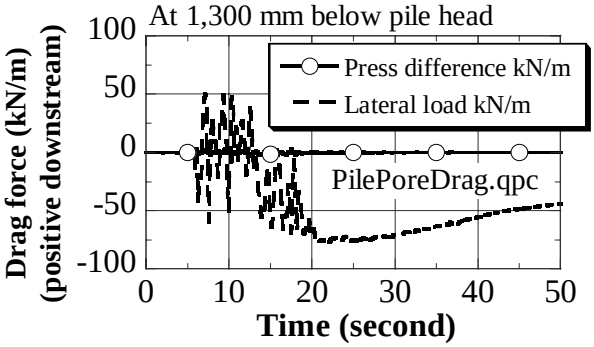

Fig. 2.8 Variation of net drag force due to excess pore water pressure and measured drag force recorded in E-Defense full-scale test

To further confirm the rate dependent nature of liquefied sand, triaxial compression shear tests were conducted on loose sand under low stress level. Two of the tests were especially characterized by their zero-gravity environment which made it possible to achieve extremely low effective stress. Shear tests on sand under low effective stress have such advantages over shaking model tests as clear identification of stress and strain states. On the other hand, its disadvantage is that stress varies

within a sample due to weight of sand grains, which becomes significant as the mean effective stress is made lower. Hence, the present study carried out tests in a zero-gravity environment. This environment was achieved by running tests in a free-fall testing facility (Fig.2.9). Fig.2.10 shows a free-fall capsule in which a triaxial shear device is encased.

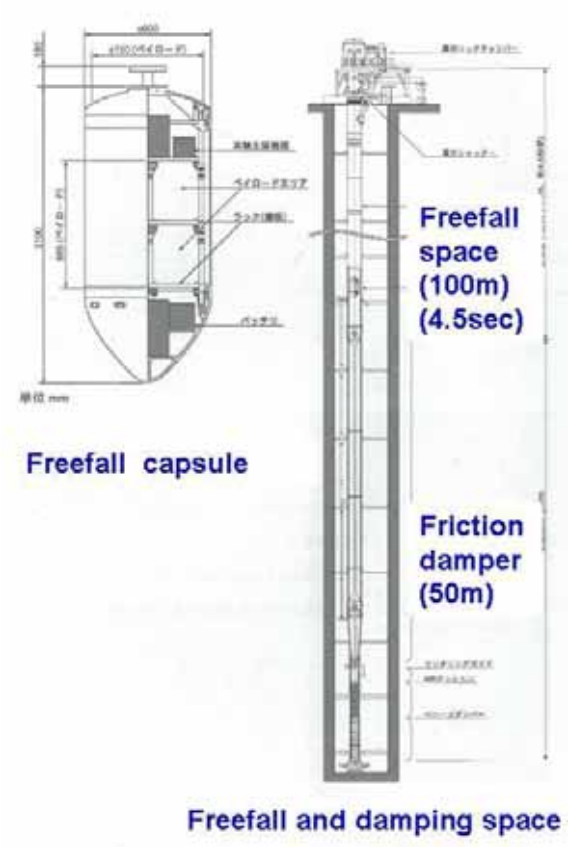

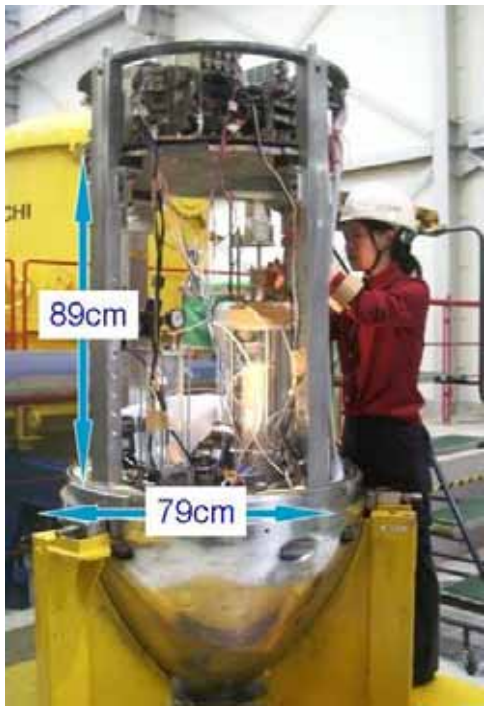

Fig. 2.9 Free-fall test facility (MG Lab. in Toki City) **Fig. 2.10** Free-fall capsule (MG Lab)

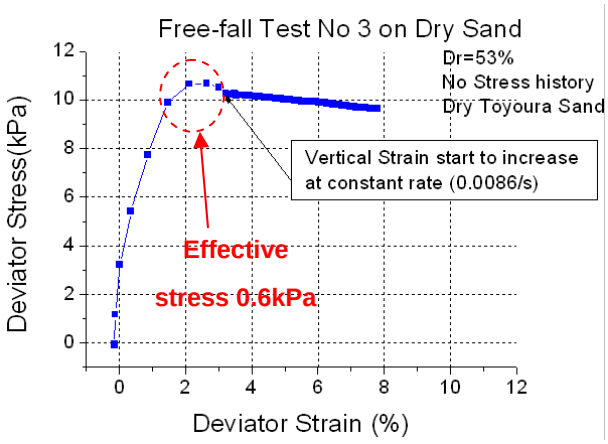

Fig. 2.11 Stress-strain behavior in a free-fall test

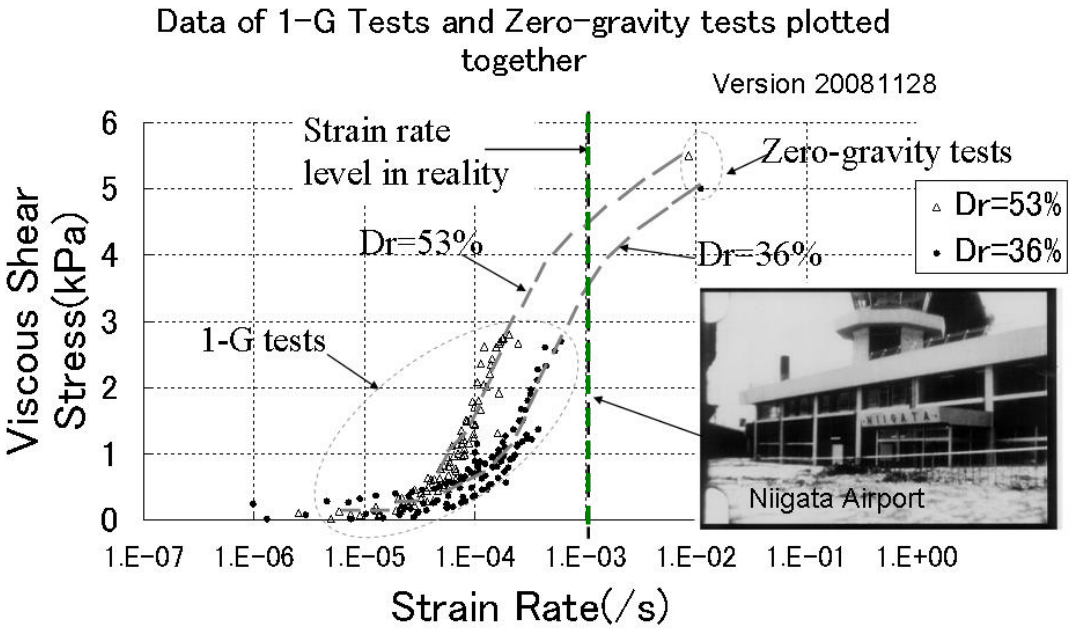

Fig. 2.12 Continuity between conventional low-stress tests and zero gravity tests (shear stress of $(\sigma_1 - \sigma_3)/2$ is plotted as the vertical coordinate)

Fig.2.11 illustrates results of one of the free-fall tests. It is seen that strain increased at a constant rate under constant shear stress, thus clearly showing that sand under very low effective stress behaves like a viscous liquid. Fig.2.12 shows the variation of viscous stress with the strain rate. Since the mechanical property of sand is always nonlinear, changing with the strain or strain rate, the viscous stress level changes in a nonlinear manner as well. However, there seems to be a consistency in the variation of viscous stress with the strain rate whether the tests were conducted in a zero-gravity environment with very low stress and higher strain rate, or under 1G gravity field where the effective stress was slightly higher and the strain rate was lower. Moreover, for a reference, the rate of strain in a real liquefaction event was inferred from the case of Niigata Airport in 1964 where the terminal building sank into ground at a rate of about 1 cm/sec. Since the thickness of liquefied sand was about 10 m, the rate of strain was about (1 cm/sec.)/(10 m) = 0.001 /sec. It is possible now to analyze the behavior of liquefied ground by using a viscous liquid model (Towhata et al., 1999).

2.1.3 Interpretation of Large Group Pile Tests

Models of a large group pile consisted of 6×6 or 11×11 piles and were shaken in a 1-G shaking table facility. Lateral soil flow was induced by the surface gradient. The aforementioned shadow effect (Fig. 2.3) is illustrated again in Fig. 2.13 in which the most upstream and downstream pile

rows were subjected to the greatest lateral pressure, while the middle rows were protected by the shadow effect. The upstream row was pushed directly by the soil flow, and the downstream piles by the pressure difference (difference in ground elevation) as stated earlier. This finding is important in seismic retrofitting of an existing pile foundation. It is supposed that additional rows of piles are installed in front of and behind a foundation and that those added rows do not bear the load of a superstructure. Being called sacrifice piles, those added piles receive the liquefaction induced earth pressure during a strong earthquake, and protect the middle piles. Even if the sacrifice piles are damaged, there occurs no damage in the superstructure because the sacrifice piles do not bear its weight.

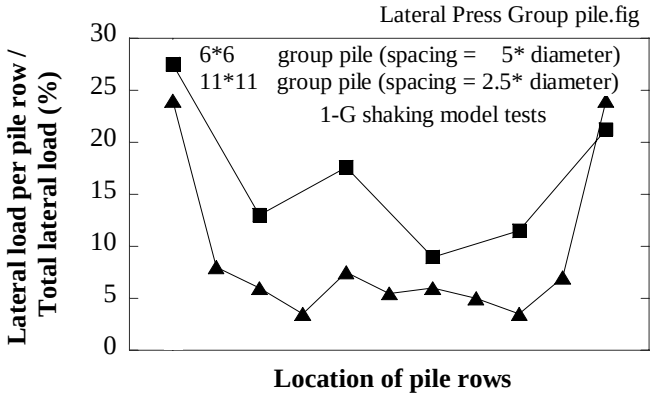

Fig. 2.13 Shadow effect in large group pile model

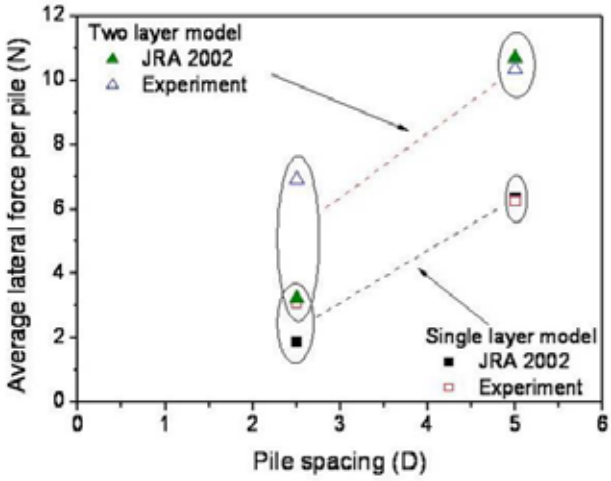

Fig. 2.14 Magnitude of total earth pressure in experiment and design code

Another finding is the total lateral load during liquefaction. Fig. 2.14 compares the average lateral force per pile (total summation of earth pressures on individual piles divided by the number of piles) with the current design specification (JRA2002) that is equal to 30% of the total vertical stress multiplied by the projected area of the group pile. It is therein seen that the design specification is

consistent with the test results, with some safety margin.

2.2 Dam Tests and Analysis

2.2.1 Shaking model tests in 1G field

Shaking of dam models was carried out in order to understand the nature of deformation of a dam body subjected to strong shaking. Following the convention of dam construction, the dam model in the first test had a central clayey core, sandwiched by sandy shell on both upstream and downstream sides (Fig. 2.15). Since the reservoir (lake) on the upstream side was filled with water, the upstream part of the dam body was saturated with water. Hence, development of excess pore water pressure and possible liquefaction were the key issue during strong shaking. Time history of base shaking is shown in Fig. 2.16. Therein the frequency and acceleration of amplitude are 10 Hz and 500 Gal (500 cm/sec^2) respectively.

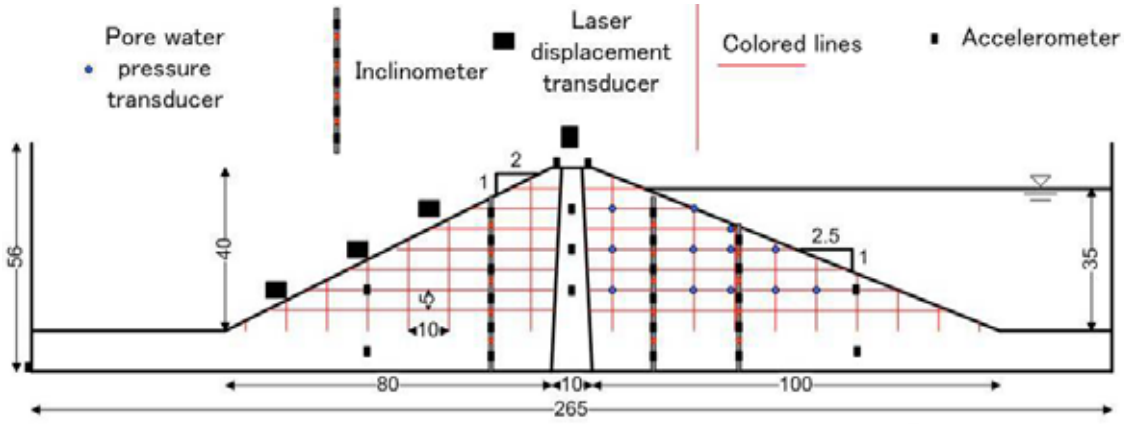

Fig. 2.15 Cross section of dam model of central-core type (unit: mm)

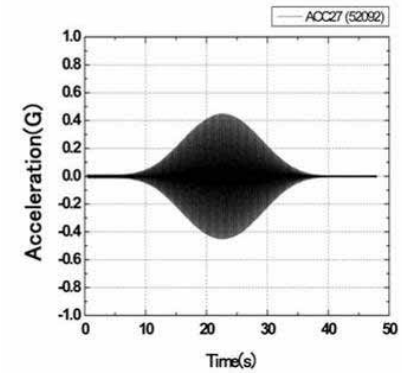

Fig. 2.16 Time history of base shaking

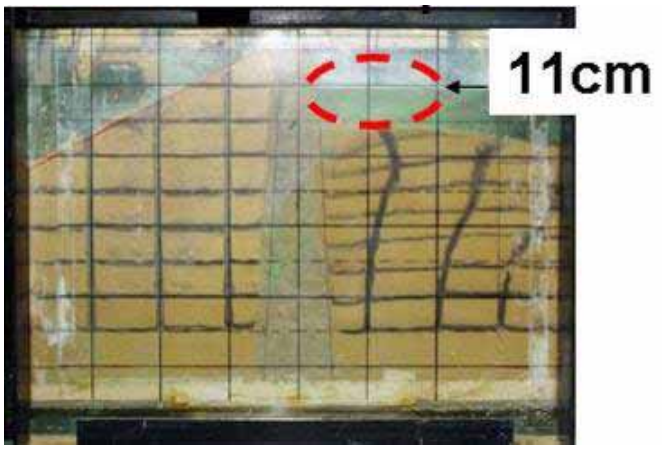

Fig. 2.17 Deformed shape of earth dam model with central core and uncompacted shell (relative density = 20%)

Fig. 2.17 demonstrates a damaged shape of the dam model. Note that this model test was conducted in order to see the behavior of uncompacted shell, which is the case of hydraulically filled dam. The subsidence on the upstream side reached 11 cm out of the total height of 40 cm. Thus, the deformation ratio is 100×(11cm/40cm) = 28 %. Note that most modern earth dams have compacted shell and have much greater seismic resistance. The observed seismic deformation in Fig. 2.17 was reproduced by a numerical analysis (Fig. 2.18). What is important is that this analysis was conduced by DEM which is one of the most elaborate numerical methods and is able to reproduce large deformation. Generally, numerical methods can achieve good results if detailed input data of soil properties, configuration, and base shaking are available. Since this situation is not necessarily the case, most geotechnical analyses, particularly on seismically-induced deformation, achieve less precise results.

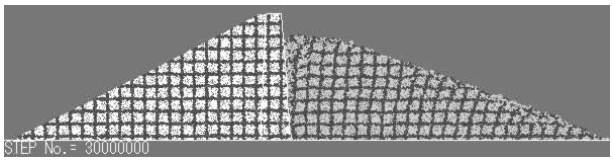

Fig. 2.18 Numerical analysis on deformation of uncompacted shell of earth dam model

In this situation, a question arises on how to evaluate the quality of prediction. Since the main goal of numerical prediction in this study is the evaluation of life cycle cost (LCC), the aim of numerical prediction should meet this goal. As will be stated later, most part of the seismic cost comes from the economic loss whose amount is strongly affected by the time needed for restoration. Although the restoration time depends on the extent of deformation, this dependency is not so sensitive with the extent of deformation. For example, subsidence of 30 cm in an expressway embankment of 5 m in height and subsidence of 50 cm in the same embankment do not cause significant difference in the restoration time. Therefore, the numerical prediction of seismically-induced deformation does not have to be so accurate. In this regard, the present study proposes to classify the damage extent of an embankment as shown in Table 2.1.

Table 2.1 Classification of damage level in embankment

Damage level	Remark	Subsidence/Height ratio
4	Collapse	>10%
3	Function lost, urgent restoration needed	1-10%
2	Minimum function held, restoration needed	0.1-1%
1	Minor damage, restoration needed	<0.1%
0	No detectable deformation	0%

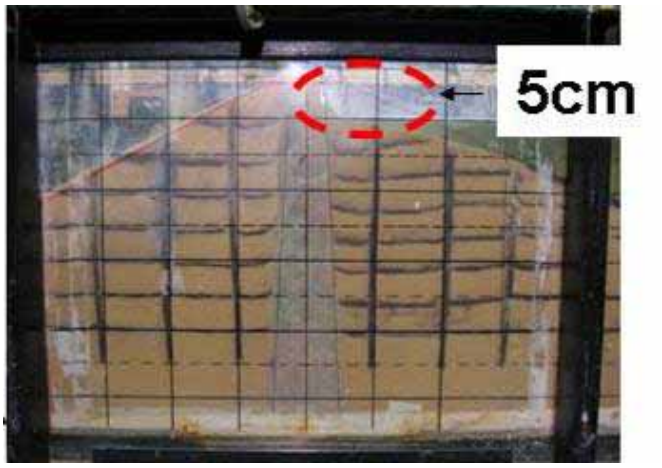

Fig. 2.19 Deformed shape of earth dam model with central core and slightly compacted shell (relative density = 50%)

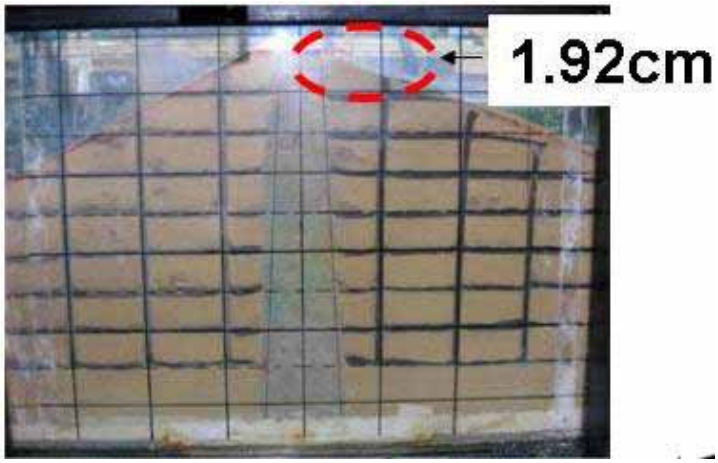

Fig. 2.20 Deformed shape of earth dam model with central core and more compacted shell (relative density = 70%)

Shaking tests on dam models were continued. Figs. 2.19 and 2.20 show that greater efforts of compaction in the shell can reduce the extent of subsidence. In the case of relative density of 70% In Fig. 2.20, the subsidence ratio is 100×(1.92cm/40cm) = 4.8 %.

One of the remarkable technologies in dam construction is the lining (pavement) on surface of the upstream slope surface. Being made of either reinforced concrete or asphalt, this lining prevents reservoir water from seeping into the dam body, and keeps the dam body without much moisture. Hence, liquefaction and softening of the dam body are made unlikely. Moreover, the hydrostatic pressure due to the reservoir (lake) water is converted by the lining to effective stress in the dam body, and the shear strength of the dam body is increased. Fig. 2.21 indicates the cross section of the constructed model. The surface lining was made by a sheet of rubber membrane. Care was taken of water tightness not to allow reservoir water to seep into the dam model.

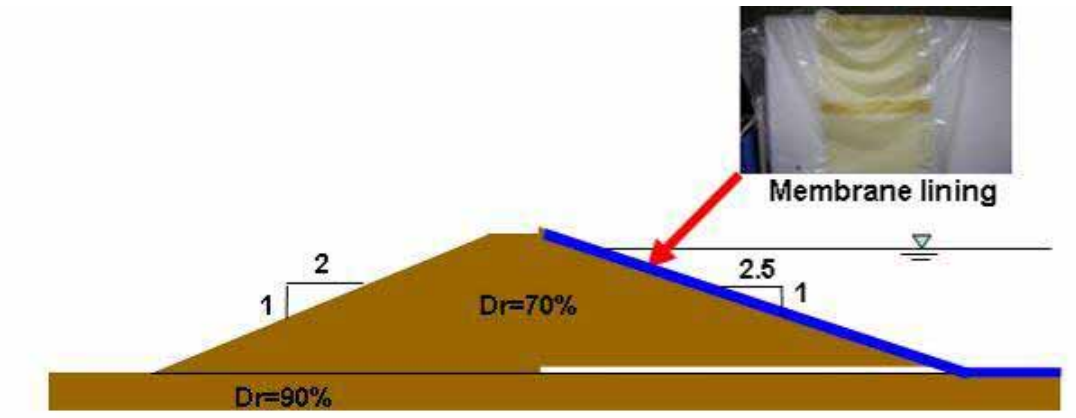

Fig. 2.21 Model of earth fill dam with surface lining on upstream side

Fig. 2.22 Shape of surface lining dam after shaking

Fig. 2.23 Zipingpu Dam after 2008 Wenchuan earthquake, China

Fig. 2.22 indicates the shape of the dam model after shaking. Evidently, no significant subsidence occurred. It has been feared on surface lining dams that earthquake-induced subsidence of the dam body may cause cracking in the concrete facing, possibly leading to water leakage, erosion, and in the worst case the entire failure of the dam body. The recent Wenchuan earthquake in China, 2008, hit the Zipingpu (紫坪鋪) Dam that was of concrete lining type. It is reported that minor cracks occurred in the lining only above the water level. When the author visited the site in October, 2008,

the reservoir water level was getting higher. Hence, it seems that the lining under water did not have a serious problem.

2.2.2 Deformation analysis on earth dam subjected to strong shaking

Earth dam, which is made of soil, may be subjected to earthquake-induced deformation and in the worst case a total breaching if the quality of construction is not sufficiently good. This was particularly the problem when dams were constructed by hydraulic filling technology that cannot achieve well compacted body of a dam. The liquefaction-induced failure of San Fernando Dam is a typical example of this type (Fig. 2.24). See a cliff at the top of the failed slope in Fig. 2.24, which is similar to the situation in a model test (Fig. 2.29). More modern technology has been able to compact dam body and hence the overall breaching is less likely today. However, the extent of deformation is still a matter to be focused from the viewpoint of performance-based design, which is the topic of the present project.

Fig. 2.24 Failed shape of San Fernando Dam in California, 1971

Fig. 2.25 Liyutan Dam in Taiwan after 1999 ChiChi earthquake

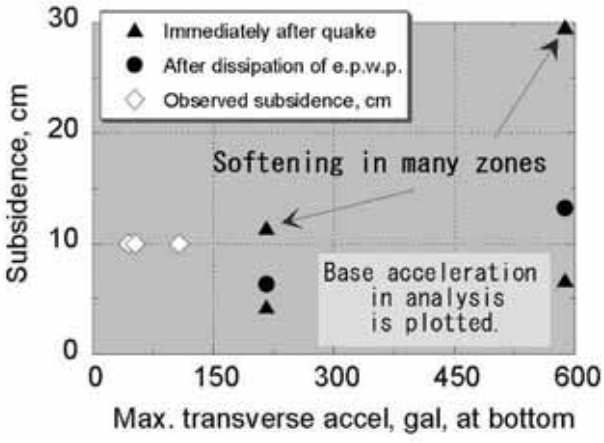

Fig. 2.26 Prediction of subsidence of Liyutan Dam under design earthquakes

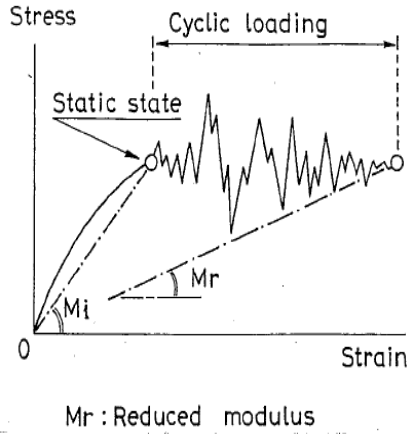

Fig. 2.27 Principle of strain potential method of deformation prediction

Fig. 2.25 illustrates the shape of Liyutan (鯉雨潭) Dam after the 1999 ChiChi earthquake in Taiwan. Out of its height of nearly 100 m, this dam body subsided only about 10 cm after the quake because of the good construction. Prior to the construction, the seismic performance of this dam was assessed by the author's group (Shi et al., 1989). Fig. 2.26 plots the magnitude of subsidence against intensity of acceleration of design earthquakes. On the basis of this prediction, it was judged that this dam would be safe under future earthquakes. It is then interesting to compare the prediction with what happened to the dam during the 1999 ChiChi earthquake. It is good that the performance prediction and judgment worked well. On the other hand, it was fortunate as well that the shaking during the ChiChi earthquake was much weaker than design earthquakes in spite of the short distance between the dam site and the earthquake causative fault of as short as 5 km. The reason for this unexpectedly weak shaking is still unknown.

Fig. 2.27 indicates the method of deformation prediction (Lee, 1974) that was employed for the Liyutan Dam project. Being called strain potential method, this method applies to soil samples stress histories that occurs in reality both before (consolidation stress) and during an earthquake in order to investigate the earthquake-induced deformation of a dam body. The applied stress histories are not necessarily identical with what happens reality and are allowed to modify in consideration of the limitation of soil testing machines. For example, triaxial machines can apply only axisymmetric stress conditions.

Fig. 2.27 schematically illustrates that strain of a soil sample increases due to earthquake-induced cyclic stress. Although this behavior of soil in the laboratory is qualitatively consistent with the reality, the induced stress increment is not quantitatively identical with reality. The reason for this lies in the boundary conditions. In a soil testing machine in the laboratory, soil specimens are subjected to stress-controlled boundary conditions. Hence, large deformation can take place if soil becomes very soft during cyclic loading. Conversely in a real dam, a softened soil may not be able to deform significantly if surrounding soil maintains rigidity. Similarly, a soil element may deform substantially if the surrounding parts of soil liquefies. Thus, the strain increment in laboratory tests is called not strain but strain potential, and realistic deformation analysis should relevantly take into account the interaction between soil elements.

The interaction is considered by interpreting the strain increment in Fig. 2.27 as decrease of modulus from the pre-earthquake value of M_i to the post-earthquake value of M_r. Then two FE analyses are conducted; one with the pre-earthquake modulus and the other with the p9ost-earthquake modulus. The difference of displacements from these two analyses is considered to be the earthquake-induced deformation. Shi et al. (1989) used M_r from two situations that are immediately after undrained cyclic loading and after dissipation of induced excess pore water pressure. See Fig. 2.26 for results.

The advantage of the strain-potential method is that complicated behavior of soil is well taken

into account by running laboratory shear tests. Use of complicated elasto-plastic modeling and unreliable determination of soil parameters are avoided. Since M_i and M_r are equivalent linear moduli, the required analyses are conducted by a simple linear elastic FE computer code. On the other hand, the limitation of the method is the need for many laboratory tests. In principle, all the finite elements in deformation analyses are subjected to different initial static and earthquake-induced stress histories, and require many different laboratory tests. To avoid this time-consuming procedure, tests are run on a limited number of elements and modulus reduction for other elements is decided by an interpolation.

Laboratory tests were run by a torsion shear device in Fig. 2.28. This apparatus can control and apply two components of cyclic shear stress that are namely the torsional shear stress and stress difference between the vertical and horizontal directions. This complicated stress control was not possible during the past similar attempts. Fig. 2.29 shows the upstream half of an analyzed dam model (height = 40 m and slope width = 90 m) and soil elements that were analyzed. This dam model was supposed to be shaken by Kaihoku motion (1978 Miyagiken Earthquake) with the adjusted maximum acceleration of 500 gal. One of the test results from tests on element 334 in Fig. 2.29 is illustrated in Figs. 2.30 and 2.31. Fig. 2.32 shows the variation of modulus reduction with the increase of cyclic shear stress ratio. Similarly, Fig. 2.33 shows the variation of Poisson ratio. These experimental relationships were used to determine modulus reduction in other soil elements for which laboratory shear tests were not conducted.

Fig. 2.28 Torsion shear device

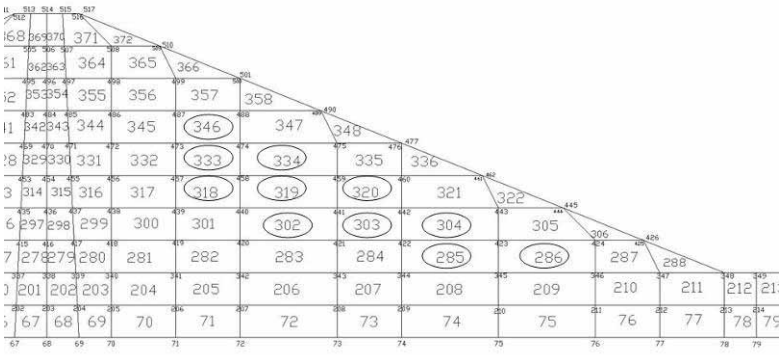

Fig. 2.29 Upstream half of analyzed dam model and soil elements for laboratory tests

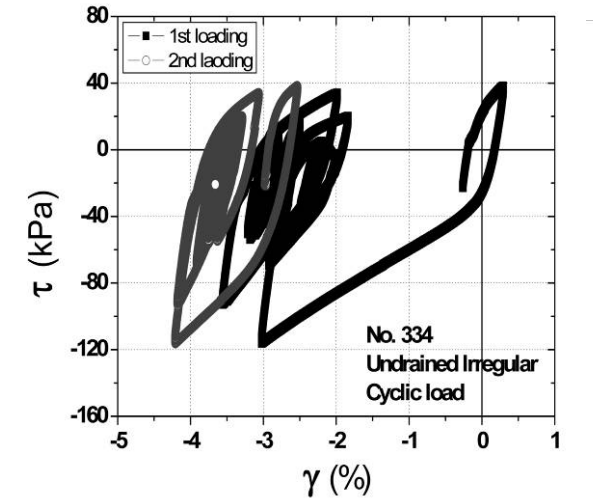

Fig. 2.30 Observed torsional stress-strain behavior (Element 334 in Fig. 2.29)

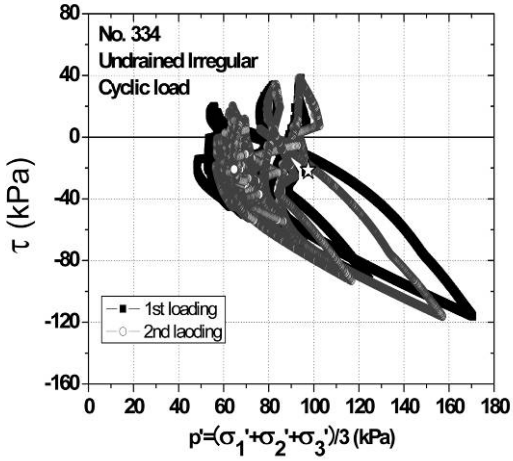

Fig. 2.31 Observed stress path (Element 334 in Fig. 2.29)

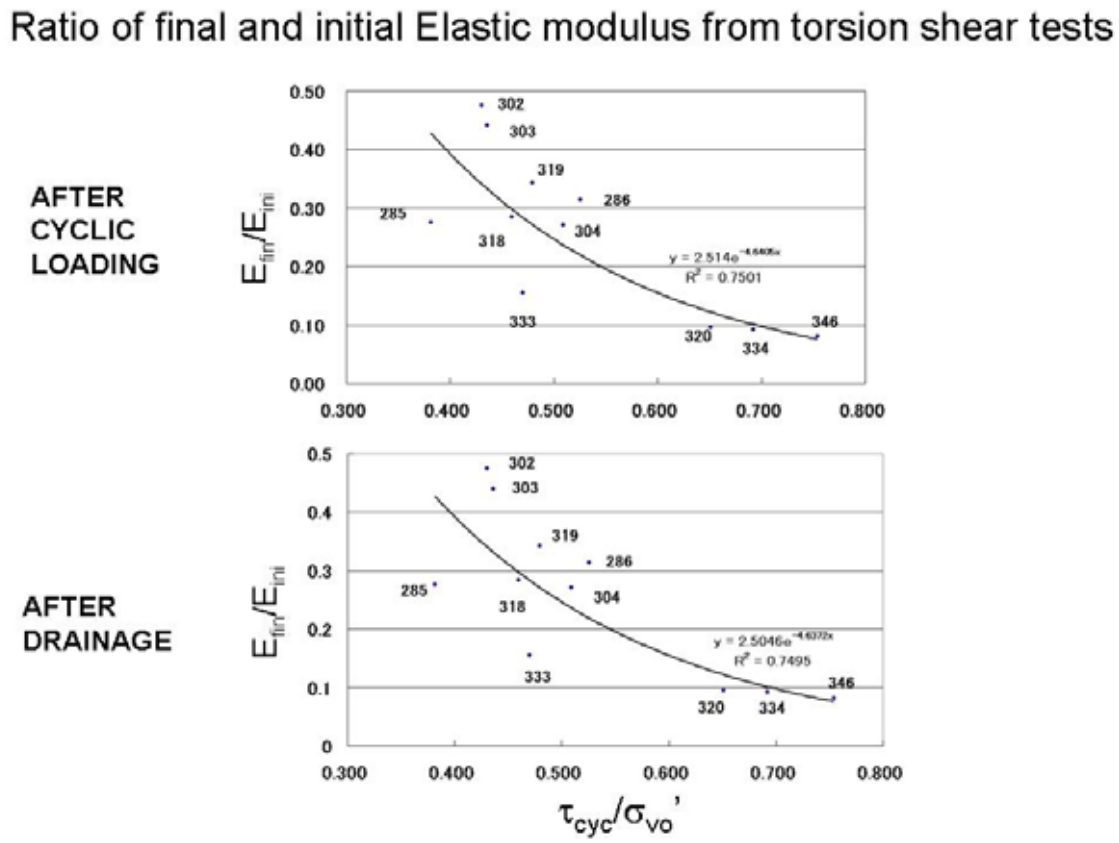

Fig. 2.32 Interpolation of modulus reduction by using cyclic shear stress ratio

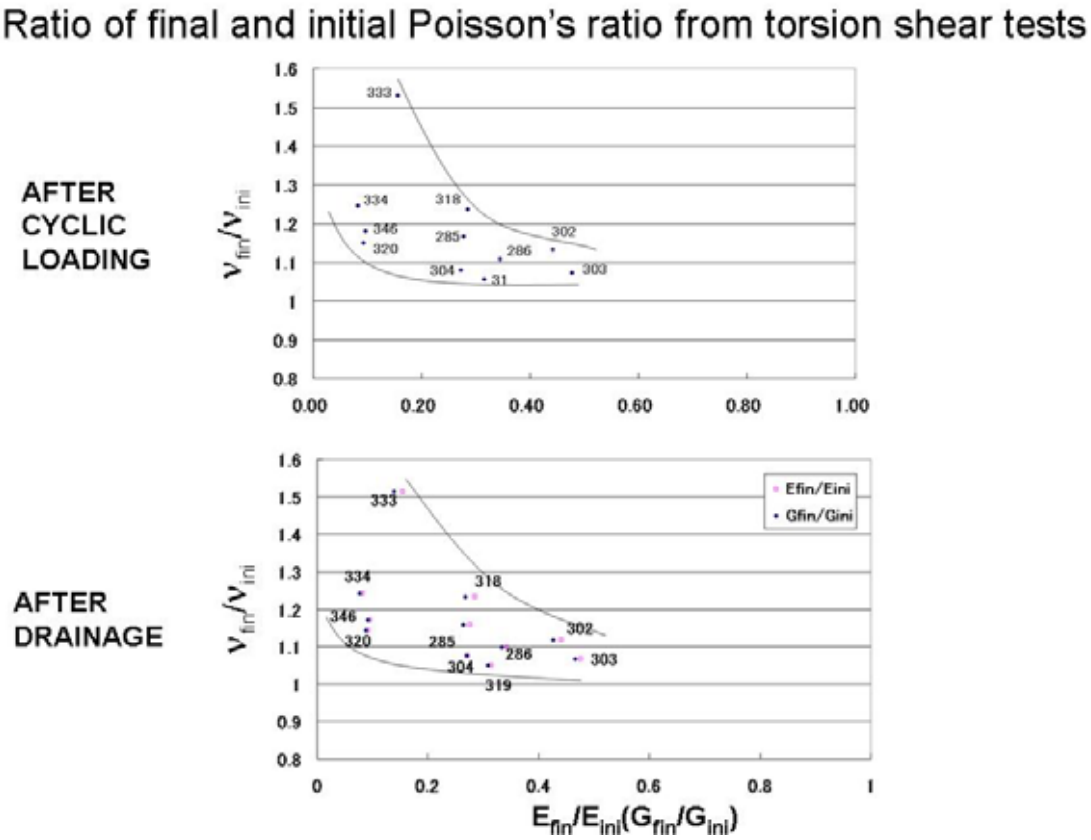

Fig. 2.33 Interpolation of change in Poisson ratio by using cyclic shear stress ratio

Figs. 2.34 and 2.35 demonstrate the calculated deformation of a dam immediately after earthquake shaking and after dissipation of excess pore water pressure (more volume contraction). Since the dam material was compacted as is in the current practice, volume contraction was limited. These figures show that the magnitude of displacement is greater near the slope surface than inside the dam because earthquake shaking (cyclic shear stress) is greater near the surface. Moreover, the displacement near the shoulder of the dam is greater than near the toe because of the same reason. Fig. 2.36 compares the state of shear stress prior to earthquake loading and the direction of strain increment vectors. It is evident that there are plastic potential curves in the stress space to which the strain increments are normal.

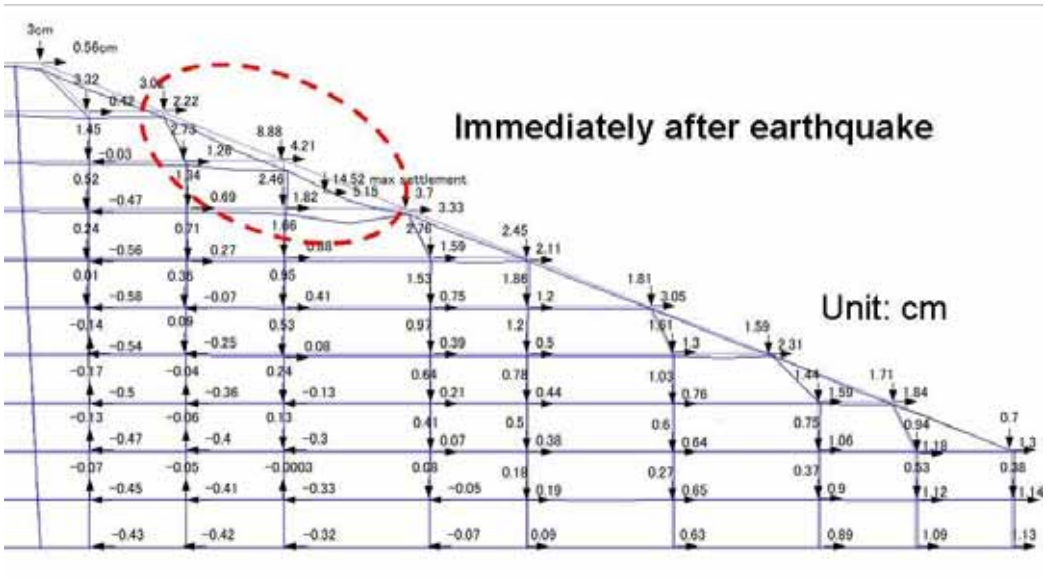

Fig. 2.34 Calculated deformation of dam body immediately after earthquake

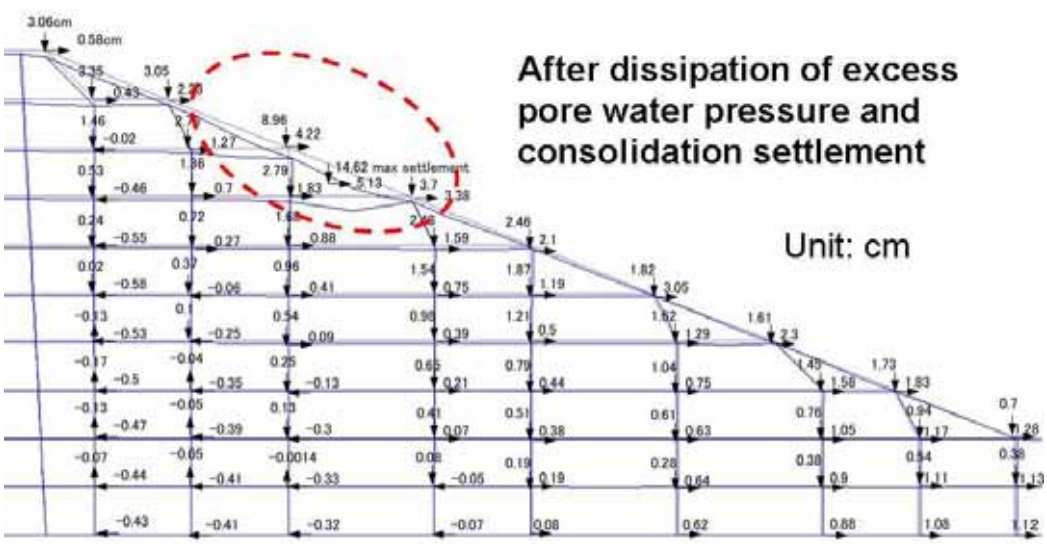

Fig. 2.35 Calculated deformation of dam body after consolidation settlement

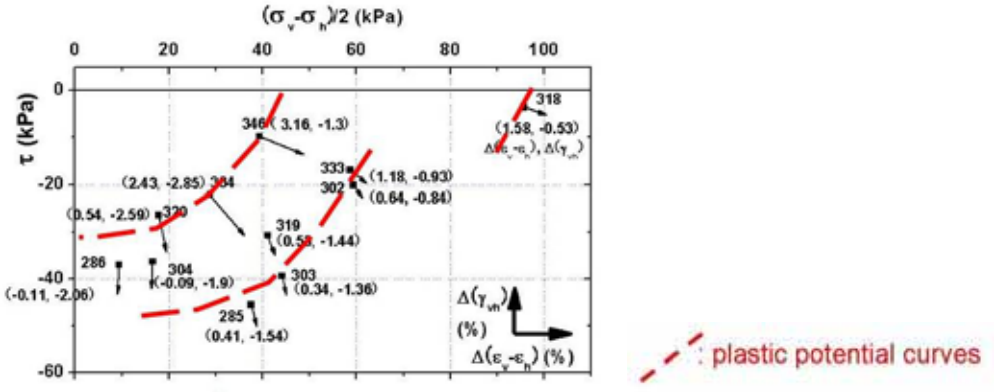

Fig. 2.36 Existence of plastic potential functions

2.3 Dynamic Behavior of Harbor Quay Wall

2.3.1 Centrifugal Model Tests on Gravity Quay Wall

Deformation of a gravity quay wall, which is made of caisson boxes with backfill soil, affects the operation of harbor directly. Therefore, it is important to study this structure from the viewpoint of seismic performance and life cycle cost. Fig. 2.37 shows the configuration of a tested quay-wall model. As the time histories of input acceleration motion (Fig. 2.38) suggest, a special interest lay in the effect of long duration time of strong earthquake motion. The expected earthquake in the Nankai subduction zone has particularly a long duration time because of its large seismic magnitude.

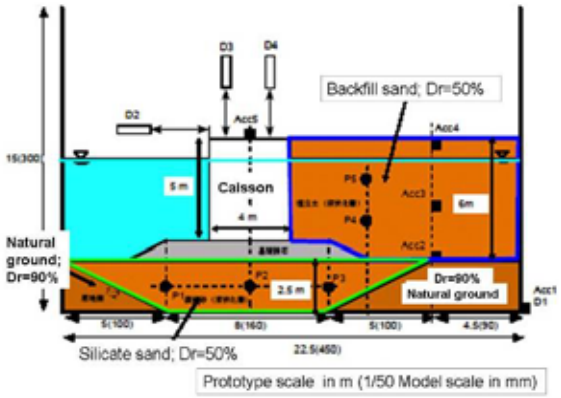

Fig. 2.37 Centrifugal model of gravity quay wall

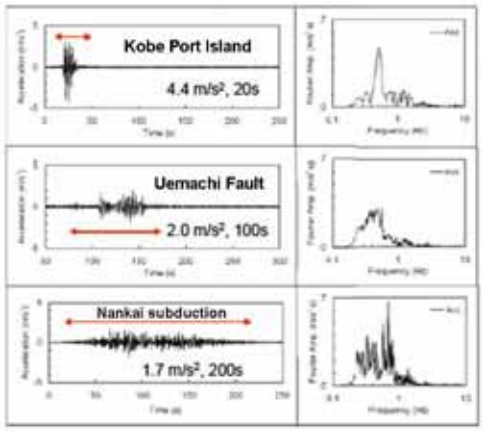

Fig. 2.38 Input motions for quay wall tests

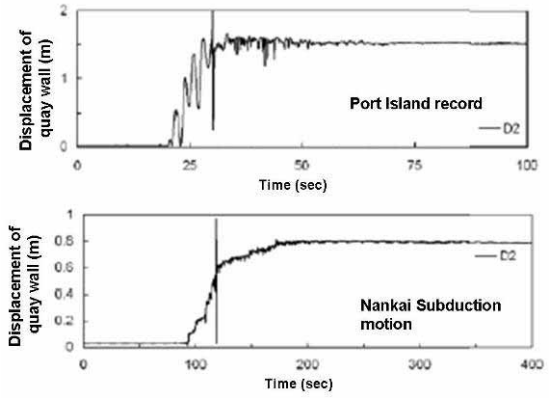

Fig. 2.39 Time history of displacement of quay wall

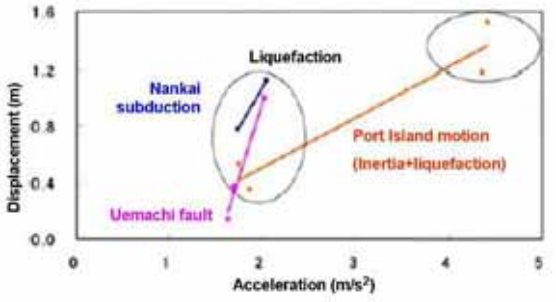

Fig. 2.40 Deformed shapes of quay wall

Fig. 2.39 illustrates the time history of lateral displacement at the top of a quay wall model. The elongated motion of Nankai subduction zone allows the displacement to develop for a longer time. Fig. 2.40 examines the relationship between the maximum acceleration of three earthquake records and horizontal displacement. The different trends for three types of input shaking suggest that the elongated shaking of Nankai record can achieve greater displacement than others for the same

magnitude of acceleration. This suggests that the performance prediction needs to consider time in some sense in contrast to the current design practice in which only the maximum acceleration and its equivalent seismic coefficient are considered. This point is made clear by comparing model responses undergoing three different motions with the identical maximum acceleration. In Fig. 2.41, the Nankai motion was able to maintain the state of high excess pore water pressure and liquefaction for a longer time, thus allowing more ground deformation.

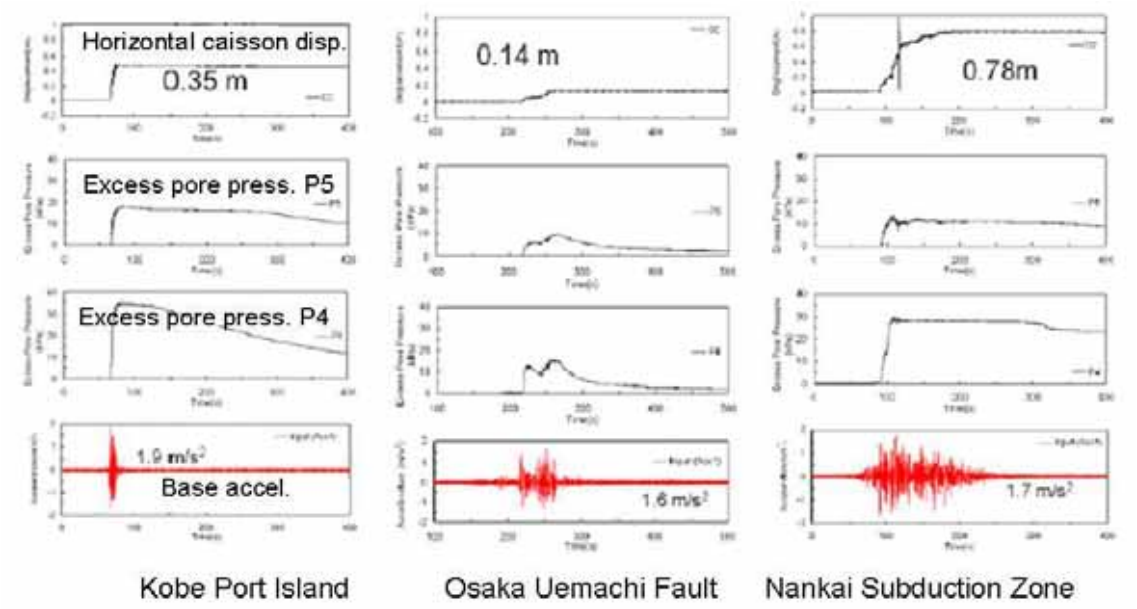

Fig. 2.41 Comparison of ground response (horizontal displacement of caisson model and excess pore water pressures) under identical magnitude of maximum acceleration in three records

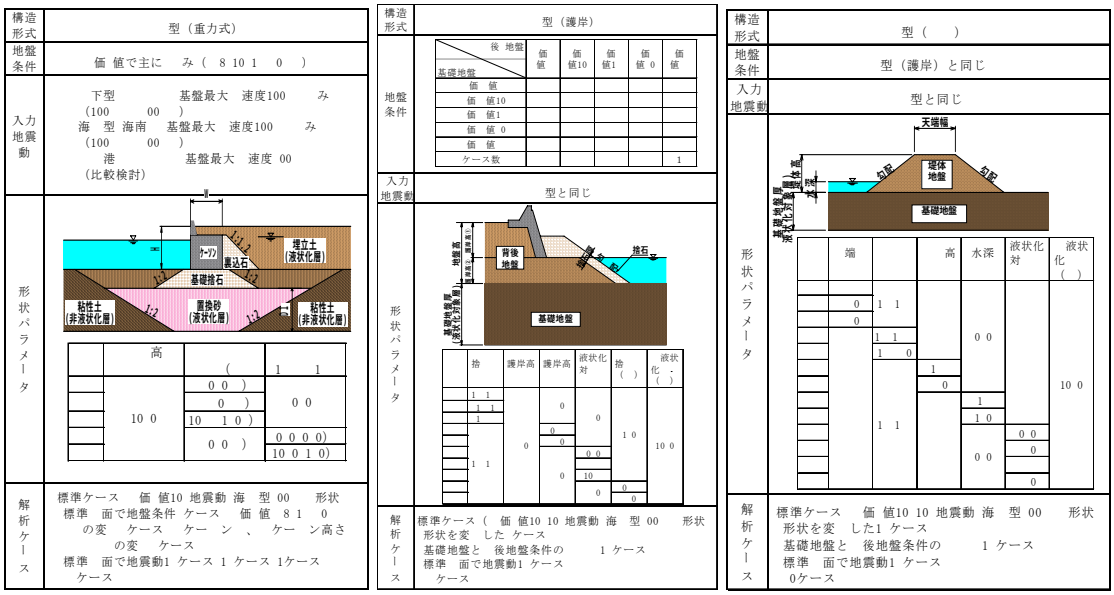

(a) Gravity quay wall (b) Inclined wall (c) River levee

Fig. 2.42 EXCEL files for quick evaluation of earthquake performance.

A frequently pointed problem in advanced numerical analysis is that the computation time and cost are too much for design procedures in which many trial calculations are required. To overcome this problem, design codes have been relying on close-form formula or design diagrams. However, those methods cannot fully consider detailed distribution of materials and configurations. The present project proposes to develop empirical formulae by conducting regression analyses on results of many nonlinear dynamic analyses that were run on different configurations and material properties. The obtained formulae are able to work out the residual displacement instantaneously by simply putting in configuration and material data in an EXCEL file. Examples are illustrated in Fig. 2.42. The life cycle cost analyses on gravity quay wall in Sect. 3.2 needed many complicated numerical analyses. It was made possible by using the EXCEL file.

2.3.2 1-G Shaking Model Tests on Gravity Quay Wall

(1) Shaking Model Tests

The present section addresses a series of 1-G model tests on displacement dissipation effects of a soft material placed behind a quay wall. It is thereby expected that dynamic earth pressure during an earthquake is reduced so that the residual deformation of the wall may be mitigated. Fig. 2.43 illustrates the idea of two types of dissipaters; cartonplast panel and a jagged bracing system. Furthermore, Fig. 2.44 shows a different idea in which a sheet-pile wall and backfill ground are connected by mechanical shock absorbers, thereby mitigating the transmission of dynamic earth pressure from the backfill to the wall. The shaking table facility and a model container are shown in Fig. 2.45. The scale of the model is 1/25 and the observed displacement of the model should be multiplied by 25 to infer the prototype behavior. All the tests were conducted by using Firoozkooh sand No.161 whose material properties are Gs=2.658, e_{max}=0.943, e_{min}=0.603, D_{50}=0.3mm, and fines content = 0%. PDPs (pressure dissipater panels) as sketched in Fig. 2.43 were constructed for model tests as depicted in Fig. 2.46. Shaking was conducted with harmonic excitation with a constant amplitude.

Fig. 2.47 depicts the deformation of a model shaken under 8 Hz. The amplitude of acceleration is shown in Figs. 2.47 and 2.48. The duration of shaking was around 10 second. Lateral displacement of the quay wall model is evident. By comparing this figure with Fig. 2.48 for a model with PDP, it is found that the lateral displacement of the wall was reduced to some extent.

The time histories of lateral displacement as well as the earth pressure from the backfill to the wall are compared in Figs. 2.49 and 2.50. As stated before, the observed model displacement should be multiplied by 25 to infer the prototype displacement. At this moment, it is concluded that the mitigative effects in earth pressure is very significant, even creating tensile force, while the lateral

displacement is reduced to a limited state because the inertia force acting on the quay wall model caused displacement as well.

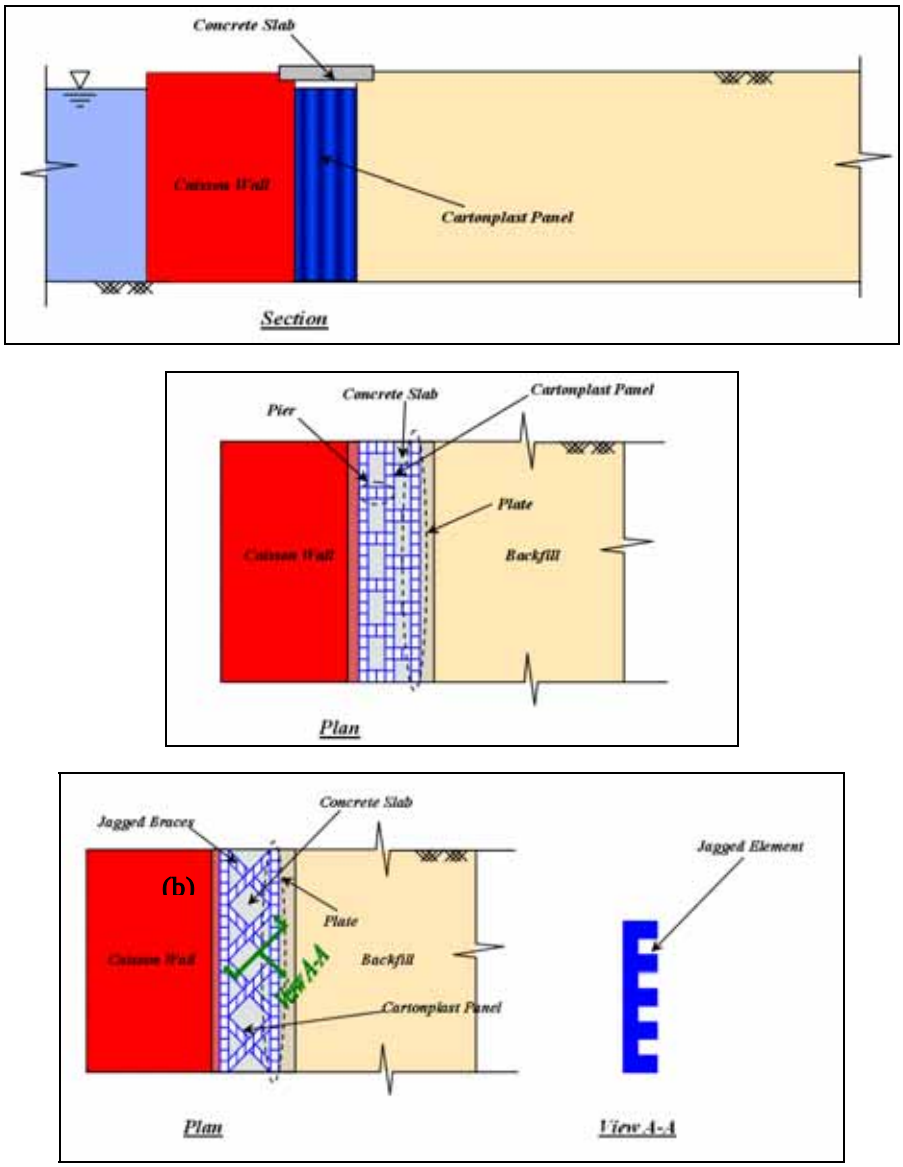

Fig. 2.43 Schematic view of the application of cartonplast panels at the back of the quay wall: (a) Section, (b) Pier-plate system type in plan, (c) Jagged-bracing system type in plan

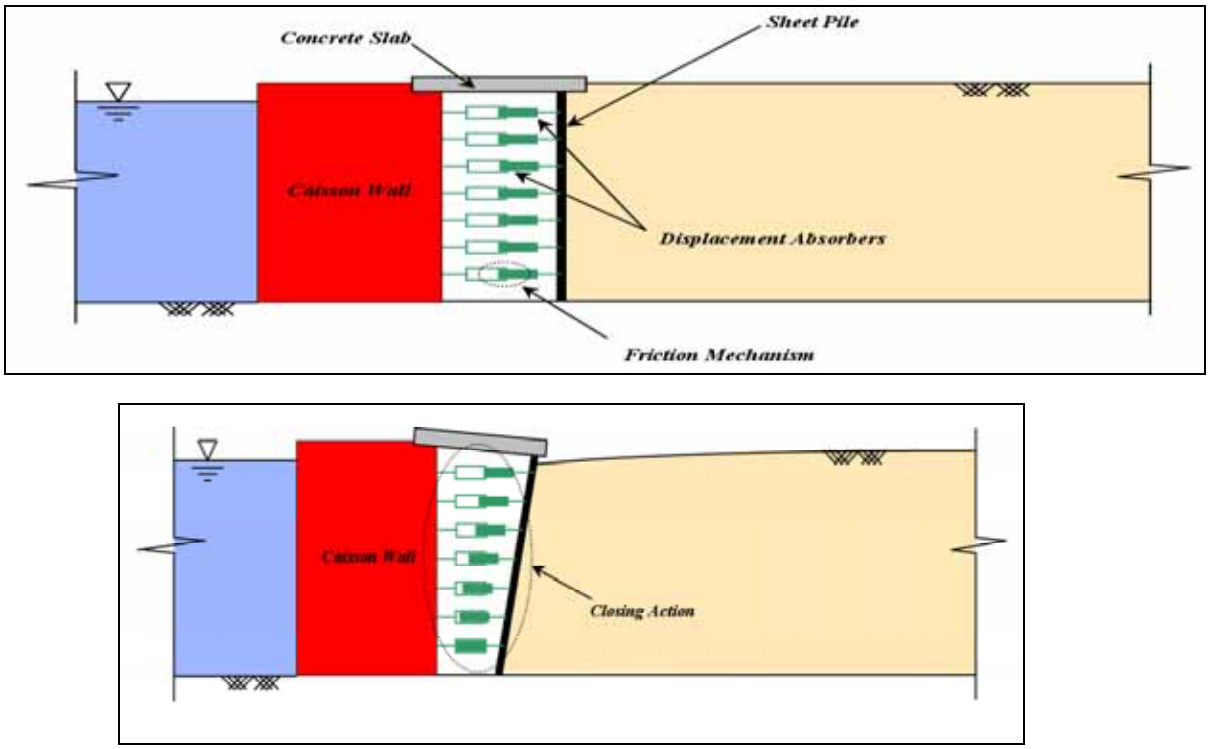

Fig. 2.44 Schematic view of the application of sheet pile wall with Pressure Dissipater Elements (PDEs) behind the quay wall: (a) Undeformed shape, (b) Deformed shape

(a) Manual Device (b) Hydro-Mechanical Device

Fig. 2.45 Shaking table facilities located at the University of Tehran, School of Engineering

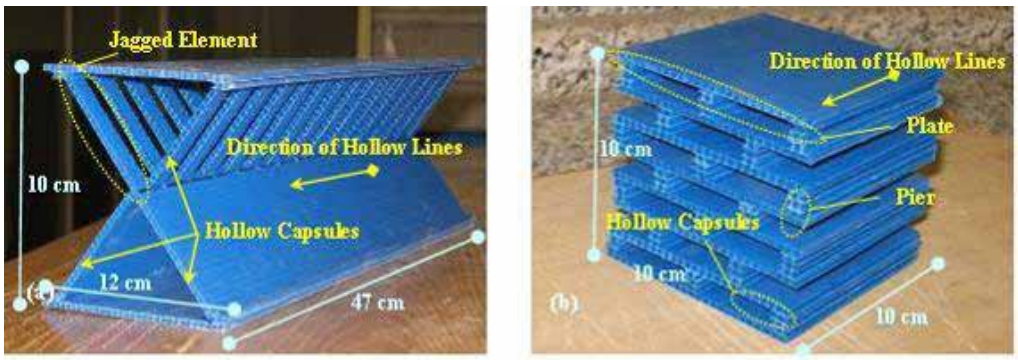

Fig. 2.46 Details of PDP models

(a) Before shaking (b) After shaking

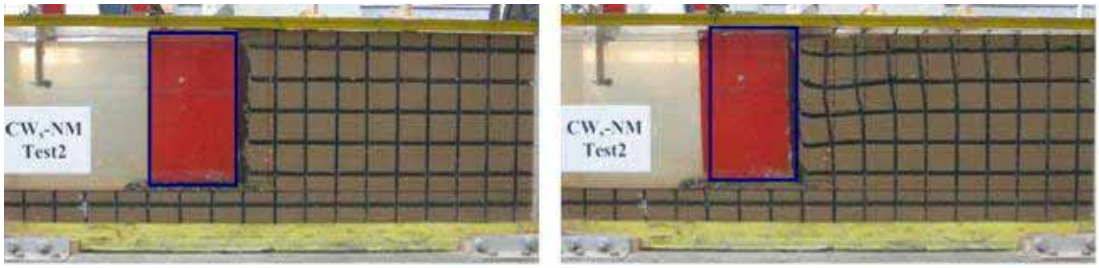

Fig. 2.47 Photographs of CWs-NM-Test 2 No mitigation, (acceleration: 0.30g, frequency: 8 Hz)

(a) Before shaking (b) After shaking

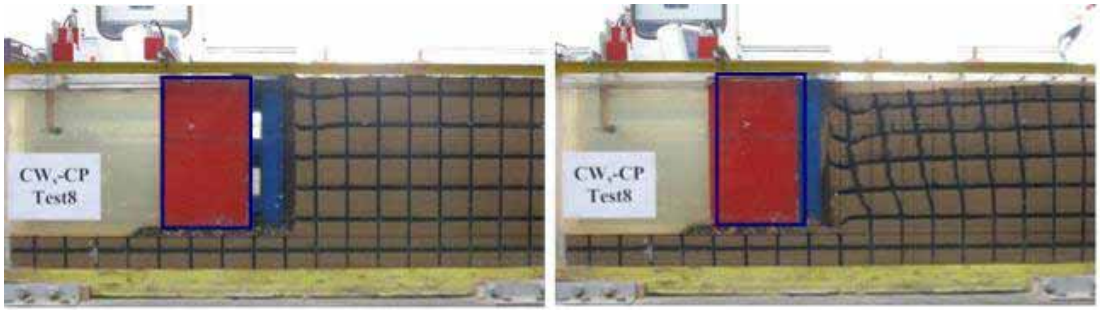

Fig. 2.48 Photographs of CWs-CP-Test 8 (acceleration: 0.30g, frequency: 8 Hz)

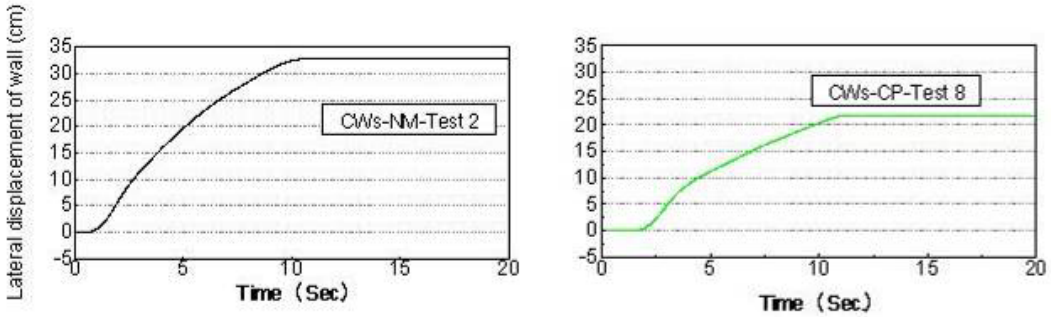

Fig.2.49 Time histories of lateral displacement of quay wall models with and without PDP

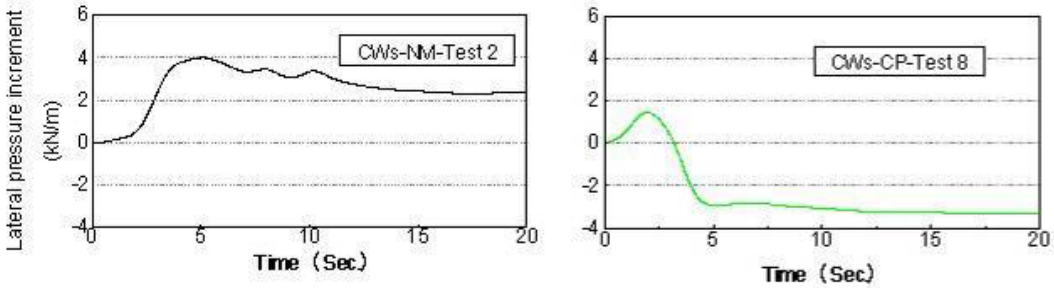

Fig. 2.50 Time histories of lateral earth pressure on quay wall models with and without PDP (earth pressure increment during shaking is plotted)

(2) Numerical Analysis

The analyses were conducted by nonlinear dynamic method in a finite difference formulation. The analyses were conducted on a prototype scale. The employed acceleration input is drawn in Fig. 2.51. Fig. 2.52 shows the configuration of the numerical model.

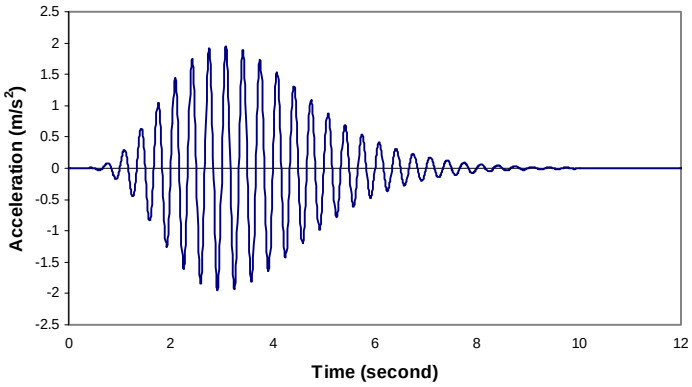

Fig.2.51 Seismic excitation applied to the bottom of numerical model

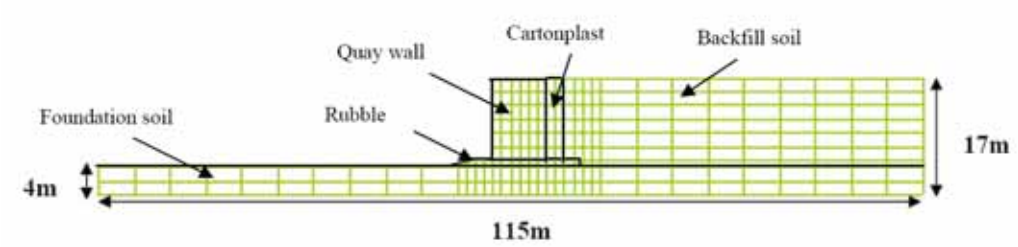

Fig. 2.52 Numerical model for finite difference analysis

The results of computation are presented in what follows on the effects of using cartonplast materials behind caisson type quay walls as mitigation against deformation and earth pressure acting on quay wall.

(i) Computed Displacement

Figs. 2.53 and 2.54 show the post-earthquake permanent horizontal and vertical displacements of top of quay wall, respectively. In these figures, negative displacements imply a seaward direction of movement. From Fig. 2.54, one can observe that the displacements of the caisson were gradually induced after 1 second after the arrival of earthquake wave. The maximum residual horizontal and vertical displacements computed at the end of shaking (see Fig. 2.53) including the post-liquefaction volumetric strain are summarized in Table 2.2. Progressive seaward displacement of the quay wall is

observed during all the simulation runs. The accumulated dynamic portion of the lateral displacement of the wall is significant in all the cases.

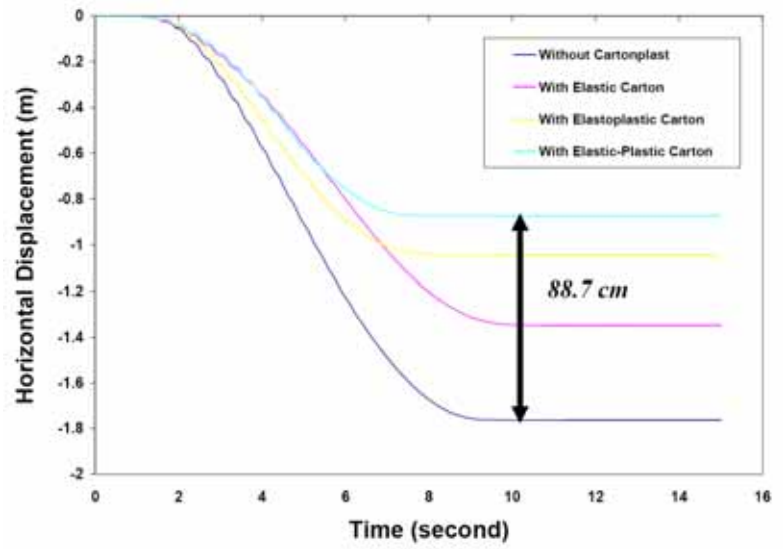

Fig. 2.53 Horizontal displacement time histories for top of quay wall

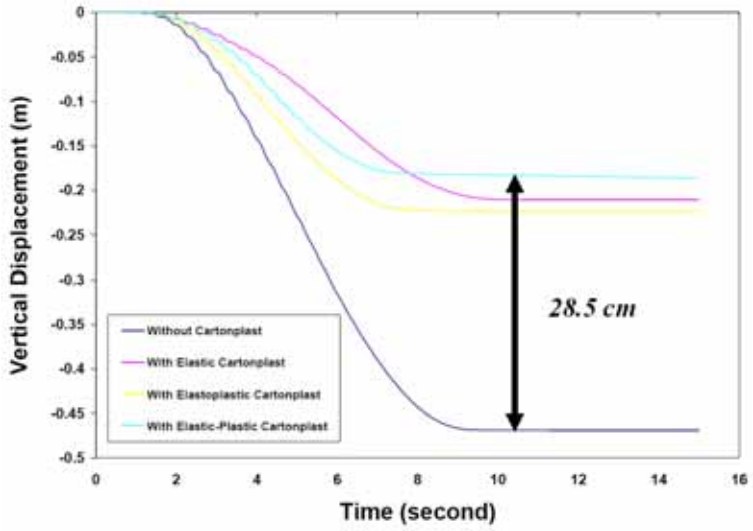

Fig. 2.54 Vertical displacement time histories for top of quay wall

Subsidence and lateral displacement behind the caisson is widely observed in all numerical models. On the other hand, subsidence and lateral displacement of quay wall are induced in mitigated models. It was found from Figs. 2.53 and 2.54 that cartonplast can reduce horizontal and vertical displacement by about 50 % and 40% respectively. Therefore, the results show that using cartonplast as a mitigation system can reduce lateral displacement and subsidence of quay wall. The results clearly demonstrates that analysis model captures very well the seismic behavior of the

caisson-type quay wall and surrounding soils in comparison with the results of model tests. Trend of vertical and horizontal displacement of structure are predicted reasonably well with respect to model tests. Therefore the numerical model is judged to provide useful, representative results for the dynamic behavior of caisson type quay walls.

Table 2.2 Computed horizontal and vertical displacement at top of quay wall

	No Mitigation	Elastic Cartonplast	Elastoplastic Cartonplast	Elastic-plastic Cartonplast	Reduction Percent (%)
Horizontal displacement (cm)	176	135	104	87	50
Vertical displacement (cm)	47	21.1	22.5	18.3	60

Fig. 2.55 Computed post-earthquake deformed shape for the quay wall without cartonplast

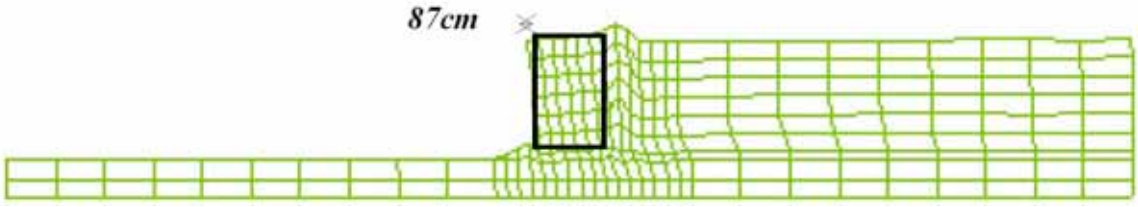

Fig. 2.56 Computed post-earthquake deformed shape for the quay wall with elastic-plastic cartonplast

Fig. 2.55 and 2.56 show the deformed grid of the wall-soil system after the completion of the earthquake shaking, magnified by a factor of two. One may observe from these figures that there is a significant movement of a quay wall. Note also that the lateral spreading of soil is clearly visible near the areas influenced by the quay wall. In addition, differential settlement between the caisson and the apron are also observed. This is consistent with the actual mode of deformation see in model tests.

In this study the failure mode which is observed is sliding with a slightly rotation failure. The calculated failure mode and the observed in model tests one are in good agreement with each other.

It is noticed that, similar to the observed behavior in experimental tests, light caisson on rigid foundation trends to slid and move toward the seaward.

(ii) Computed Acceleration

Acceleration response is a very important issue in seismic performance because acceleration-induced inertial force can easily lead to damage in superstructures on the ground surface. Fig. 2.57 shows the horizontal acceleration atop the quay wall. Note that the maximum acceleration increased, opposite from the expectation, when a soften cartonplast was installed. Table 2.3 compares accelerations of different models.

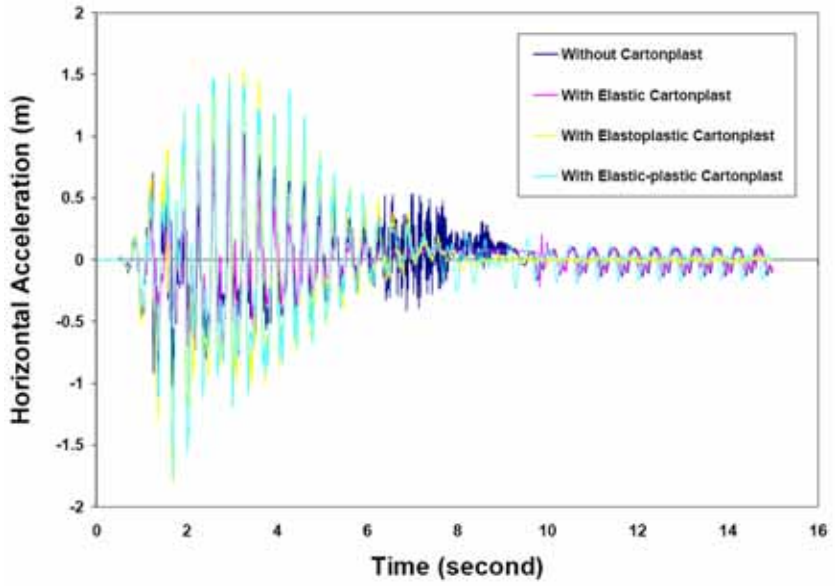

Fig. 2.57 Horizontal acceleration time histories for top of quay wall

Table 2.3 Comparison of computed maximum horizontal acceleration at top of quay wall

	No Mitigation	Elastic Cartonplast	Elastoplastic Cartonplast	Elastic-plastic Cartonplast
Horizontal acceleration (m/s^2)	1.11	1.15	1.7	1.78

(iii) Computed Earth Pressure

In this part a comparison is made between the earth pressures predicted with numerical simulation

for different systems. It is found that cartonplast can reduce the earth pressure on quay wall and can restrict caisson's displacement.

The total dynamic incremental resultant forces acting on quay wall and cartonplast are shown in Fig. 2.58 and 2.59. In Fig. 2.58, the total earth forces in all models are presented and it can be seen that the total force acting on quay wall is reduced by mitigation system about 90 percent. For comparison purposes, the results of total forces acting on quay wall and also cartonplast are summarized in Table 2.4.

Table 2.4 Computed horizontal and vertical displacement at top of quay wall

	No Mitigation	Elastic Cartonplast	Elastoplastic Cartonplast	Elastic-plastic Cartonplast	Reduction Percent (%)
Resultant Total Force acting on quay wall (N)	2.16e6	2.02e6	1.97e6	1.92e6	10
Resultant Total Force acting on cartonplast (N)	-	2.16e6	2.12e6	2.10e6	3

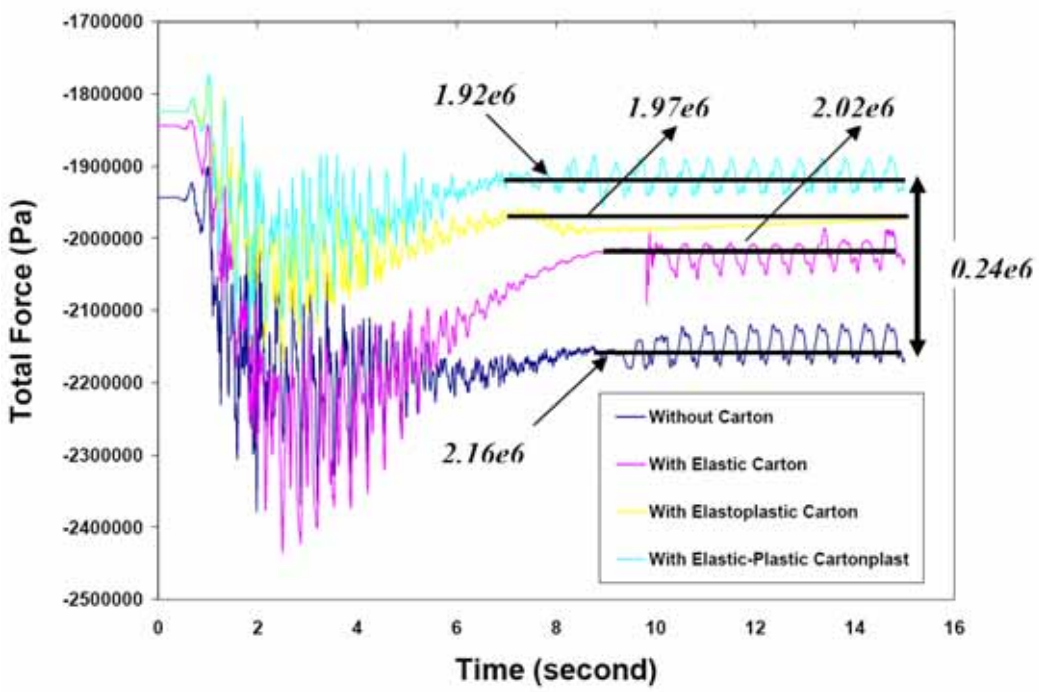

Fig. 2.58 Resultant total force time histories acting on quay wall

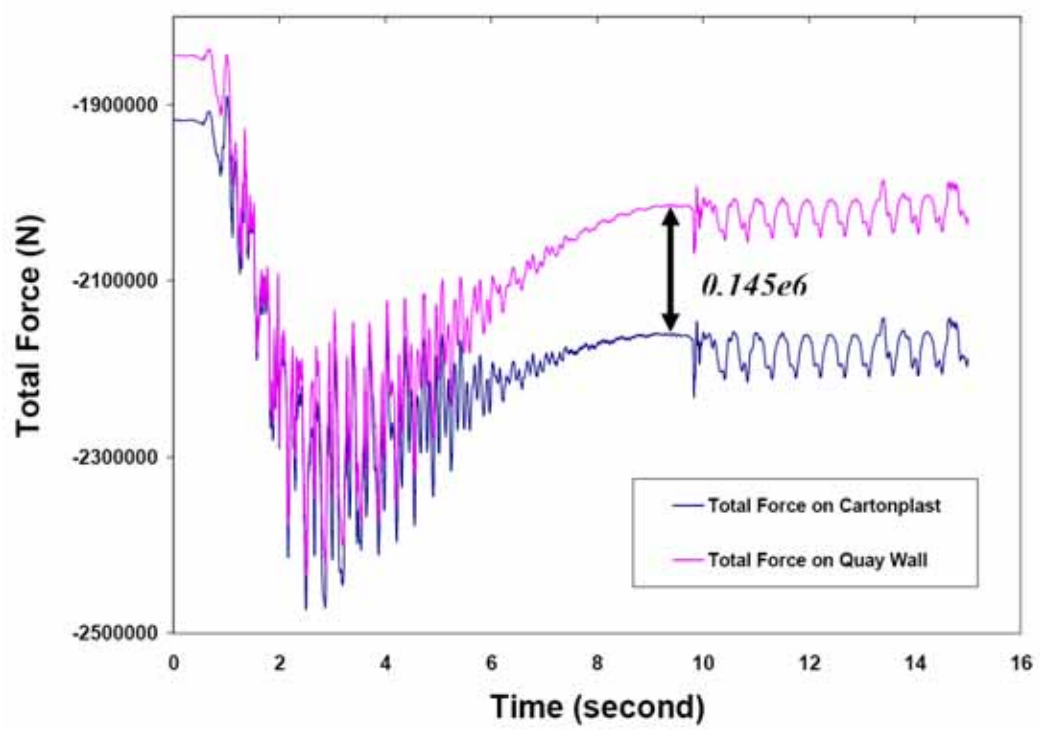

Fig. 2.59 Resultant total force time histories acting on quay wall and elastic cartonplast

2.4 Studies on Embankment

Centrifugal tests were conducted on embankment. The results are presented later together with the related life cycle cost analyses. For details, refer to Sect. 3.3.

The present report shows the state-of-art FE dynamic analysis that is often encountered in design practice. Fig. 2.60 shows a finite element model of a large sandy embankment. The analysis followed the stress variation during the construction of this embankment because the stress state in a nonlinear material such as sand is significantly affected by the stress history. Fig. 2.61 indicates the time history of base basing. The employed stress-strain model can reproduce the variation of secant shear modulus and damping ratio with the strain amplitude as illustrated in Fig. 2.62. Thus, the current practice is able to conduct very advanced analyses. The calculated behavior is illustrated in Figs. 2.63 through 2.66. However, the procedure for determination of relevant soil parameters is time-consuming and is not necessarily supported by experimental data.

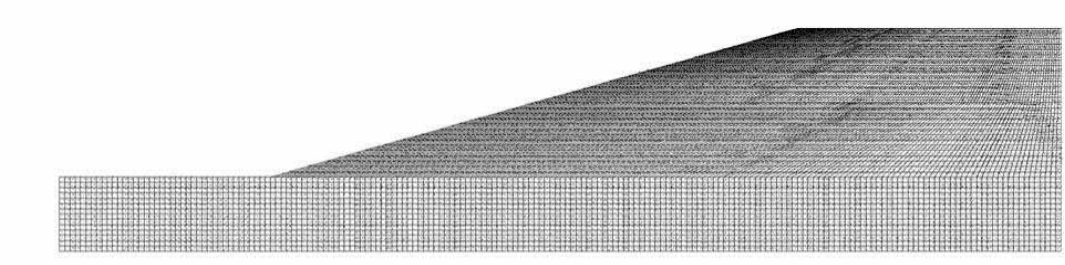

Fig. 2.60 Finite element model of sandy embankment

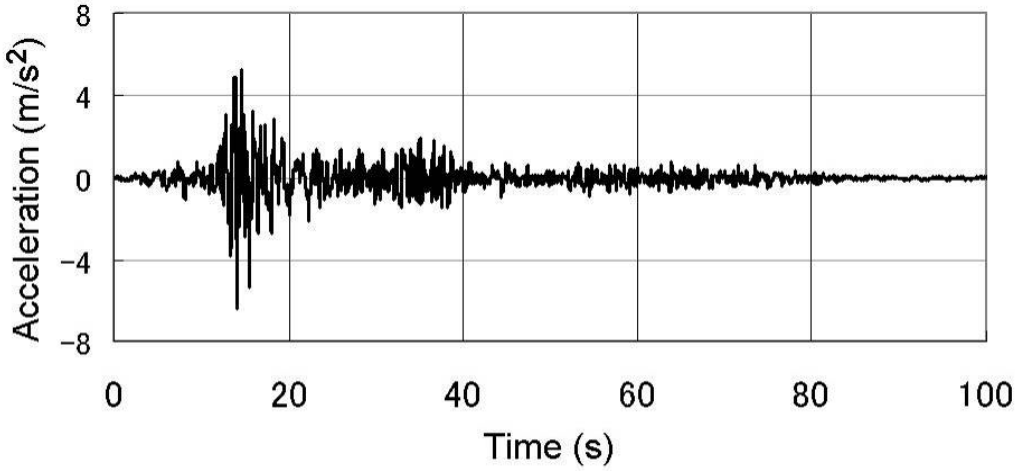

Fig. 2.61 Time history of input acceleration

(a) Loose sand

(b) Medium sand

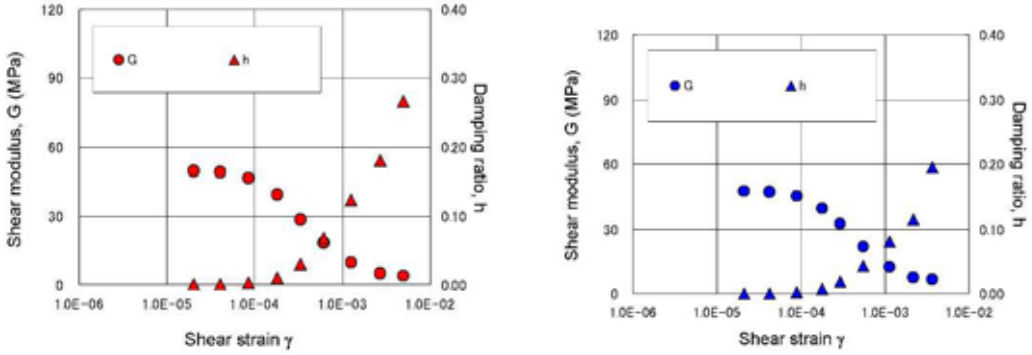

(c) Dense compacted sand

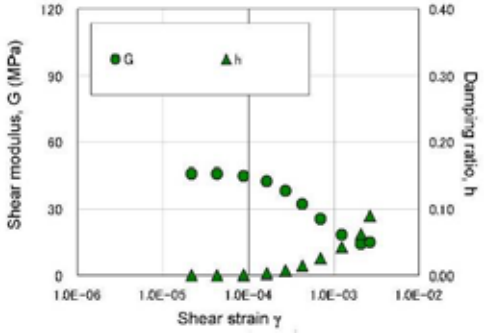

Fig. 2.62 Nonlinear deformation characteristics employed in analysis

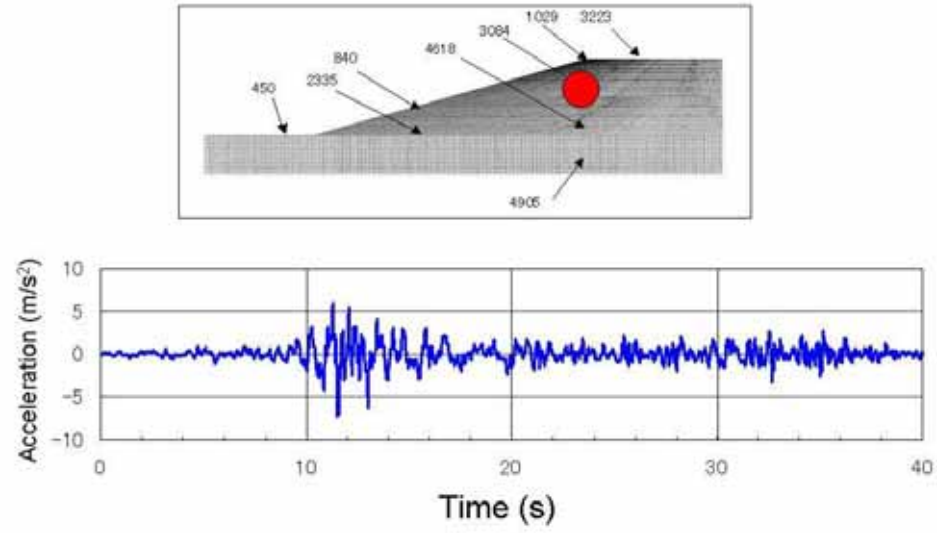

Fig. 2.63 Time history of acceleration at the top of embankment

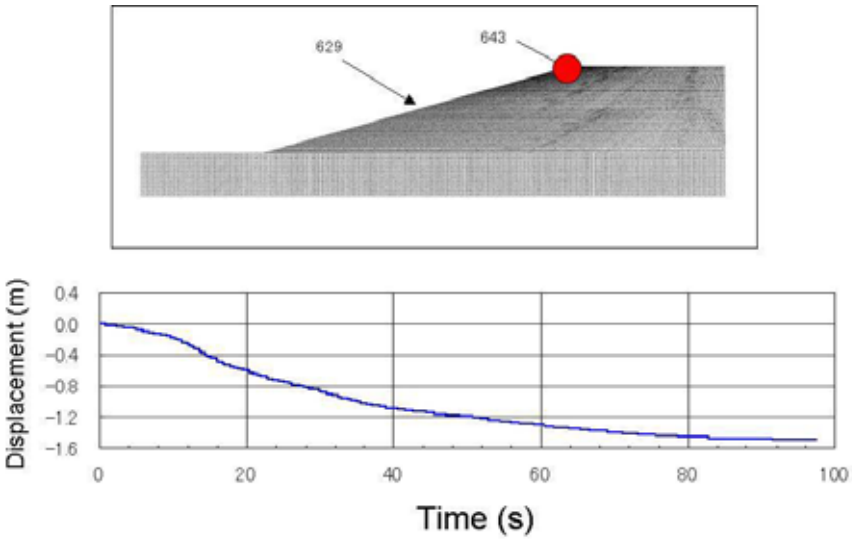

Fig. 2.64 Time history of subsidence at the top of embankment

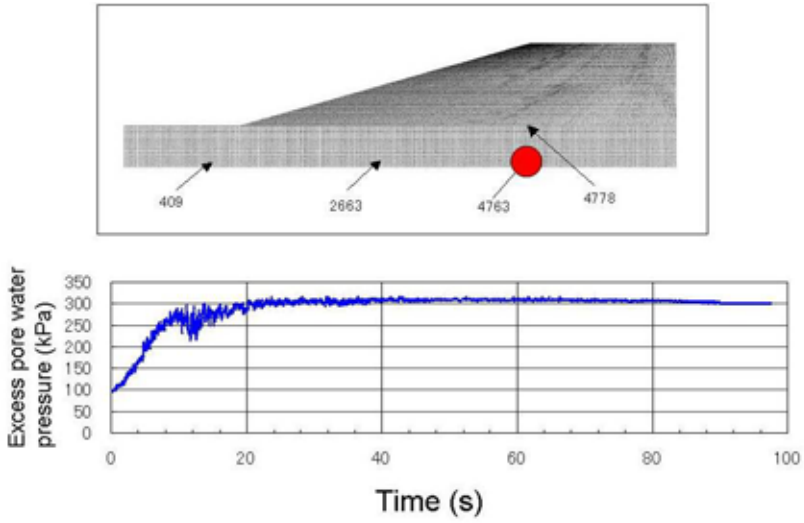

Fig. 2.65 Time history of excess pore pressure development at the bottom of embankment

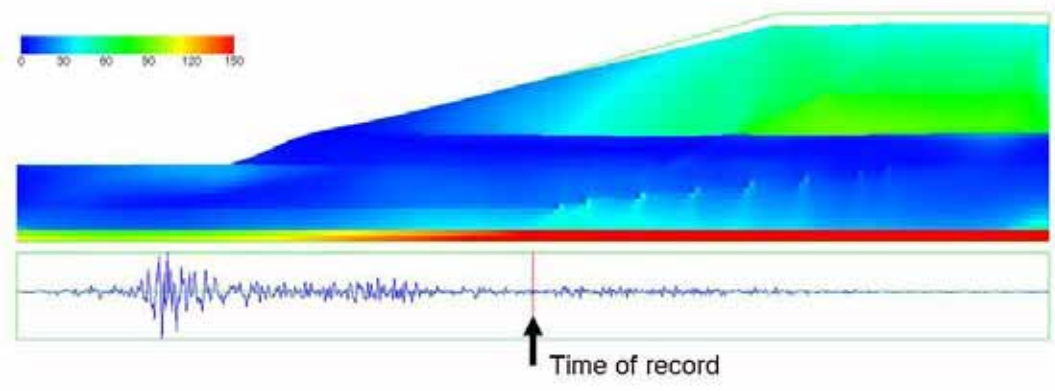

Fig. 2.66 Distribution of excess pore water pressure (Blue shows liquefaction)

3. Trial Designs Based on Seismic-Performance and Life-Cycle-Cost Principles

3.1 Example design of express motorway

3.1.1 Introduction

The structural design code in Japan has changed from a conventional allowable stress design to a limit state design. Moreover, the shift to a performance-based design system, which clearly specifies the performance of a structure, is also at present being considered. The ISO code for earthquake geotechnical engineering (ISO23469, 2004) put a special emphasis on performance based design. The performance of a structure is also important from an economic or financial view point. In recent years, there has been an increasing demand from expressway companies, governments and organizations that manage infra-structures, for cost optimization strategies of design and maintenance of structures during their service life. Usually, construction costs, inspection costs, maintenance costs, user costs, and expected failure costs are included as essential factors for a life-cycle cost (LCC) analysis. During their design working life, structures are exposed to hazards that could lead into unfavorable states and which in turn would lead to negative consequences, in other words, expected failure costs or risk. ISO/IEC Guide 73 (2002) gives a definition that risk is a combination of the consequence of an event and its probability. In this paper, risk is defined as the expected failure cost, which is the product of the consequence in monetary terms and its probability.

The risk corresponding to such events must be maintained under an acceptable level. Any design code prescribes a series of design criteria in the design of structures. These criteria are often based on the target reliability levels which must be predetermined by judging the risk due to the exceedance of the limit states of interest. The concept of LCC minimum provides a basis for codes writers as well as designers to reasonably set the target reliability level. The objective of a LCC-based design is to allocate limited resources optimally for stakeholders such as the general public, local community, individuals, and various organizations. The definition of stakeholder is also given in ISO document (ISO/IEC Guide 73, 2002), which is any individual, group, organization or authority that can affect, be affected by, or perceive itself to be affected by, a risk. Detailed explanations as to the management or assessment of risk are given in several guidelines or books, such as Australian/New Zealand Standards (2004), and Stewart and Melcher (1997).

Structures may be exposed to various possible hazards occurring during their service lives. Representative natural hazards are typhoon and earthquake in Japan. The frequency of failure event caused by a large earthquake is rare yet its consequences are substantial. Seismic risk assessment of buildings or infra-structures has been studied by Takahashi, et al. (2004), Yoshida (2005), and Furuta and Frangopol (2005) among others. However, the considered consequence of a seismic failure event has been limited to restoration cost and economic loss of the owner or has simply been assumed. Moreover, there are problems in LCC approach which are specific to geotechnical engineering,

which will be discussed later on.

In this paper, an example of LCC-based geotechnical design with seismic risks taken into consideration is demonstrated using a hypothetical expressway embankment model. The benefit loss to the public is considered to be the interruption of an expressway. This consequence is modeled by developing a function in terms of subsidence caused by earthquakes. Thus, the risk is estimated on the basis of a continuous limit state, which is namely the magnitude of subsidence.

3.1.2 Conventional Design of Seismic Slope Stability

(1) Model of Embankment

In this paper an embankment of a hypothetical expressway in an area where seismic activity is high is studied. Furthermore, the embankment rests on a soft ground, which requires soil improvement to provide sufficient earthquake resistance. When this type of embankment is connected with a bridge that is supported on a pile foundation and is free of subsidence, the differential settlement between them could be fatal to road transportation (Fig. 3.1). Fig. 3.2 shows the cross sectional view of the embankment model. Design parameters for the improvement consist of the width of the area and the improvement ratio of either sand compaction pile (SCP) or deep mixing method (DJM). Soil properties of the embankment and subsoil are also shown in Fig. 3.2. They stand for soil properties prior to soil improvement. The shear strength of soft subsoil is improved to different extents depending on the improvement ratio. When SCP is practiced, soil properties of sand piles are given by unit weight = 19.0 kN/m^3 and internal friction angle = 37 degrees. When DJM is employed, on the other hand, the undrained strength, C_u, of the grouted soil is assessed by the improvement ratio multiplied by 300 kN/m^2. Fifty design plans were examined for the best choice of soil improvement work, which are illustrated in Fig. 3.3. In this figure, five improvement widths of 0, 5, 10, 15, and 20 m, and two methods of soil improvement, SCP and DJM, were compared. The improvement ratio was also variable, being such as 20, 25, 30, and 35% for SCP, and 20, 30, 40, 50, 60, and 70% for DJM. This brings to a total of fifty design plans.

Fig. 3.1 Differential settlement between road embankment and bridge

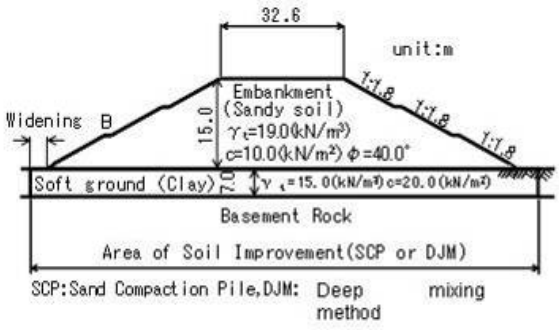

Fig. 3.2 Cross section of embankment model

Costs for the soil improvement work were calculated by using the improvement ratio, volume of improved soil, and the unit price as indicated in Table 3.1. The length of the improvement is assumed to be 100 m. For example, the cost for design plan of SCP with improvement ratio of 30% is estimated in Japanese currency of Yen as 3,700 times the improved soil volume (m^3). The cost for DJM with improvement ratio of 50%, for example, is estimated by 0.5 × 8,000 × the soil volume (m^3). This soil improvement cost is going to be called the initial cost hereinafter.

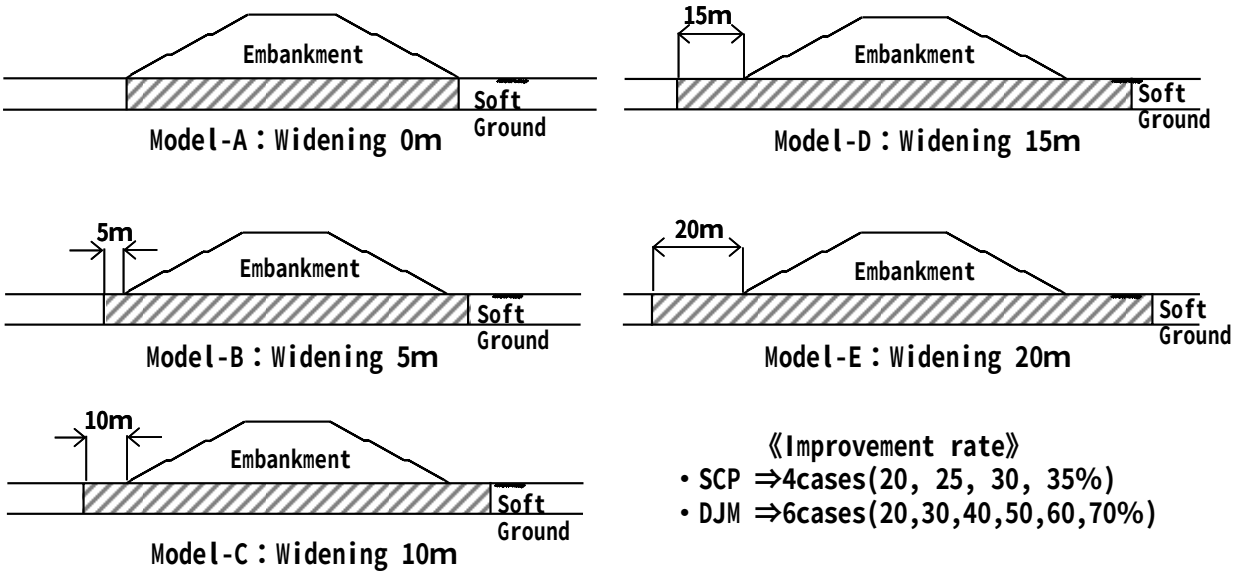

Fig. 3.3 Fifty design plans for soil improvement with respect to improvement width, methods, and improvement ratio

Table 3.1 Unit cost for soil improvement and restoration

Unit: Yen/m^3

Item	Unit cost	
Subgrade Pavement Embankment	2,250 2,280 2,150	
Sand compaction pile (SCP)	Improvement ratio 20% 25% 30% 35%	 2,400 3,100 3,700 4,300
Deep mixing method (DJM)	8,000	

(2) Estimation of Safety Factors and Construction Costs

In order to compare the conventional design with a LCC-based design, the result obtained by conventional design procedure is briefly summarized in this section. A limit state is defined in terms of the safety factor, which is defined as the ratio of the resisting force and the driving force along the sliding surface in conventional design practice. Those forces are calculated following the design procedure (Japan Road Association, 1999). Static lateral force defined by a seismic coefficient is applied to the embankment, and then the safety factor is calculated by using the limit equilibrium of a rigid body, which is known as Fellenius Method. Seismic coefficient of $K_h = 0.16$ is specified by a road design code (Japan Road Association, 1999) at a site that is situated on a base ground type I (firm soil) in the Tokyo Metropolitan Area. The most critical sliding mechanism is detected by a random search, in which slip surfaces are randomly generated and the one with the lowest safety factor is found.

Fig. 3.4 shows the seismic safety factor thus estimated that varies with the initial cost. The safety factor should be greater than 1.0. The design plan of which cost is minimum and safety factor is larger than 1.0 is the case of SCP with no widening and an improvement ratio of 20%.

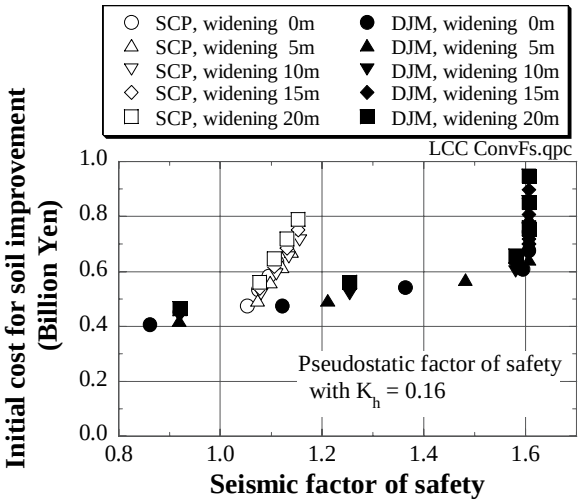

Fig. 3.4 Seismic safety factor estimated by conventional design procedure and its initial cost (improvement cost)

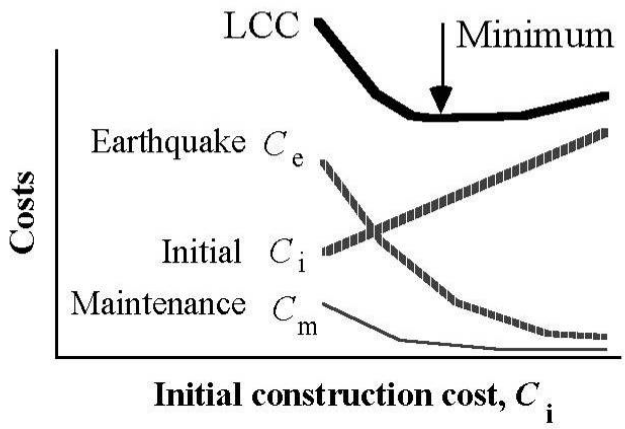

Fig. 3.5 Conceptual illustration of life cycle cost

3.1.3 Basic Principles in LCC-Based Design of Soil Improvement

(1) General Remarks

The life cycle cost is conventionally defined as the total monetary cost that consists of the initial construction cost (C_i), the maintenance cost (C_m), and the seismic risk cost (C_e):

$$LCC = C_i + C_m + C_e \qquad (3.1)$$

The maintenance and seismic costs are assessed over the entire life (service period) of a concerned structure. It is supposed that a design option that minimized LCC is the most optimal design. As Fig. 3.5 illustrates, the greater initial construction cost would improve the quality of a structure, and hence reduce both maintenance and seismic risk costs.

Although this idea is easy to understand for most types of structures, the life period of a geotechnical structure cannot be determined clearly. There are dikes and road embankments that have been in service for hundreds of years or longer, for which the life is not clearly defined. To cope with this problem, the authors visited governments and authorities which are in charge of the maintenance of dikes and embankments. It was first found that most part of the maintenance cost is spent on cutting grasses, inspection of drainage pipe, and similar business that have nothing to do with the construction quality. Moreover, although it was initially expected that good quality of construction would reduce later subsidence of embankments and its restoration cost, it was found that road pavement is repaired not only due to subsidence but also due to weathering and abrasion. Similarly, the height of a river dike is raised not because of the subsidence but for improving the quality of regional flood disaster mitigation. Consequently, it was decided in the present study to eliminate the maintenance cost from the current study. This does not affect the conclusion of this

study, because the maintenance cost is smaller than the seismic risk, as will be presented later, and also because the maintenance cost is independent of the construction cost, without affecting the choice of the soil improvement option. This is considered to be a characteristic of geotechnical structures except very extreme situations. It seems, in contras, that maintenance efforts of concrete and steel structures depend on the quality of initial construction, and therefore, their LCC calculation requires maintenance cost to be considered.. The life of geotechnical structure is assumed to be 80 years, furthermore. After this time period, the life style of people and public demand would change completely and the value of the original structure would be lost. Finally, the initial cost in this paper designates that for soil improvement only. This is because the construction cost for an expressway embankment is independent of the choice of soil improvement. The seismic risk is a product of monetary consequence and its probability, namely expected failure cost. The design plan is determined from the viewpoint of minimum LCC among the above fifty design cases in a LCC-based design.

(2) Consequence of Earthquake Effect

Details of seismic cost (C_e in Eq. 3.1) or scenario consequence due to failure of an embankment are going to be described. For clarity, the present paper employs an embankment of expressway resting on cohesive subsoil that is adjacent to a bridge and is subject to differential subsidence upon a strong earthquake. The consequence includes damage of structures, loss of functionality, human injury and death, and economic loss caused by the failure of a particular structure that concerns stakeholders. It is assumed that a strong earthquake causes subsidence or dip in an expressway embankment (Fig. 3.6), which in turn leads to traffic accidents and interruption for a certain period. Injury, loss of human life, and restoration cost of the structure are classified as direct loss, whereas economic loss caused by the expressway interruption is called indirect loss.

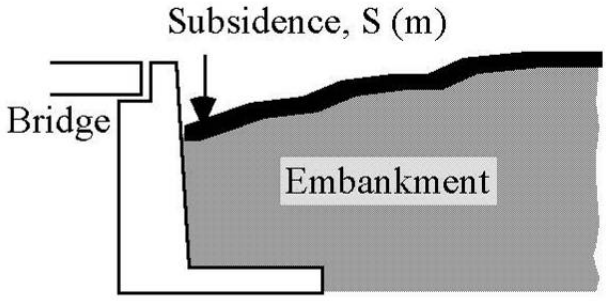

Fig. 3.6 Subsidence of embankment adjacent to bridge abutment

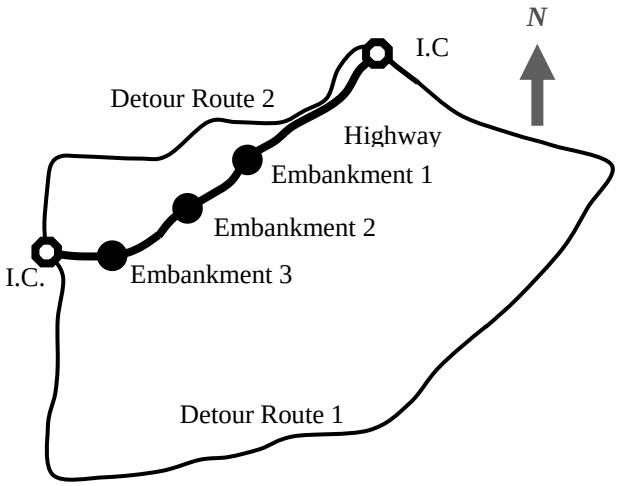

Fig. 3.7 Investigated routes of expressway and detours

The expressway embankment discussed in this paper is hypothetical. However, in order to have a realistic numerical example, real traffic volume and other data were utilized. These data were taken from the Tomei expressway between Atsugi and Yokohama-Machida Interchanges. Note that the Tomei expressway is a part of the nation's No.1 expressway connecting Tokyo and Osaka. Hence, it is a good example to investigate the economic indirect loss upon a strong earthquake. Fig. 3.7 shows the expressway and local routes for detour. There are three embankments in the studied section. Hence, the following cost calculation concerns three critical embankments. The traffic volume of the expressway and assumed detour routes are summarized in Table. 3.2. Table 3.3 shows the traffic volume of detour routes when the expressway is interrupted. The traffic volumes after the interruption are estimated by traffic flow analyses, assuming that all the interrupted traffic of the expressway takes either route 1 or 2.

The present study employs the subsidence of the top of the expressway embankment as an index for the extent of seismic effects. In particular, the subsidence, *S*, at an interface between cut and fill or between fill and a bridge abutment (Fig. 3.6) may cause car accidents if it is significant. In accordance with the practice by Railway Technical Research Institute (2003), the subsidence was calculated by using the Newmark rigid block analogy (Newmark, 1965) on the cross section in Fig. 3.2 in which a gigantic earthquake of magnitude = 8 in the tectonic subduction zone and an inland one of magnitude = 7 at a shorter epicentral distance were employed (Fig. 3.8). Since the intensity and occurrence of these earthquakes are of probabilistic nature, the calculated subsidence was probabilistic as well.

Both direct and indirect losses are modeled as a function of subsidence. The estimated consequences are restoration, human, detour, traffic accident and environmental losses which are summarized in Table 3.4. The first two are direct losses while the rest are indirect losses. Details of

these losses are described in the following chapters.

Table 3.2 Traffic volume without interruption of expressway

	Traffic volume (cars/day)				
	Automobile	Bus	Van	Truck	Total
Expressway	59,600	1,289	11,091	48,699	120,679
Detour route 1	38,191	401	8,820	17,077	64,489
Detour route 2	27,233	206	7,489	7,594	42,522

Table 3.3 Traffic volume after the interruption of expressway

	Traffic volume (cars/day)				
	Automobile	Bus	Van	Truck	Total
Expressway	0	0	0	0	0
Detour route 1	92,069	1,566	18,846	61,101	173,582
Detour route 2	32,955	330	8,554	12,269	54,108

Table 3.4 Considered Losses in LCC estimation

Direct	D1: Human Loss D2: Restoration Cost	Traffic accident due to failed embankments Restoration of failed embankments
Indirect	D3: Detour Loss D4: Environmental Loss D5: Traffic Accident Loss D6: Toll Loss	Economic loss due to extension of time and distance Emission of CO_2, NOx, Noise Traffic accident due to the traffic congestion in detour route Missing toll of expressway

(1) Inter-plate earthquake of magnitude 8

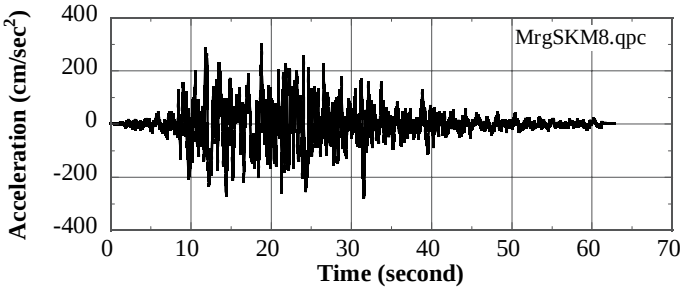

(2) Earthquake of magnitude = 7 caused by inland crustal, intra-plate, and smaller inter-plate mechanisms

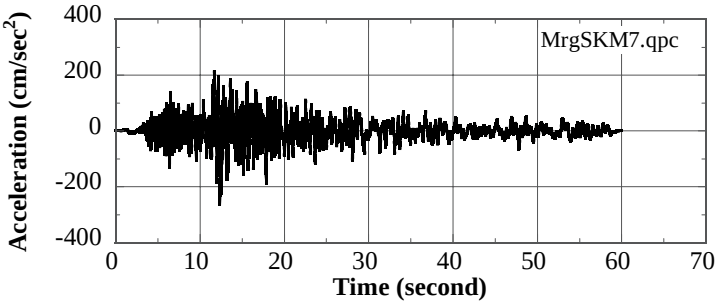

Fig. 3.8 Input seismic motions for dynamic analyses

3.1.4 Calculation of Direct Losses

Human loss/injury and restoration cost are evaluated in what follows. First, in cost-benefit analyses, monetary value must be determined for human life and injury, often causing great controversy. This human loss is caused by car crash at a significant subsidence. Human life is conventionally assumed to be 31.5 MY (million Yen) per person in cost-benefit analyses for road investment in Japan. However, this value is much lower than real loss in the bereaved family. It is also very small as compared with those in other nations: see Fig. 3.9.

One of the reasons for the difference is the way of calculation. In the previous Japanese method, the life cost calculation is based on the missing income during the rest of life. This generally leads to lower costs. Conversely, the GNP-based method calculates the life cost of a person by dividing the total product by population. For example, ICAF (Rackwitz, 2002 and 2004) calculated with statistics in 2004 to give 247 MY in US, 226 MY in UK, and 238 MY in Japan. Considering these figures, the present study employs 200 MY/person.

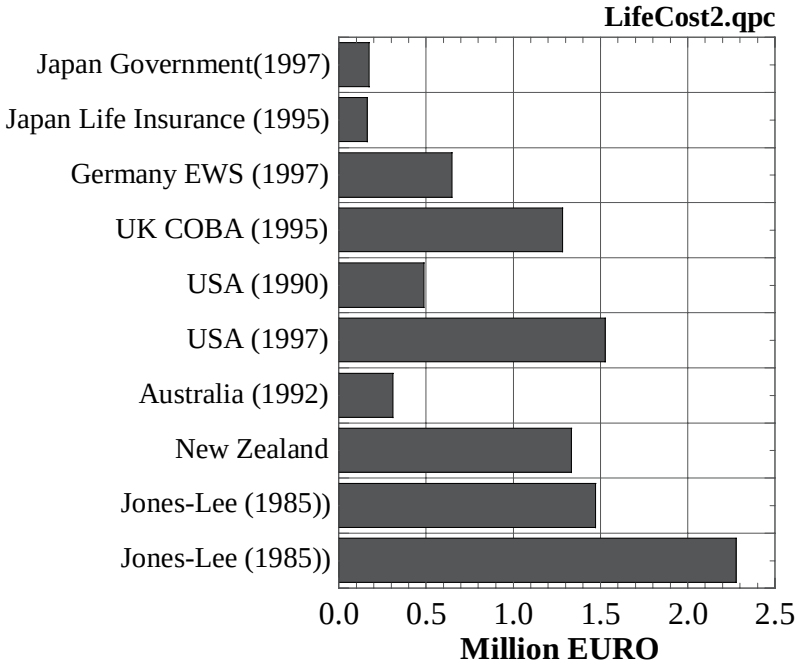

Fig. 3.9 Costs of human life in different nations (after Jones-Lee, et al., 1985).

The human loss is calculated by Eq. 3.2 in this study.

$$D_1 = 0.5YP, \quad Y = 189.8S^2 + 10.7S - 0.5 \text{ (million Yen)} \tag{3.2}$$

where Y stands for the mean human loss per person, being inclusive of life loss as well as heavy and light injuries. This equation was derived by assuming that the human loss is equivalent to human life loss when subsidence S is 1.0 m, 70% of human life loss when S is 0.5m, and 0% when S is 0.03m.

P is the number of passengers in all the vehicles involved in a possible car crash at the seismic subsidence. Since the present study assumes that vehicles that cannot stop before the subsidence is involved in the accident, P is a function of the number of traffics in the expressway (Q / hour in Table 3.2), vehicle velocity, V (km/sec), and the mean number of passengers per car (p):

$$P = \frac{Q}{1000 \times V} \times p \times B(V) \tag{3.3}$$

It is hypothesized that the average car velocity is V = 80 km/h and cars need B = 80 m to stop completely. Those cars within 80 m from the subsidence are involved in a crash to different extents, depending on the final velocity. The number of passengers per car (p) is set equal to 1.5, considering 1.44 on weekdays and 2.01 on weekends/holidays (Public Works Research Institute, 2004). The coefficient 0.5 in Eq. 3.2 accounts for the difference of crash severity because some vehicles near a

subsidence cannot reduce the speed, while others at a greater distance can reasonably slow down before crash. See Fig. 3.10 for variation of human cost with *S*.

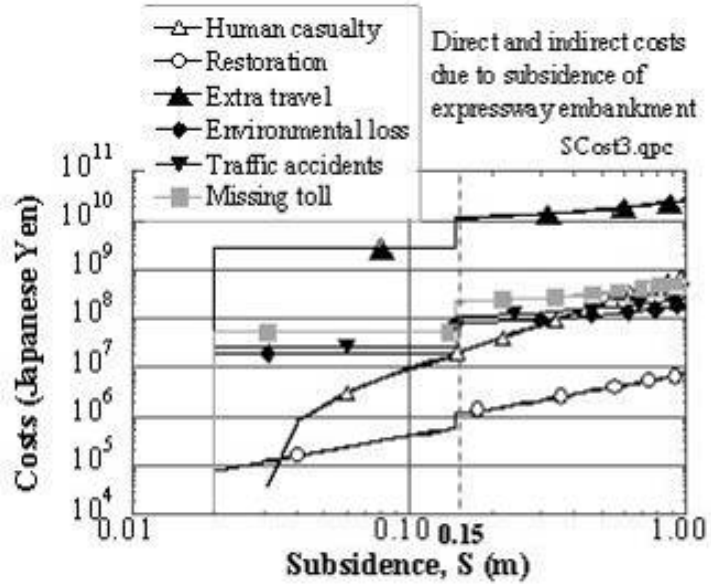

Fig. 3.10 Failure costs model costs based on subsidence of expressway embankment

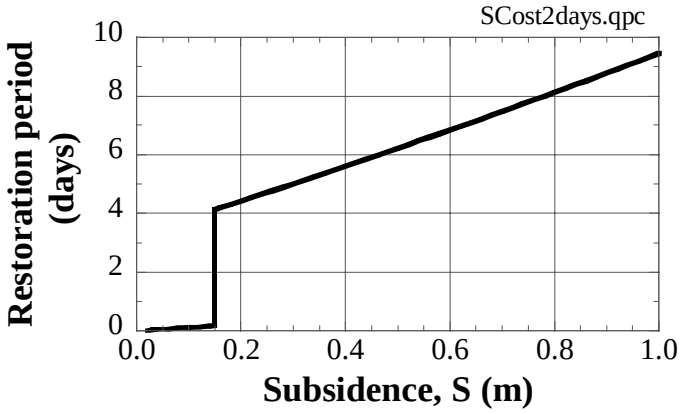

Fig. 3.11 Expected restoration time changing with subsidence

Restoration cost is calculated using the following simple equation;

$$D_2 = 1.3\sum_i 25\, S\, W H_i C_i \qquad (3.4)$$

where *S* is the subsidence caused by an earthquake (m), *W* the width of the expressway (m), H_i the depth of a material *i* for restoration construction, C_i the unit price of the material *i*, and 1.3 a

coefficient for consideration of overhead cost. The length of the restored road is assumed to be 25 S (m) so that the surface slope after restoration would be reduced to 4 %. Furthermore, when the subsidence is less than 0.15 m, the overlay method is adopted. In contrast when the subsidence exceeds 0.15 m, the damaged pavement is removed, the embankment is reconstructed, and the road is newly paved. Discontinuity at S = 0.15 m is seen in Fig. 3.11 due to the differences of the restoration method. The threshold to minimum damage state is assumed to be 2 cm because of the 5 m thickness of the very surface asphalt pavement. The obtained restoration loss is illustrated in Fig. 3.10. Finally, on the basis of experiences of similar restoration works, the restoration time, which is the traffic interruption time, was assessed as illustrated in Fig. 3.11.

3.1.5 Calculation of Indirect Loss

It is assumed that there are three embankments as shown in Fig. 3.7 and their seismic fragilities are the same for simplicity. If any of the embankments fails, expressway traffic is interrupted. The interruption period, T, in days was assessed as shown in Fig. 3.11.

The traffic from the interrupted expressway causes traffic congestions in detour routes (Fig. 3.7) and the travel time is elongated. This time elongation is one of the indirect losses and is designated by D_3. It obstructs the economic activities, and increases fuel consumption. This loss is evaluated by

$$D_3 = \sum_i \sum_j (Q_{ij} C_{ij} - Q'_{ij} C'_{ij}),$$
$$C_{ij} = t_i a_j + l_i b_j, \quad C'_{ij} = t_i' a_j + l_i b_j \tag{3.5}$$

where, D_3 stands for the detour loss per day (Yen/day), Q'_{ij} and Q_{ij} the number of vehicles per day of vehicle type j on the route i before and after interruption of the expressway, C'_{ij} and C_{ij} the general expense before and after interruption, t *and* t' the travel time (minutes) before and after interruption, a_j the time value of vehicle type j, l_i the link length (km) of route i, and b_j the driving expense of vehicle type j. Details of economic loss estimation procedure is described in many cost-benefit manuals. Note that D_3 and the following indirect losses are multiplied by the interruption period, T, in Fig. 3.11 to determine the entire indirect loss.

The environmental loss, D_4, is the monetary loss due to the increase of CO_2 and NO_x emission and the traffic noise level. It is noteworthy that these problems decreases along the interrupted expressway, while they increases along detour routes where traffics increase. The estimated environmental loss based on a guideline by Research Committee on Assessment of Investment on

Road (1998) is demonstrated in Fig. 3.10.

The traffic congestion in detour roads increases the number of traffic accidents, while it disappears in the interrupted expressway. The traffic accident loss, D_5, in the monetary loss was assessed by the aforementioned guideline as seen in Fig. 3.10.

Finally, the missing toll of the expressway, D_6, was calculated by using the number of daily traffics under normal conditions and the toll money particularly concerning the interrupted section of the expressway.

$$\mathrm{D}_6 = \frac{\mathrm{Q}_\mathrm{p} \times l_p}{\sum_k \mathrm{Q}_\mathrm{k} \times l_k} \times \mathrm{f} \quad (Yen\ /\ day) \qquad (3.6)$$

in which Q_k and l_k stand for the daily traffics and length of expressway section "k", while Q_p and l_p designate those in the interrupted section. Moreover, f is the daily toll income of the entire expressway. Consequently, the result is shown in Fig. 3.10. In spite of the calculation shown above, the relevancy in including the missing toll is controversial. It is also considered that the missing toll is a loss to the highway authority alone, creating no loss to the regional and national economies. When the indirect loss to the national economy is interested in as is the present case, this loss may have to be eliminated from the LCC calculation. Although this opinion deserves attention, the present study includes the missing toll. This would not affect the final conclusion because the toll loss is much smaller than the aforementioned detour loss.

In conclusion, it is evident in Fig. 3.10 that the indirect loss concerning the elongated travel time is the most significant component. The entire earthquake cost is obtained by adding all the components in Fig. 3.10 and is denoted by $D_\mathrm{e}(S)$ in what follows.

3.1.6 Probabilistic Calculation of Seismic Cost

As was mentioned above, the present study is based on a probabilistic consideration of the design input earthquake, and consequently, the subsidence, S, in the previous chapter is of probabilistic nature. It is aimed therefore in this chapter to calculate the seismic cost in a probabilistic manner as well. The probabilistic nature of subsidence, S, which is termed limit state in this section is estimated by 1) seismic hazard analysis, 2) fragility analysis, and 3) estimation of limit state probability

(1) *Seismic Hazard Analysis*

A seismic hazard curve defines the probabilistic nature of an index that expresses the intensity of an expected earthquake. The peak ground acceleration is frequently employed as this index. Annaka and Yashio (2000) proposed a probabilistic model, which consists of a seismic source model and an attenuation model which was developed on the basis of records obtained by the JMA-87 strong motion accelerometer network of the Japan Meteorological Agency (JMA). Note that Tokyo Metropolitan Area is a region of high seismicity, where large inter-plate, intra-plate, and inland crustal type earthquakes occur frequently.

The present study requires a time history of seismic acceleration to be defined because the subsidence of an embankment is calculated by the Newmark (1965) analogy. Hence, many earthquake motions have to be employed with varying type of earthquake, epicentral distance, and magnitude (M). Sensitivity analyses on the seismic hazard in the concerned region, however, suggests that the most influential earthquakes are the inter plate type of M = 8 class and the one with M = 7 class at a short epicentral distance. Accordingly, two seismic hazard curves are constructed.

Response spectra were developed for both earthquake types by the model of Annaka and Nozawa (1988), which is an attenuation model of response spectra constructed from the observation data set in Tokyo metropolitan area. Then time histories of two artificial earthquake motions are made so that they may be compatible with the given response spectra. Phase spectra of an observed earthquake motion with its epicentral distance and magnitude similar to the target earthquake was used to generate the artificial earthquake motions. The hazard curves and corresponding earthquake motions are shown in Figs. 3.12 and 3.8, respectively. Note that these two design motions are of different frequency components because of their different earthquake magnitudes. Moreover, the hazard curve, F_h(a), demonstrates the probability that the peak acceleration of a is exceeded in reality within a unit time. By using the probabilistic density function, $f_h(a)$ for a,

$$F_h(a) = \int_a^\infty f_h(a)da \tag{3.7}$$

More precisely, this curve gives the probability of exceedance during the life period of n = 80 years. It is hence given by using an annual probability of exceedance, $F_h^1(a)$:

$$F_h(a) = 1 - \left\{1 - F_h^1(a)\right\}^n \tag{3.8}$$

Note that there are two hazard curves, F_{h1}(a) and F_{h2}(a), because two kinds of design earthquakes are employed. Moreover, the discount ratio is assumed to be zero, which means that the amount of loss is independent of the year of earthquake occurrence.

(2) *Fragility Analysis*

The seismic fragility is also a key ingredient of seismic risk assessment, describing the conditional probability of failure as a function of seismic intensity. A fragility curve shows the probability of seismic consequence exceeding the limit state value for a given seismic intensity. In this study, the peak ground acceleration (a) is employed as the seismic intensity index.

The present study focuses on the subsidence of an expressway embankment, S, induced by earthquakes, and limit states are defined in terms of S. The following discussion addresses the probability that S exceeds an example limit state of $S = S_r = 0.5$ m. The fragility, $F_f(a)$ is defined by

$$F_f(a) = \int_0^{R_r} f_f(r)dr \tag{3.9}$$

in which $f_f(r)$ stands for the probabilistic density of resistance, r, against subsidence or deformation, and R_r is the resistance that generates the subsidence exactly equal to S_r. Evidently this resistance varies with the acceleration, a. See Fig. 3.13 for an example.

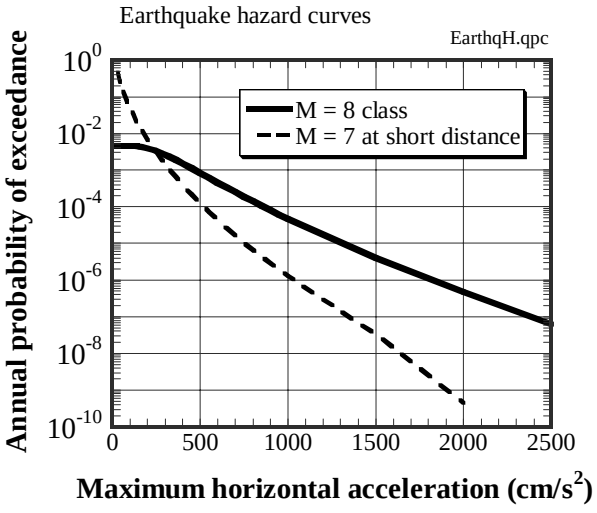

Fig. 3.12 Seismic hazard curves for two kinds of design earthquakes

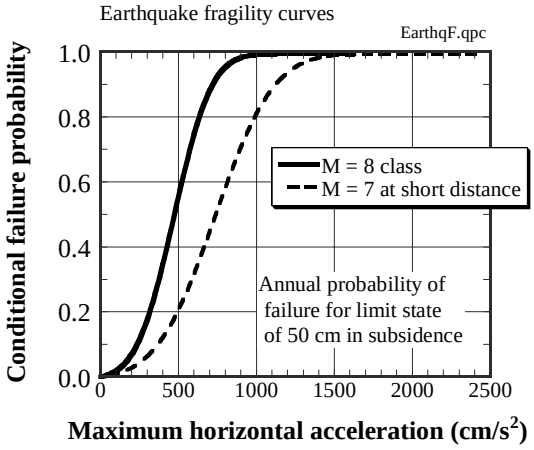

Fig. 3.13 Examples of fragility curves for limit state of 50-cm subsidence

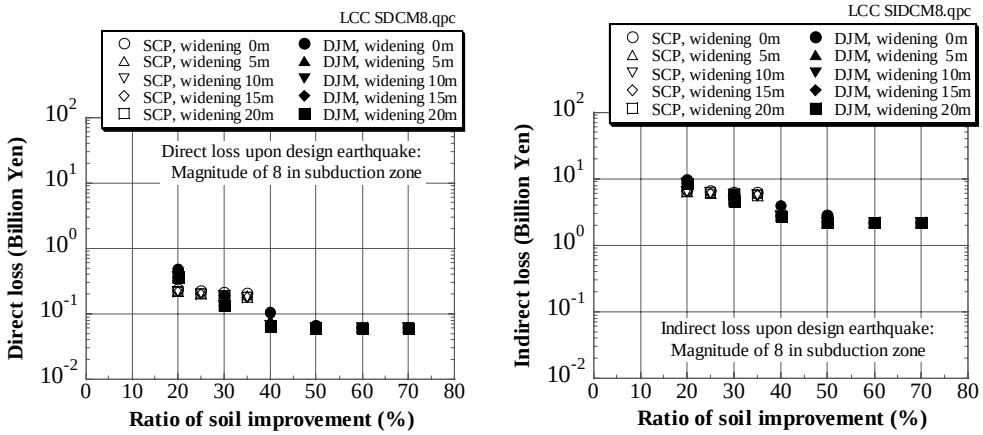

(1) Direct cost (2) Indirect cost

Fig. 3.14 Seismic risk due to M8-type earthquake

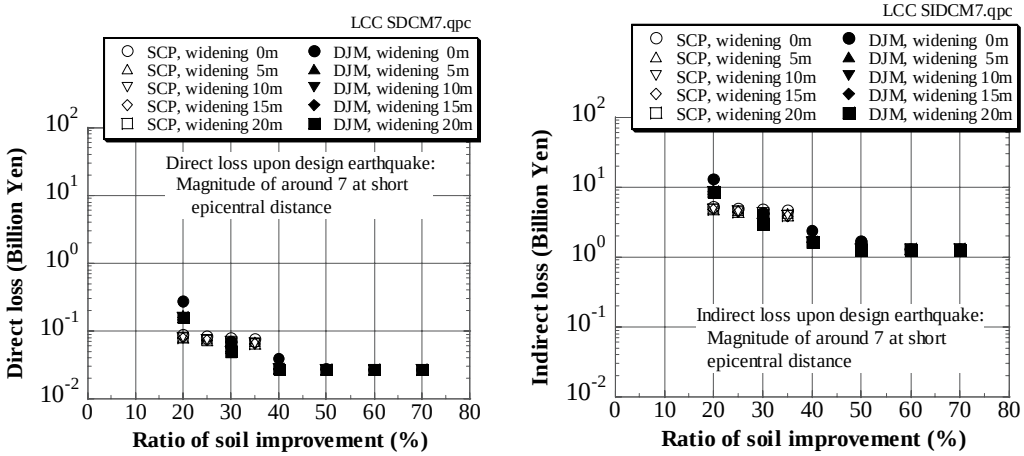

(1) Direct cost (2) Indirect cost

Fig. 3.15 Seismic risk due to earthquakes of M=around 7 at short epicentral distance

While subsidence, S, is calculated by the Newmark rigid block analogy, the state of $S > S_r$ is considered to be damage. In principle, subsidence is affected by such uncertain factors as types of earthquakes (j = 1 or 2), the peak acceleration (a), and parameters of $\boldsymbol{x}$ that represent local conditions (soil and geometry). It is, however, believed that the uncertainty in ground motion is more significant than the effects of all other uncertainties (Celik and Ellingwood, 2007). This suggests that a variation of fragility is relatively insignificant.

It is important in the present study to take into account many kinds of uncertainty involved in material properties of soils, modeling, etc. Consequently, fragility curves are assumed to follow a lognormal distribution. Coefficient of variance (COV) of the distribution is assumed to be 0.4. Although the authors examined the consequence of COV = 0.3 and 0.5, the obtained LCC was similar. The median value of the lognormal distribution is given by the peak acceleration (a) at which the estimated subsidence, S, is equal to the prescribed S_r.

Fig. 3.13 presents two fragility curves for the limit state subsidence of S_r = 50 cm. They correspond to two different seismic motions. The significant difference between them comes from the fact that the earthquake motion of M = 8 class has a longer duration time and greater low frequency components, generating greater seismic displacement.

(3) *Estimation of Seismic Risk for Expressway Model*

The probability of failure is calculated by using the hazard and fragility curves discussed above for which two types of earthquakes are considered. The probability of subsidence exceeding S (= 0.5 m for example) is given by

$$P(S) = \sum_{j=1}^{2} \int_0^{\infty} f_{hj}(a) \int_0^{R_r} f_{fj}(r)\, dr\, da \tag{3.10}$$

as a summation for two types of earthquakes. By changing the order of integration,

$$\begin{aligned} P(S) &= \sum_{j=1}^{2} \int_0^{\infty} f_{fj}(r) \int_a^{\infty} f_{hj}(\eta)\, d\eta\, dr \\ &= \sum_{j=1}^{2} \int_0^{\infty} F_{hj}(a) \frac{\mathrm{d}F_{fj}}{\mathrm{d}a} da \end{aligned} \tag{3.11}$$

The seismic cost, C, is determined by integrating the product of the probabilities and its consequences. Since P(S) is a probability of exceedance,

$$C = \int_{S_{min\,imum}}^{\infty} \left(-\frac{\mathrm{d}P}{\mathrm{d}S} \right) D_e(S) dS = \left[-P\, D_{\mathrm{e}} \right]_{S_{min\,imum}}^{\infty} + \int_{S_{min\,imum}}^{\infty} P \frac{\mathrm{d}D_e}{\mathrm{d}S} dS \qquad (3.12)$$

Since P (probability of exceedance) is null at $S = \infty$ and D_{e} is null at the minimum subsidence, the first term in Eq. 3.12 vanishes. Accordingly,

$$C = \int_{S_{min\,imum}}^{\infty} P \frac{\mathrm{d}D_e}{\mathrm{d}S} dS \qquad (3.13)$$

The indirect cost is related to the interruption of the expressway that occurs when any of the three embankments in Fig. 3.7 collapses. On the other hand, the direct cost is related to the failure of each embankment. Therefore, the seismic risk C_{e} is determined by

$$C_e = C^{in} P\left(\bigcup_{i=1}^{3} E_i \right) + \sum_{i=1}^{3} \left(C^{d} P(E_i) \right) \qquad (3.14)$$

where C^{in} is the indirect cost, E_i designates a failure event in embankment i, and C^{d} is the direct cost of a single embankment.

(4) *Detailed Calculation*

In an ordinary approach, several limit states are defined, and then a fragility curve is developed to describe the probabilities that a structure exceeds each defined limit state when subjected to a specific seismic intensity level. The present study, in contrast, takes a different way in which limit state is continuous. This implies that the subsidence of S in the cost calculation is not a discrete variable but a continuous variable as illustrated in Fig. 3.10. By combining equations so far presented, the seismic risk C_e is calculated by assuming continuity in limit state,

$$C_e = \sum_{j=1}^{2} \int \int \frac{dC^{in}(s)}{ds} F_{hj}(a) \frac{dF_{fj}^{in}(a|s)}{da} da\, ds$$

$$+ \sum_{j=1}^{2} \sum_{i=1}^{3} \int \int \frac{dC_i^{d}(s)}{ds} F_{hj}(a) \frac{dF_{fij}^{d}(a|s)}{da} da\, ds \qquad (3.15)$$

in which $F^{in}_{fj}(a|s)$ and $F^{d}_{fij}(a|s)$ designate indirect and direct fragility curves for a limit state defined by subsidence *S*. Moreover, $C^{in}(s)$ and $C^{d}(s)$ are indirect and direct losses at subsidence of *S*, respectively. The indirect loss in the first term occurs if one of the three critical embankments is damaged, and, in contrast, the direct loss in the second term is calculated for each of the critical embankments separately (i = 1, 2, and 3). $F_{hj}(a)$ stands for a seismic hazard curve for a seismic event of type j and F^{d}_{fi} denotes a fragility curve for indirect loss, which is the fragility against failure of any of the three embankments, while F^{d}_{fi} expresses the fragility of an individual embankment *i*. The first and second terms in Eq. 3.15 indicate indirect and direct risk, respectively. It is assumed that seismic forces at the three sites are perfectly correlated, and fragilities of the three embankments are independent. The fragility for indirect loss is expressed with the fragility of each embankment:

$$F^{in}_{fj}(a|s) = 1 - \prod_{i=1}^{3} \left(1 - F^{d}_{fij}(a|s)\right)^{3} \tag{3.16}$$

Hazard curves in Fig. 3.12 show annual probability of exceedance. In order to estimate failure probability during *n* years, the annual hazard curve F^{1}_{hj} is transformed as follows:

$$F_{hj}(a) = 1 - \left(1 - F^{1}_{hj}(a)\right)^{n} \tag{3.17}$$

In the risk estimation below, working period or the life cycle is assumed to be 80 years.

3.1.7 Remarks on Calculated Life Cycle Cost

Seismic risks were calculated on all of the fifty design cases in Fig. 3.3. Figs. 3.14 and 15 present the estimated risk for a design earthquake of magnitude (M) = 8 and the other with smaller magnitude . It is noteworthy therein that the risk of indirect loss is remarkably greater than that of direct loss. This indirect loss will later make the LCC consideration meaningful. It should be understood, therefore, that those structures with less economic importance are not appropriate for LCC-based design. In Figs. 3.14 and 3.15, moreover, at high improvement ratio, the risk that associates the M=8 quake is greater than that of lower magnitude because large seismic intensity of the former quake is able to induce damage. Fig. 3.16 reveals the total seismic risk, concerning two types of design earthquake, and the initial cost. The high ratio of subsoil improvement is able to reduce the seismic

risk significantly, while it generally increases the initial cost needed for improvement. The seismic risk is nearly constant in the range of high improvement ratio, because, in this situation, the slip plane as employed by the Newmark sliding analysis occurs within the embankment and is not affected by further improvement in the subsoil. For this reason, the extent of SCP in excess of 40% does not affect the seismic risk.

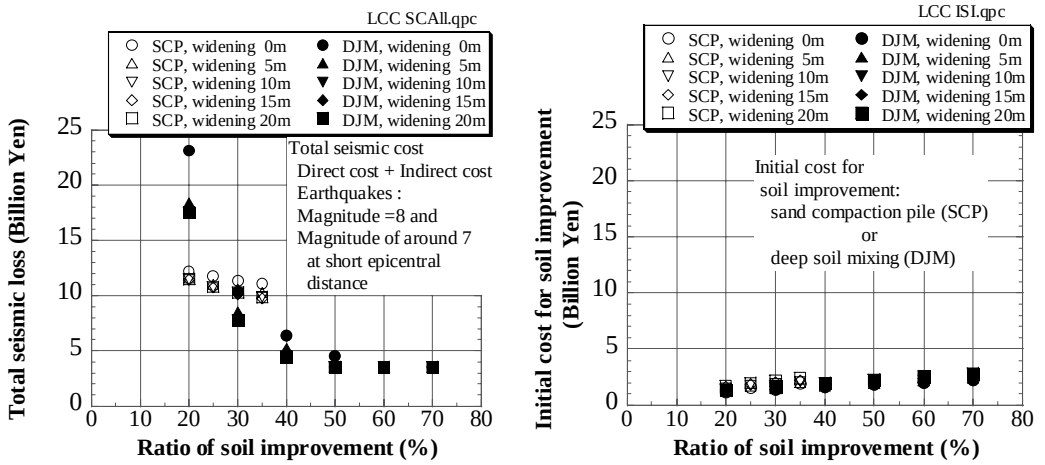

(1) Total seismic risk (2) Initial cost

Fig. 3.16 Total seismic risk and initial cost

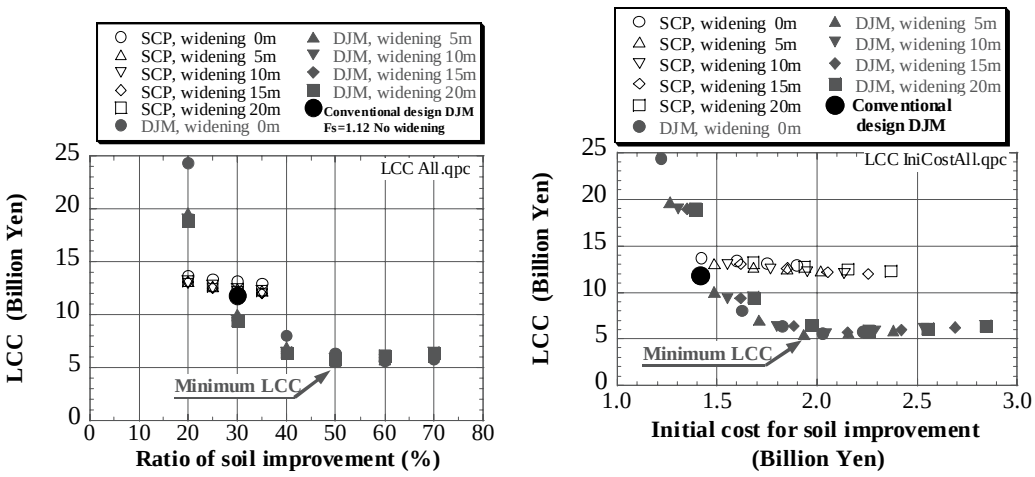

(1) LCC vs. improvement ratio (2) LCC vs. initial cost

Fig. 3.17 Comparison of LCC for all design alternatives

LCC is defined as the sum of initial cost and seismic risk. The estimated LCC values for all the cases are indicated in Fig. 3.17. In the case of DJM, the seismic risk decreases rapidly with respect to the improvement ratio, and the LCC curve attains virtually the minimum value. This implies that the soil improvement effort of 1.9 Billion Yen with the ratio of 50% at three embankments is sufficient and optimum, and that further increase in the initial cost is unnecessary. The design plan determined

by the conventional method is also shown in Fig. 3.17. The initial cost of minimum LCC case is 1.9 billion Yen, while that of the conventional design is 1.4 billion Yen. This suggests that more initial investment is needed to construct the expressway embankment in this area from the viewpoint of minimum LCC.

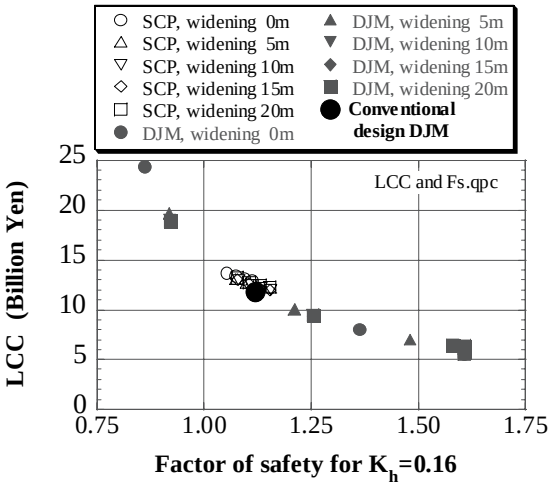

Fig. 3.18 Variation of LCC with conventional seismic factor of safety

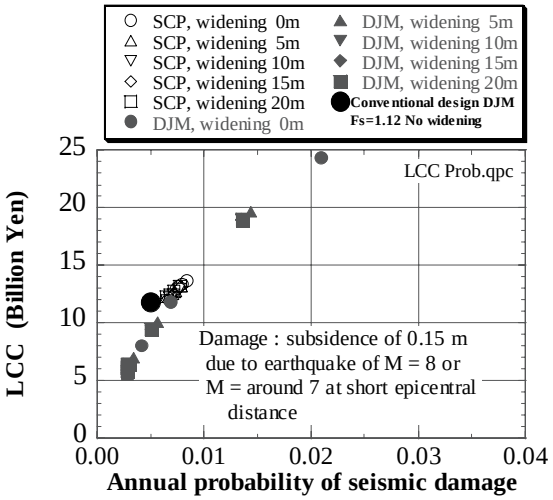

Fig. 3.19 Relationship between LCC and damage probability

To compare the conventional and LCC-based principles in more detail, Fig. 3.18 illustrates the variation of LCC with the conventional seismic factor of safety. It is interesting that LCC monotonously decreases as the factor of safety increases. Thus, types and extents of subsoil improvement do not affect the general trend of LCC. Similarly, Fig. 3.19 exhibits the relationship between the annual probability of damage and LCC. The damage is defined by the subsidence of 0.15 m due to an earthquake. Evidently, details of soil improvement does not affect the illustrated relationship.

Finally, the effects of the traffic interruption in the expressway on the regional and national economy have to be addressed. The authors discussed on this issue significantly, considering the following points:

(1) the industrial activities and production may be reduced by the traffic problem,

(2) clients and consumers may find a new place of production,

(3) consequently, the new manufacturer may get more profits from the increased business.

Thus, both gain and loss occur in parallel. The conclusion of the present study is that the negative effect to the economy is not explicitly calculated because this effect is somehow taken into account in the detour loss (D_3) due to elongated travel time.

3.1.8 Conclusions

An attempt was made to demonstrate and compare seismic designs of an embankment on the basis of a conventional pseudo-static principle and a new principle of life cycle cost. The following conclusions were drawn from this study.

1) The seismically-induced subsidence was employed as an index of limit state that varies continuously with the extent of earthquake effects.
2) Procedures to calculate the risk and consequence with respect to the subsidence were developed and demonstrated.
3) Seismic hazard and fragility curves were estimated separately for an M=8-class inter-plate earthquake and the one of smaller magnitude at a shorter epicentral distance. After seismic damage was probabilistically estimated separately for each of the two design earthquakes, the total probability was obtained by summing them up.
4) Consequence analysis is a very important part in risk estimation. The indirect loss was assessed using a cost-benefit analysis procedure for road investment. It is shown that the indirect loss, especially the elongated travel time due to detour, exerts a strong influence on the decision making in a LCC-based design.
5) Consideration on LCC may give a design conclusion that is different from that from the conventional design. This is particularly the case when a concerned structure plays an important role in the regional and the national economy. It, however, does not directly mean that the conventional design is not rational. Design procedures (specification) should be written considering many aspects. LCC considering seismic risk can be used as one of useful information for better code writing.

3.2 Seismic Performance and Design of Port Structures

3.2.1 Introduction

Seismic performance of port structures, such as caisson quay walls, sheet pile quay walls, and pile-supported wharves, are significantly affected by ground displacements and soil-structure interaction phenomena, and pose complicated engineering problems. In particular, seismic performance of these structures in the past earthquakes indicate that deformations in ground and foundation soils and the corresponding structural deformation and stress states are key design parameters and, unlike the conventional limit equilibrium-based methods, some residual deformation may be acceptable in design. Since 1995 Kobe earthquake (Fig. 3.20), significant advances have been made in the effective stress analyses for evaluating the degree of damage to port structures due to seismic shaking and ground displacement, including soil liquefaction (Iai, 1998; Iai *et al.*, 1998). Confidence has been gradually born among the port engineers on the applicability of these analytical methods as a new option of engineering design tools. In addition, there is a growing awareness that uncertainty in ground motions and geotechnical conditions should be adequately evaluated in geotechnical engineering practice (e.g. Iai, 2005; Kramer *et al.*, 2006).

This section presents an emerging methodology for seismic evaluation and design of port structures incorporating these recent advances discussed above. The principles in the methodology and their implications in geotechnical earthquake engineering are discussed through an example.

Fig. 3.20 Kobe port paralyzed at 1995 Kobe earthquake, Japan

3.2.2 Performance Objectives

The principles in the performance-based approach applied for port structures may be summarized as follows by following the guidelines presented in International Standard (ISO23469) (Iai, 2005). In this approach, the objectives and functions of port structures are defined in accordance with broad categories of use such as commercial, public and emergency uses. While the objectives and

functions of port structures managed by most of the US port authorities are commercial, there is a certain category of port structures designated as an essential part of emergency bases in Japan with objectives and functions being emergency use.

Depending on the functions required during and after an earthquake, performance objectives for seismic design of port structures are specified on the following basis;

- serviceability during and after an earthquake: minor impact to social and industrial activities, the port structures may experience acceptable residual displacement, with function unimpaired and operations maintained or economically recoverable after temporary disruption:
- safety during and after an earthquake: human casualties and damage to property are minimized, critical service facilities, including those vital to civil protection, are maintained, and the port structures do not collapse.

The performance objectives also reflect the possible consequences of failure.

For each performance objective, a reference earthquake motion is specified as follows:

- for serviceability during or after an earthquake: earthquake ground motions that have a reasonable probability of occurrence during the design working life;
- for safety during or after an earthquake: earthquake ground motions associated with rare events that may involve very strong ground shaking at the site.

Although these descriptions are very general, they constitute essential principles of emerging methodologies for performance-based evaluation and design of port structures as described in the next section.

3.2.3 Evaluation of Serviceability through Life Cycle Cost

While safety should be one of the primary performance objectives for ordinary buildings, serviceability and economy become higher priority issues for ordinary port structures. For these port structures, a methodology based on the principle of minimum life cycle cost may be ideal (e.g. Sawada, 2003). This methodology is emerging and will be eventually adopted as the state-of-practice in the coming decade.

Life cycle cost is a summation of initial construction cost and expected loss due to earthquake induced damage. Probability of occurrence of earthquake ground motion (i.e. earthquake ground motions with all (or varying) return periods) is considered for evaluating the expected loss due to earthquake induced damage. The life cycle cost also includes intended maintenance cost and cost for demolishing or decommissioning when the working life of the structure ends.

When evaluating serviceability through life cycle cost, failure of a port structure is defined by the state that does not satisfy the prescribed limit states typically defined by an acceptable displacement, deformation, or stress. If a peak ground motion that is put in to the bottom boundary of soil structure systems is used as a primary index of earthquake ground motions, probability of failure $F_{\mathrm{F}}(a)$ at peak ground motion a is computed considering uncertainty in geotechnical and structural conditions. A curve described by a function $F_{\mathrm{F}}(a)$ is called a fragility curve (Fig. 3.21(a)). Probability of occurrence of earthquake ground motions is typically defined by a slope (or differentiation) of a function $F_{\mathrm{H}}(a)$ that gives annual probability of exceedance of peak ground acceleration a. A curve described by a function $F_{\mathrm{H}}(a)$ is called a seismic hazard curve (Fig. 4.11(b)).

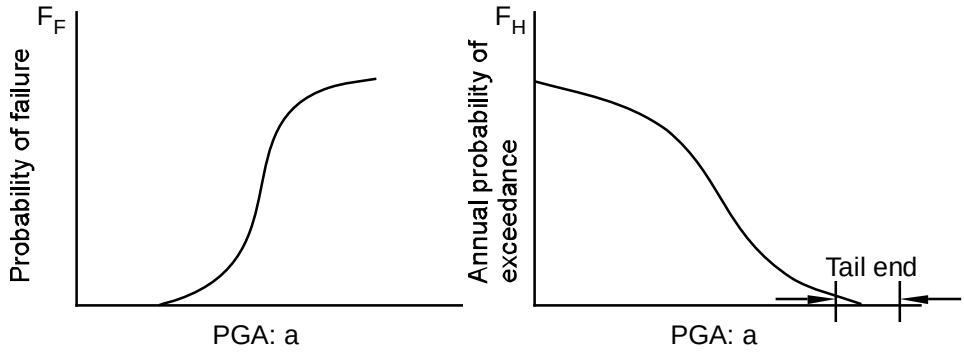

(a) (b)

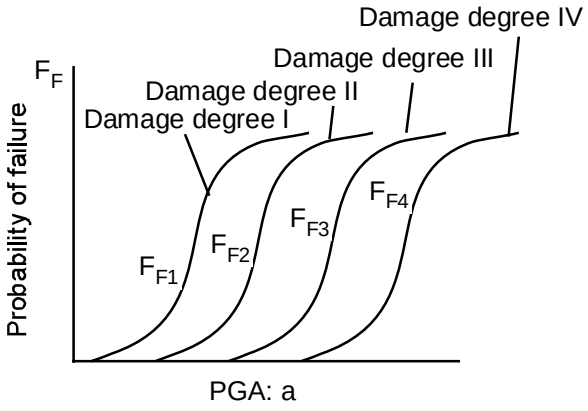

(c)

Fig. 3.21 Schematic figures of a fragility curve (a), a seismic hazard curve (b), and a group of fragility curves for multiple limit states (c)

Given the fragility and seismic hazard curves for a port structure, annual probability of failure of the port structure P_1 is computed as follows:

$$P_1 = \int_0^\infty \left(-\frac{dF_{\mathrm{H}}(a)}{da} \right) F_{\mathrm{F}}(a) da \qquad (3.18)$$

If a design working life is T years, probability of failure of the port structure over the design working life is given by

$$P_T = 1 - \left(1 - P_1\right)^T \qquad (3.19)$$

If loss due to earthquake induced damage associated with the prescribed limit state is designated by c_{D}, expected loss over the design working life of a port structures C_{D} is given by

$$C_{\mathrm{D}} = P_T c_{\mathrm{D}} \qquad (3.20)$$

Thus, the life cycle cost C_{LC} is given by adding initial construction cost C_{I}, maintenance cost C_{M} and demolishing cost C_{END} as

$$C_{\mathrm{LC}} = C_{\mathrm{I}} + C_{\mathrm{D}} + C_{\mathrm{M}} + C_{\mathrm{END}} \qquad (3.21)$$

This is generalized further by introducing more than one serviceability limit state. Given the fragility curve defined for the i^{th} limit state as $F_{\mathrm{F}i}(a)$ (Fig. 3.21(c)), Eqs. 3.18 through 3.21 are generalized as follows:

$$P_{1i} = \int_0^\infty \left(-\frac{dF_{\mathrm{H}}(a)}{da} \right) F_{\mathrm{F}i}(a) da \qquad (3.22)$$

$$P_{Ti} = 1 - \left(1 - P_{1\mathrm{i}}\right)^T \qquad (3.23)$$

$$C_{\mathrm{D}i} = P_{Ti} c_{\mathrm{D}i} \qquad (3.24)$$

$$C_{\mathrm{LC}} = C_{\mathrm{I}} + \sum_i C_{\mathrm{D}i} + C_{\mathrm{M}} + C_{\mathrm{END}} \qquad (3.25)$$

As demonstrated for liquefaction hazard evaluation by Kramer *et al.* (2006), the probability evaluated by Eqs. 3.18 and 3.19 is a consistent index of hazard and the conventional approach based on the return period prescribed in design provisions and codes can be either too conservative or unconservative depending on the site. Expected loss evaluated by Eq. 3.20 is an index that reflects the consequence of failure. Life cycle cost evaluated by Eq. 3.21 is an index that properly reflects the

trade-off between initial cost and expected loss. The design option that gives the minimum life cycle cost is the optimum in terms of overall economy. Thus, the optimum design has a certain probability of failure given by Eq. 3.19. This probability is not prescribed by an authority (such as 10% over 50 years) but rather determined as a result of the minimum life cycle cost procedure. The probability of failure can be large if a consequence of failure in meeting the performance criteria, as measured by seismic loss c_D, is minor. The probability can be small, however, if a consequence of failure, as measured by c_D, is significant. Thus, the minimum life cycle cost procedure reflects the possible consequences of failure and, thereby, satisfies the principles in performance objectives in the ISO guidelines described in the previous section.

3.2.4 Example calculation

A caisson quay wall with a water depth of 15 m is considered for a design example. The quay wall is constructed on loosely deposited sand for replacing alluvial clay layer beneath the rubble foundation as shown in Fig. 3.22. The design options considered in this example include sand compaction piles (SCP) for foundation only (Case A), cementation of foundation only (Case B), SCP both for foundation and backfill with a spacing of 1.8 m (Case C), the same as Case C but with a spacing of 1.6 m (Case D), and SCP for foundation only and structural modification by expanding the width of caisson by 3 m (Case E).

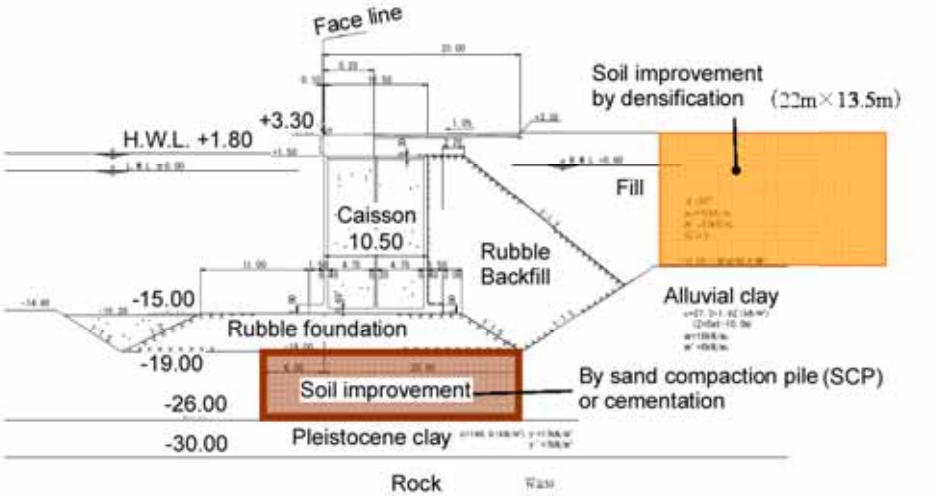

Fig. 3.22 Cross section of a caisson quay wall considered for a design example

More than one limit states are typically defined for port structures as shown in Table 4.3. Limit states as specified by the acceptable normalized horizontal displacement of a caisson is shown together with the associated repair cost (or direct loss) in Fig. 4.13. Ideally, all of these limit states

should be used for life cycle cost evaluation (Ichii, 2002). For simplicity, however, only one limit state was assigned for the example in this paper: the acceptable horizontal displacement of caisson wall is assumed to be 10% of wall height that corresponds to the displacement of 1.5m. Design working life was assigned as 50 years.

Table 3.5 Acceptable level of damage in performance-based design*

Acceptable level of damage	Structural	Operational
Degree I : Serviceable	Minor or no damage	Little or no loss of serviceability
Degree II: Repairable	Controlled damage**	Short-term loss of serviceability***
Degree III: Near collapse	Extensive damage near collapse	Long-term or complete loss of serviceability
Degree IV: Collapse****	Complete loss of structure	Complete loss of serviceability

* Considerations: Protection of human life and property, functions as an emergency base for transportation, and protection from spilling hazardous materials, if applicable, should be considered in defining the damage criteria in addition to those shown in this table.
** With limited inelastic response and/or residual deformation
*** Structure out of service for repairs for short to moderate time
**** Without significant effects on surroundings

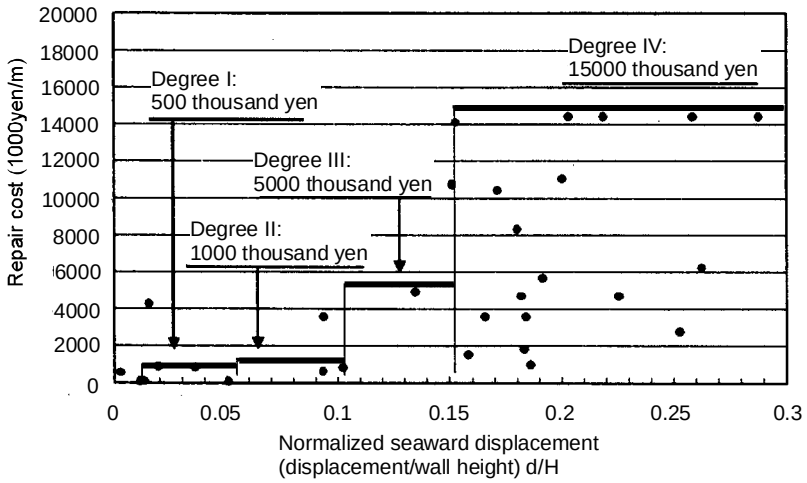

Fig. 3.23 Repair cost (or direct loss) for a gravity quay wall (Ichii, 2002)

Fragility curves $F_F(a)$ were computed by Monte Carlo simulation by considering the uncertainty in SPT N-values with 1000 trials for each peak ground acceleration a input at the base rock. Coefficient of variance in SPT *N*-values was assigned as 0.1 based on the number specified in the technical standard of Japanese ports (2006).

In the performance-based design, displacement of wall should be evaluated for each trial SPT N-value. In theory, this is achieved by running an effective stress analysis of soil-structure systems

for each trial SPT *N*-values. An example of the results of effective stress analysis specifically run for the caisson quay wall for a particular earthquake motion is shown in Fig. 3.24. In practice, this is not feasible. In order to overcome this difficulty in practice, a set of simplified performance evaluation charts that were developed through a parameter study (Iai *et al.*, 1999; Ichii *et al.*, 2002; Higashijima *et al.*, 2006).

The cross sections and primary dimensions used as input parameters are shown in Fig. 3.25. Typical examples of the results of the parameter study are shown in Fig. 3.26. These results were compiled as a comprehensive set of data for the simplified performance evaluation charts. These charts are incorporated in a spread sheet format. Input data required are (1) basic parameters defining the cross section of structures, (2) geotechnical conditions as represented by SPT N-values, and (3) earthquake data, as represented by wave form, peak ground acceleration, or distance and magnitude from the seismic source. These charts can be also conveniently used for efficiently assessing the vulnerability of coastal geotechnical structures that extends over a long distance, such as tens of kilometers, over a variable geotechnical and structural conditions.

Fragility curves computed by using these simplified performance evaluation charts are shown in Fig. 3.27(a). Together with a hazard curve at a port in Japan considered for the example exercise shown in Fig. 3.27(b), probability of failure (i.e. probability that does not meet the prescribed limit state) was computed through Eqs. 3.18 and 3.19. For example, probability of failure over 50 years was 0.96 and 0.32 for Cases A and B, respectively.

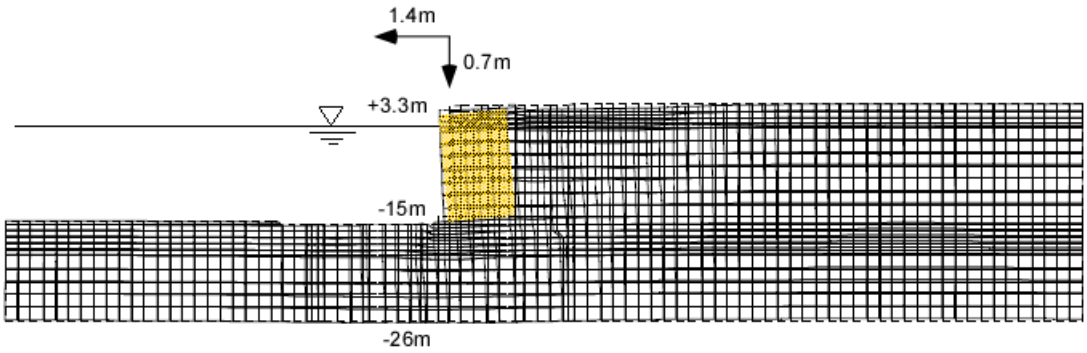

Fig. 3.24 Residual displacement of a caisson wall through effective stress analysis

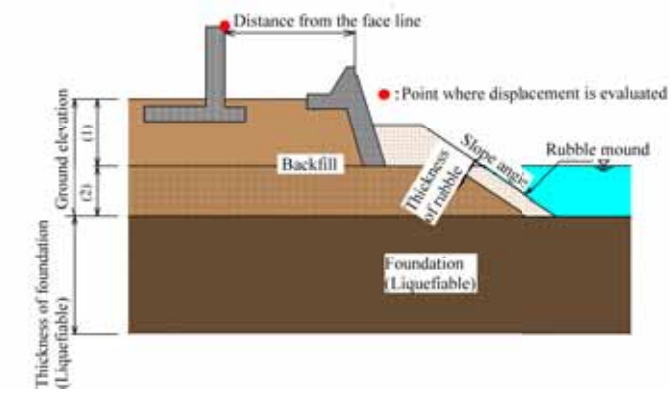

(a) Leaning bulkhead

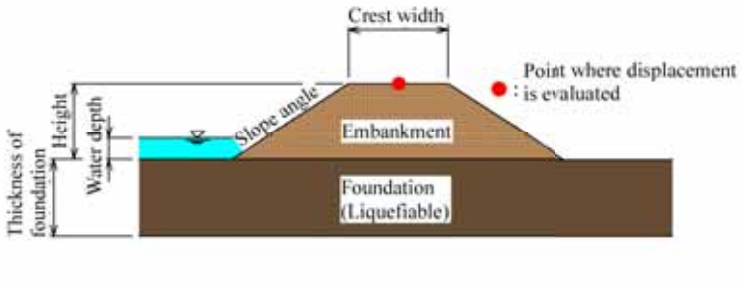

(b) Embankment type

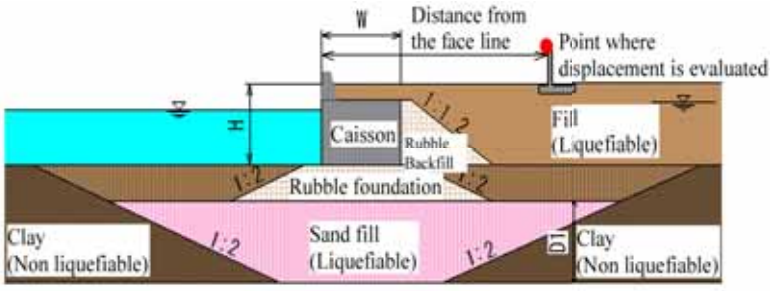

(c) Gravity type

Fig. 3.25 Cross sections and primary parameters used for the simplified design charts (Higashijima *et al.*, 2006)

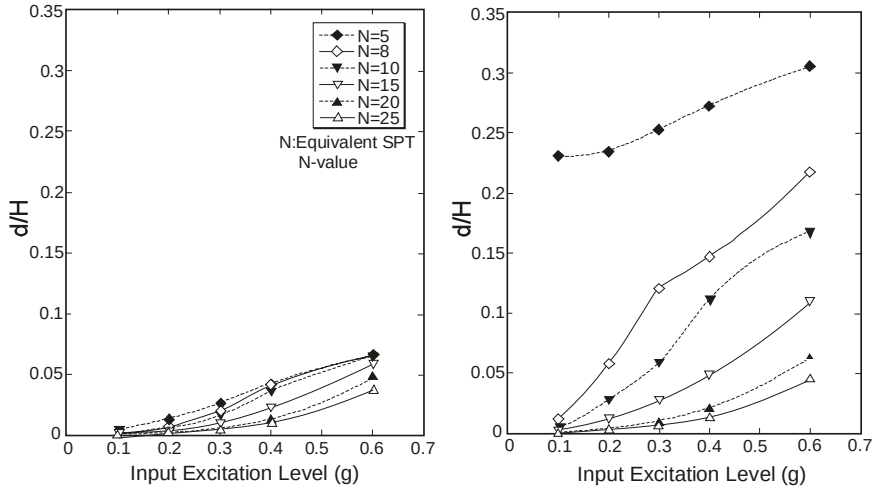

(a) D1/H=0.0 (b) D1/H=1.0

Fig. 3.26 Parameter study of normalized horizontal residual displacements of a gravity caisson wall over varying maximum accelerations (Iai et al., 1999)

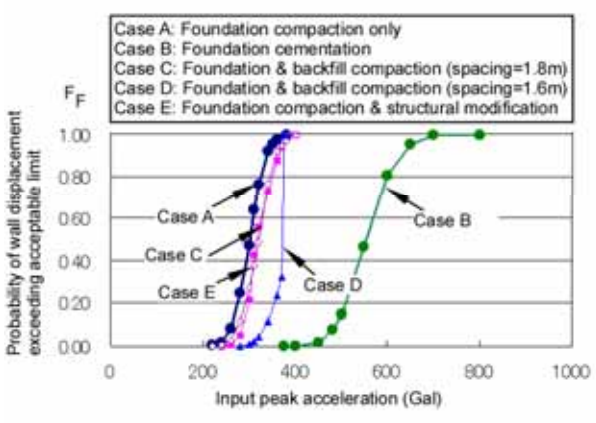

(a) Fragility curves

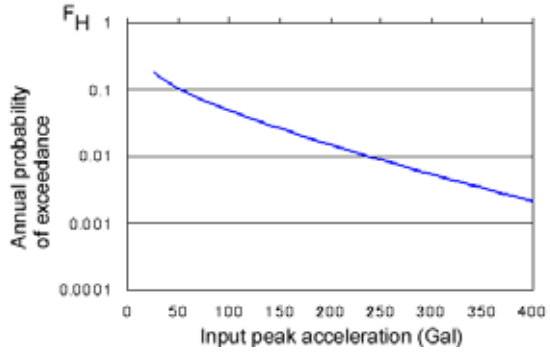

(b) Hazard curve

Fig.3.27 Fragility curves and a hazard curve

The loss due to earthquake induced damage is typically defined on the basis of the acceptable level of structural and operational damage given in Table 3.5. The structural damage category in this table is directly related to the amount of work needed to restore the full functional capacity of the structure and is often referred to as direct loss due to earthquakes. The operational damage category is related to the amount of work needed to restore full or partial serviceability. Economic losses associated with the loss of serviceability are often referred to as indirect losses. In addition to the fundamental functions of servicing sea transport, the functions of port structures may include protection of human life and property, functioning as an emergency base for transportation, and as protection from spilling hazardous materials. If applicable, the effects on these issues should be considered in defining the acceptable level of damage in addition to those shown in Table 3.5.

In the example exercise, the direct loss that is needed for restoring the damage caisson wall was assigned as one million yen/m following the results shown in Fig. 3.23 (Ichii, 2002). Together with the initial construction cost, including the cost for soil improvement or structural modification, the life cycle costs considering only the direct loss were computed as shown in Fig. 3.26(a). Design option Case B based on cementation of foundation showed the minimum life cycle cost whereas design option Case E based on structural modification showed the most expensive life cycle cost.

Indirect loss due to earthquake induced damage to port structures needs careful evaluation in economic loss of industries associated with service of port. In this example, for simplicity, indirect loss was assumed as five times as the direct loss. The results shown in Fig. 3.26(b) indicate that inclusion of indirect loss reflects the difference in design options and resulting seismic performance much more clearly than when only direct loss is considered. Serviceability during and after the earthquake is obviously related closely to the operational aspect of port structures.

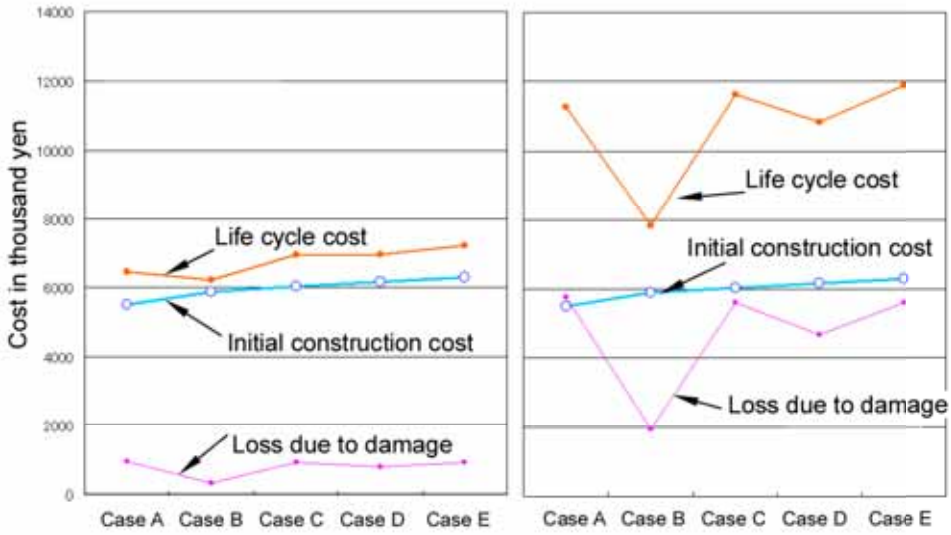

(a) Considering direct loss only (b) Considering both direct and indirect losses

Fig. 3.26 Life cycle cost of a caisson quay wall (per meter)

3.3 Life Cycle Cost Evaluation of Embankment

3.3.1 Tests and Analyses

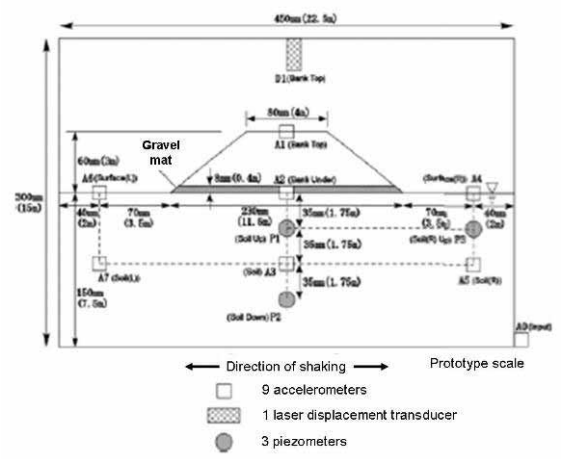

Fig. 3.27 Cross section of embankment and foundation

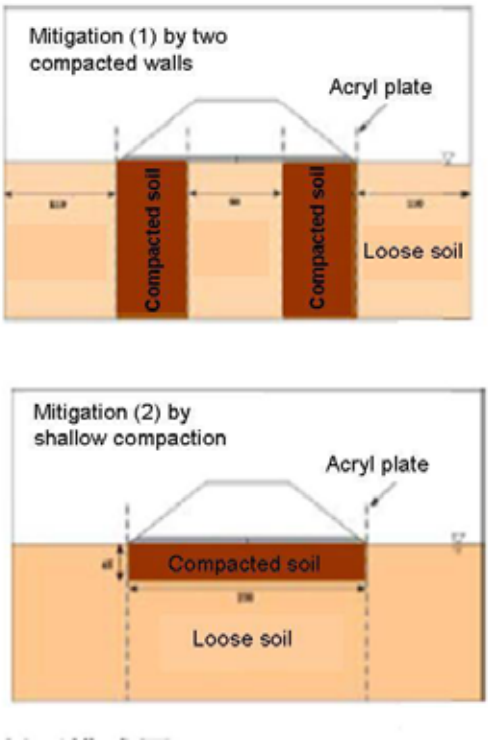

Fig. 3.28 Two options of compaction in foundation (two walls or shallow layer)

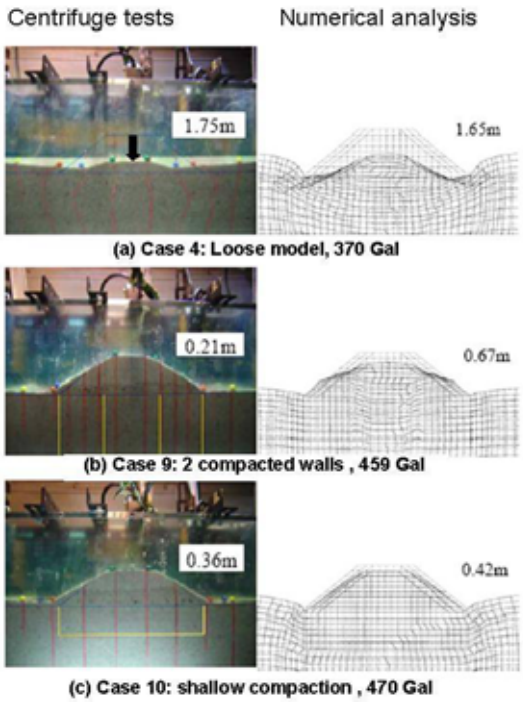

Fig. 3.29 Comparison of subsidence of embankment between analysis and centrifugal model tests

Life cycle cost was further evaluated by using advanced numerical analyses. The employed computer code is the same one as used in Section 3.2. This approach is useful when soil behavior, subject to liquefaction, is highly nonlinear. Numerical study was supported by running centrifugal model tests at the same time. Fig. 3.27 illustrates a cross section of an embankment and, to improve the seismic resistance in the foundation soil, two kinds of compaction were considered (Fig. 3.28). The considered shaking was Uemachi motion with varying acceleration amplitude. Fig. 3.29 compares the subsidence of centrifugal model tests and the numerical results. Except the case of two compaction walls, the agreement between tests and analyses are reasonable.

3.3.2 Evaluation of Life Cycle Cost of Embankment

LCC analyses were conducted in order to determine the optimum extent of shallow compaction under a hypothetical river levee. The epicentral distance, R, to the earthquake fault was varied between 0 km and 30 km. The height and the length of a concerned levee was 3m and 400 m, respectively. The cost for restoration of a damaged levee was set equal to be 1.3 times of the initial construction cost. The extent of damage varied with the extent of initial construction (subsoil improvement), and was calculated by an FE computer code. As an indirect cost, the damage due to breaching of the levee and flooding was considered, which was set equal to 1 trillion Yen owing to the industrial development in the studied area. The employed seismic hazard curves and the fragility curves are presented in Figs. 3.30 and 3.31, respectively. The degree of damage was classified into four categories as shown in Table 3.6. It is proposed here that the quality of performance prediction should be judged to be satisfactory if the prediction precisely predicts the damage degree in this table. This rather generous criterion comes from the present situation of field investigation (Chapter 4).

It should be stressed first that LCC did not decrease with the increase of initial construction cost (extent of soil improvement) when the seismic cost consisted only of the restoration (direct) cost. LCC decreased when the indirect cost was taken into account. This point implies that LCC approach is useful in densely populated or industrially important regions where economic loss is significant.

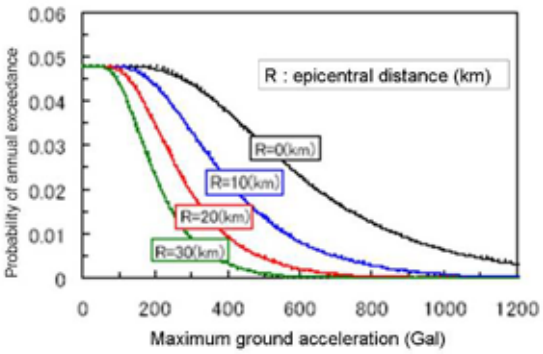

Fig. 3.30 Seismic hazard curves

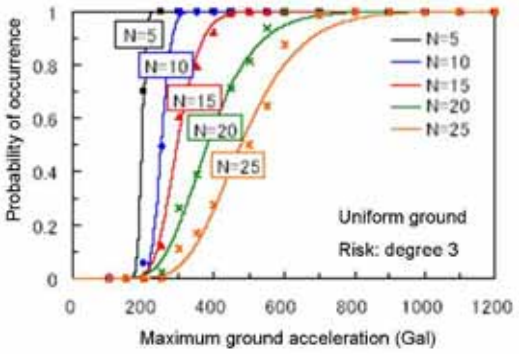

Fig. 3.31 Fragility curves

Table 3.6 Classification of damage degree

Degree	Subsidence (m
1	> 0.2 m
2	> 0.5 m
3	> 1.0 m
4	> 1.5 m

Height of levee = 3 m

Fig. 3.30 concerns the case in which the epicentral distance is very short (R = 0 km). LCC decreases as the SPT-N value in the compacted foundation increases. It is therein seen that the initial construction increases with SPT-N because of more elaborate soil improvement but that the decrease in damage cost (risk) is substantial. Noteworthy is that LCC did not achieve any minimal in Fig. 3.30. It implies that when a strong earthquake is expected to occur just beneath an industrially develop area, disaster mitigation has to be extremely elaborate. Conversely in the case of R = 30 km (Fig. 3.31), the minimum LCC was achieved for the case of SPT-N = 20.

3.4 Technical Environmental Consideration

3.4.1 Background

In the present project, new designs specified to perform against seismic effects were developed for several types of civil infrastructures. Two new indexes were introduced to measure the efficiencies of these designs: (a) the residual displacement which remains after an earthquake and (b) the Life Cycle Cost (LCC) of the structure.

As part of the project carried out in Japan, five road embankment design schemes were developed by a team of experts. The embankments were designed to have different levels of

efficiency in resisting seismic attacks. Their descriptions are as follow: 1) The basic case: 7m long sand column piles (SCP) of 30% improvement rate inserted beneath the embankment. 2) Same as case 1 but a reduced improvement rate of 20%. 3) Same as case 1 with extra compaction to enhance the soil quality on the embankment. 4) Same as case 1 but with layers of geotextiles inside the embankment. And 5) Instead of SCP, deep jet mixing technique (DJM) was adopted, with an improvement rate of 50%.

An earthquake was chosen to impose on the embankments. The earthquake was assumed to be representative and critical for a specific area in Tokyo. The LCC was calculated as the initial construction cost plus the product of the probability and financial cost of the failure. The probability of their total failure was defined as a one meter residual displacement at the crest of the embankment after the earthquake. While the failure cost was assumed to be a range of factors of the initial construction cost, to include cost of human lives, reparation cost of the embankment and traffic diversion cost due to road failure. LCC were calculated for all five designs.

In recent years, general environmental awareness has increased significantly all around the world. Nowadays, solely considering the direct monetary values of a design can be considered as incomplete for three reasons: 1) In the near future, it seems likely that some form of an emission tax will come into effect which will entail an additional cost. 2) We have a social obligation to limit the damages we impose on the environment. 3) For these earthquake designs, the probabilities of their failure and rebuilding are considered for a long life cycle. Therefore it is important to understand the environmental impacts of these designs; so that should rebuilding be required, no unconsidered or unnecessary impacts will be re-imposed onto the environment.

This study evaluates the environmental impacts of the mentioned embankment design schemes using embodied energy (EE), in the aim of providing a comprehensive picture on the efficiency of the embankments.

3.4.2 Embodied Energy

The embodied energy of an item is by definition the total energy that is attributed to bringing that item to its existing state. Generally, in construction, there are three main types of energy consuming processes: gaining of materials, transportation and installation. More specifically for this study: the materials energy includes the energy consumed in the extraction of raw materials such as soil and cement, how they are processed, and the manufacturing of composite items such as geotextile. Transportation energy includes the fuel consumed in moving the materials and construction machineries between the sites. Finally, installation energy comprises appropriate proportions of the energy consumed in manufacturing of the machineries involved in the construction processes; as well as the fuel consumed during the operations.

Embodied energy, which is abbreviated as EE, is a conceptual idea; it is often taken to be an environmental impact indicator. At current stage, how it describe the environmental impact is not understood fully. Unlike CO_2 and other emissions, it does not bear any physical impact to the environment. However, established researches indicate that EE has strong correlations with CO_2 and other gas emission; thus providing evidence that it is a valid environmental impact indicator and hence chosen for this study. For an example, a case of embankment is picked up.

3.4.3 Methodology

(1) Construction EE

To evaluate the life cycle embodied energy of the embankments, a process boundary was first defined. Fig. 3.32 shows a flow chart of the process stages, the shaded boxes are processes considered in this study and hence the boundary. Note that maintenance is ignored; and at the end of service life, embankments are assumed to be left on site, so no demolishment is required. However in this special case, when structural failure occurs, the embankment is assumed to be rebuilt on the same site using the same design.

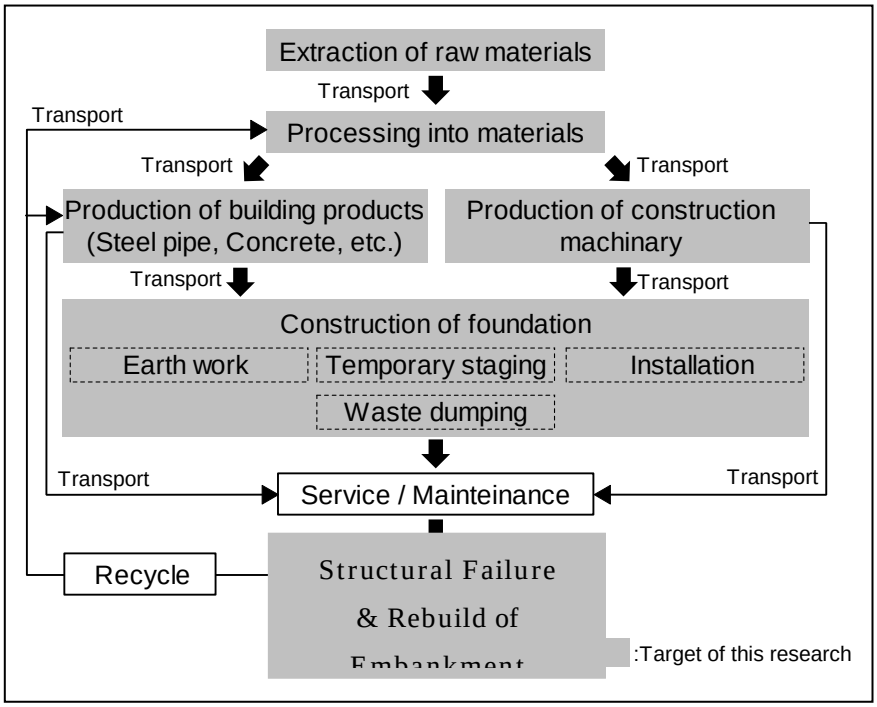

Fig. 3.32 Flow chart of the process boundary

The energy involved in each process stage was evaluated by quantifying the amount of materials or fuels used and multiply by their appropriate Embodied Energy Intensity (EEI) (more on this later). Materials and fuel were quantified through the use of design drawings and materials specifications for each embankment scheme (Appendix); and assuming distance of transportations for both the materials and machineries. The installation procedures and durations are given by contractors based on industry practise. Note that the data transportation and installation processes were acquired for UK conditions, it may differ from the data used in the original report of LCC. This can serve as part of the sensitivity analysis for international applicability of the original study.

Embodied energy intensity (EEI) has the unit of MJ/kg or MJ/l. For each construction material, it is defined by the energy inputted form a unit weight of the material. It includes the energy to extract the associated raw materials, to convert those materials into its final usable form, taking into account of appropriate proportion of energy used in the construction of the relevant equipments. For the transportation and installation stage, fuels were consumed, their EEI refer to the sum of energy used to extract the resources plus their potential energy.

Wherever available, the EEI values adopted in this study are averages of all the published sources. In this case study, the EEI used are as follows: Soil and sand were 0.1MJ/kg, cement was 5MJ/kg, geotextile was 103MJ/kg and petrol was 36MJ/l (Kiani, 2006).

(2) Life Cycle EE

To evaluate the life cycle embodied energy of the embankments, the idea is the same to that of LCC: life cycle embodied energy = construction embodied energy + probability of failure (per year)× life cycle of structure x energy of failure. Table 3.7 shows the probability of failure in any given year, for each embankment.

Table 3.7 Probability of failure (per year) for each embankment

	1. SCP 30%	2. SCP 20%	3. High quality embankment	4. Geotextile	5. DJM 50%
Probability of failure	2.56E-03	2.82E-03	2.04E-03	1.46E-03	8.07E-04

As mentioned, the cost of failure in this case includes the cost of human lives, structural reparation cost and traffic diversion cost. In terms of environmental impacts, the lost of human lives are not included; some may argue that diversions and traffic jams would entail extra emissions, but for now, it is assumed to be negligible. It leaves the reparation of the roadway and how much "failure energy" should be accounted for. There is no previous study on this topic available, so bold

assumptions were made upon the following argument: for embankment of this kind, since it is primarily soil or sand, it is needless to remove all the existing material to a dump site and re-import new material for rebuilding, unlike conventional buildings. As for the SCP and DJM, if damages were done to them during the earthquake, they will seldom be removed, but rather just construct new SCP or DJM on the existing site. Therefore, a lower bound for the rebuilding energy or failure energy was assumed to be solely the energy from the operational stages; while the upper bound failure energy would be approaching a total reconstruction of the embankment, or 100% of the construction energy.

3.4.4 Results

(1) Construction EE

Fig. 3.33 shows the construction EE for each embankment broken down into stages. The important observations are as follows: 1) EE of the DJM design far exceed the EE of the other four designs by a factor of more than two. The reason is due to relatively high EEI and density of cement; large quantity was used which further increased the transportation energy compared to other designs. 2) Comparing across the stages, materials energies are the most dominant in every design, especially in the DJM, again because of the large quantity of the cement. 3) The magnitude of installation energies are similar for every design and small compared to other stages.

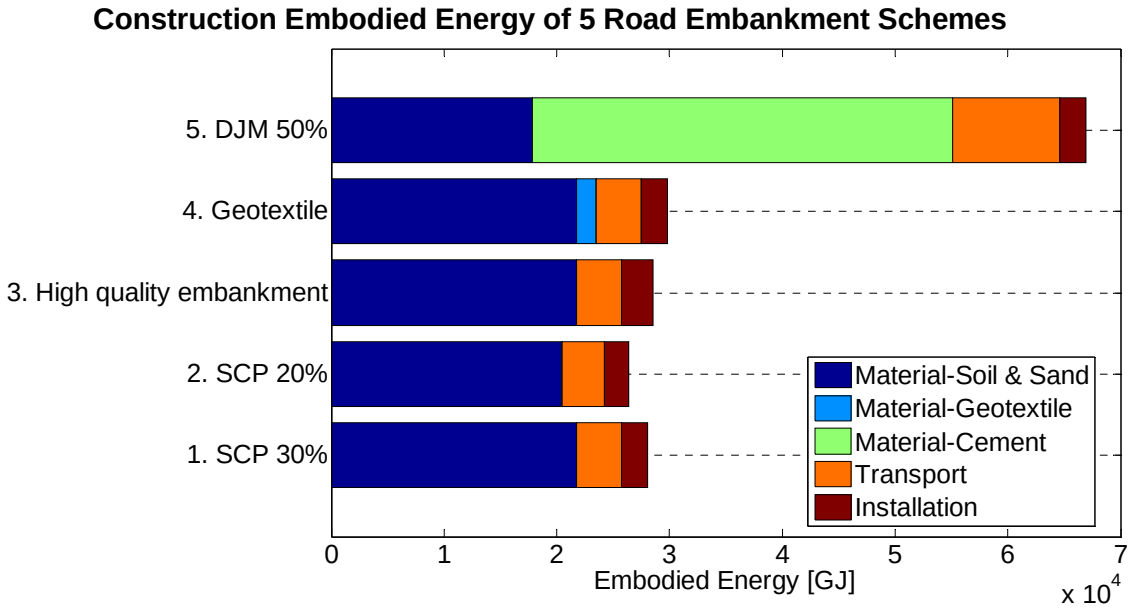

Fig. 3.33 Construction Embodied Energy of the embankment designs

(2) Life Cycle EE

Fig. 3.34 shows the results of the life cycle embodied energy for the five embankments in different colour. For reference, the construction energy was indicated again with a hollow triangle, the filled circles indicate the lower bound energy (accounting only for the operational energy) and the filled squares indicate the upper bound energy (assuming a new embankment is built to reinforce the failed embankment on the same location).

The observations from Fig. 3.34 are as follows: 1) the total energy of the DJM design on the rightmost side of the diagram far exceed the other four designs by an order of more than two. 2) The extra energies due to structure failure are relatively small compared to the construction energies for all designs, both for upper and lower bounds. 3) Over their life cycle, all of the SCP designs or the geotextile design are predicted to impose similar environmental impacts. 4) In environmental impact point of view, the geotextile design is recommended for it is predicted to have a lower probability of failure than the SCP designs without compensating much to the environment.

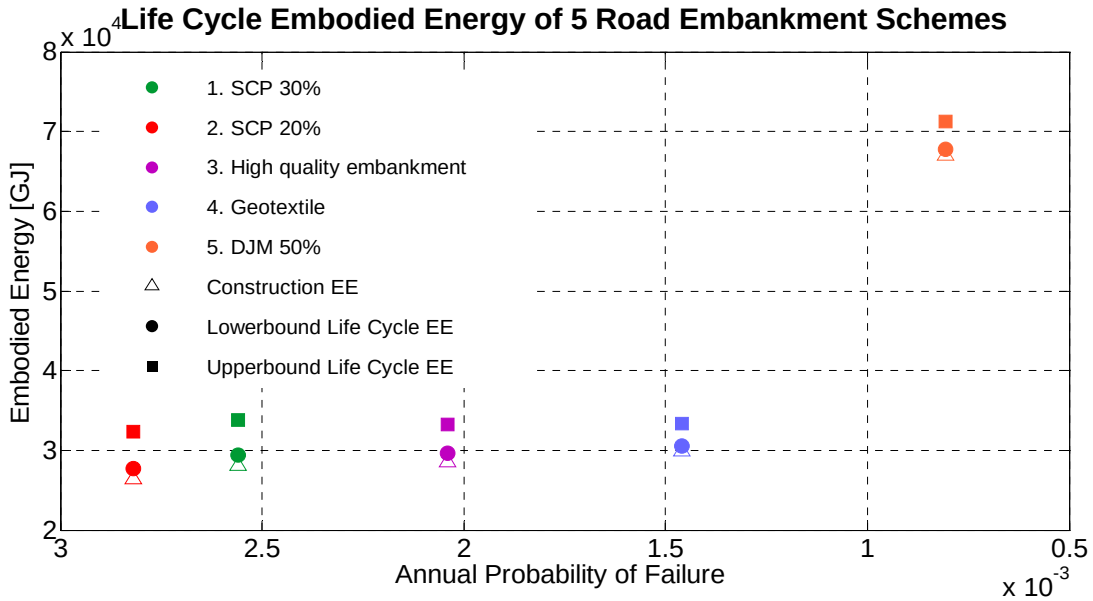

Fig.3.34 Life cycle Embodied Energy of the embankment designs

(3) Compare to Monetary Costs

Comparing to the LCC values from the original report, the main difference are the construction cost and embodied energy of design number 4 and 5, the geotextile and DJM designs. In the case of the construction cost, DJM design costs around the same as scheme 1 – 3, the SCP designs, but consumes much more energy than those schemes. The reverse is true for scheme 4, the geotextile design where the energy is similar to 1-3 but costs much more.

The reason behind this is that, although geotextile has an exceedingly high EEI, it has only a very small density, thus only small amount of material was used and limited amount of energy was consumed. (Note that the high pricing is also reflected through the high EEI.) The reverse is true for the use of cement; it has a much smaller EEI compared to geotextile, but much larger quantity is required for this design.

This study suggests two important things: 1) there is no directly proportional relationship between EE and monetary cost at construction stage. 2) If magnitude of EE indicates the magnitude of environmental impacts and hence a possible environmental tax in the future; then the DJM design may entail a larger top up cost than other design and may affect the decision made upon the optimisation of LCC.

3.4.5 Conclusion

Five established road embankment designs are known to have different levels of efficiency in seismic resistance and hence different construction cost and probability of failure. Previous study measured their performances by evaluating their life cycle cost (LCC). This report extended that study by assessing life cycle embodied energies of the embankments in the aim to predict their relative environmental impacts. The purpose of this report is not to suggest that road embankment schemes should be chosen solely according to the minimisation of environmental impacts. It should be read in conjunction with the findings on LCC to paint a comprehensive picture on the life cycle performance of the designs.

The results indicated that the embodied energy related to the failure of the structures is very small: most environmental impacts are dealt during the initial construction stage. Primary direction to minimise environmental impact should be through the reduction in the quantity of materials used since this is the main energy consumer. Whilst enhancement for the properties of the embankment through compaction should be carried out wherever possible; because the marginal energy consumed in installation processes is very small. The use of cement in the DJM method is comparatively bad for the environment and consumes at least twice as much of energy as the other methods assessed. It should be noted that this extra environmental impact may introduce extra financial cost in the future. If some sort of environmental tax comes into effect and it will possibly affect the conclusion made upon the optimisation of LCC.

4. International Survey on Soil Investigation

4.1 Introduction

As mentioned earlier, the prediction of seismic performance plays a key role in practice of performance-based design and life cycle cost calculation. Hence, the quality of field investigation that determines the soil conditions is essentially important. Being different from other industrial materials that are produced in factories under good control of quality, however, most geomaterials are products of natural procedures without care of quality or uniformity. In many cases, furthermore, we cannot see or touch those materials lying underground. In spite of this difficulty, demands for good accuracy of material properties and geometrical configuration (geological layers or stratification) are high. In case that the quality of soil data is poor, the calculated results have limited reliability. This situation cannot be improved by using the most sophisticated and advanced numerical tools for analysis.

The present project carried out an inquiry study on the current state of field investigation which is employed for geotechnical earthquake problems. A set of questions was made on imaginary construction projects and questions were asked to engineers of many countries on what kind of field investigation would be conducted by them. The asked questions and example answers based on practice in Japan are shown in Sect. 4.2.

(a) in Japan (b) in USA

Fig. 4.1 Practice of Standard Penetration Test in Japan and USA

The inquiry addressed the following four situations.

(1) Expressway or railway embankment resting on clayey soft soil

The thickness of clay soft soil is 20 m with its SPT-N <4. The embankment is 20 m high as well. The expressway is supposed to be most important one in the nation. The embankment consists of sandy soil. Dynamic properties and strength of soils are important. Moreover, the examination on quality of constructed embankment is important as well.

(2) Harbor structure prone to the risk of backfill liquefaction

This harbor is a very important harbor. Sea floor consists of clayey soil. The quay wall is made of caisson boxes of gravity type. The sea bed is replaced by sand and the same material is used for the backfill. The water depth is more than 15m. Of particular interest is the decision on details of soil improvement for mitigation of liquefaction risk.

(3) Pile foundation of reinforced-concrete building

This is a commercial building of 10 storeys. It is located in a water front area where SPT-N of subsoil is less than 10 and liquefaction risk is high. The ground water table rests at 1 m below the ground surface, which is underlain by 5 m of liquefiable sandy soil as well as a clay deposit of 10 m thickness and SPT-N = 5.

(4) Earth dam

The height of the dam is 30 m. The dam rests on such a stable soil as that of Pleistocene origin. Since there is a densely populated area in the downstream direction of the dam, the seismic safety is extremely important.

The present state of field investigation was studied by sending inquiry to many overseas institutes and societies. Answer was received from USA, Korea, Taiwan, Philippines, UK, and Argentine. This implies that most other countries do not pay much attention to the quality of soil investigation in practice, using empirical design formula that was developed by geotechnical developed countries, without considering the different quality of their own data. The received replies show that standard penetration test (SPT; Fig. 4.1) is considered to be the most important option in those countries although the geotechnical family recently pays more attention to cone penetration tests (CPT, Fig. 4.2). This discrepancy is probably because the existing design formula in earthquake design employs SPT-*N* value. Accordingly, the present study should make an appeal that the quality of SPT should be improved by keeping the equipments in a good condition (maintenance) and following the specified procedure as much as possible (practice).

Fig. 4.2 Cone penetrometer (CPT) for pushing into ground

4.2 Questions and Example of Answers (Japanese case)

Example 1 : Construction of highway road embankment on soft clay deposits

(a) Cross section across a site considered

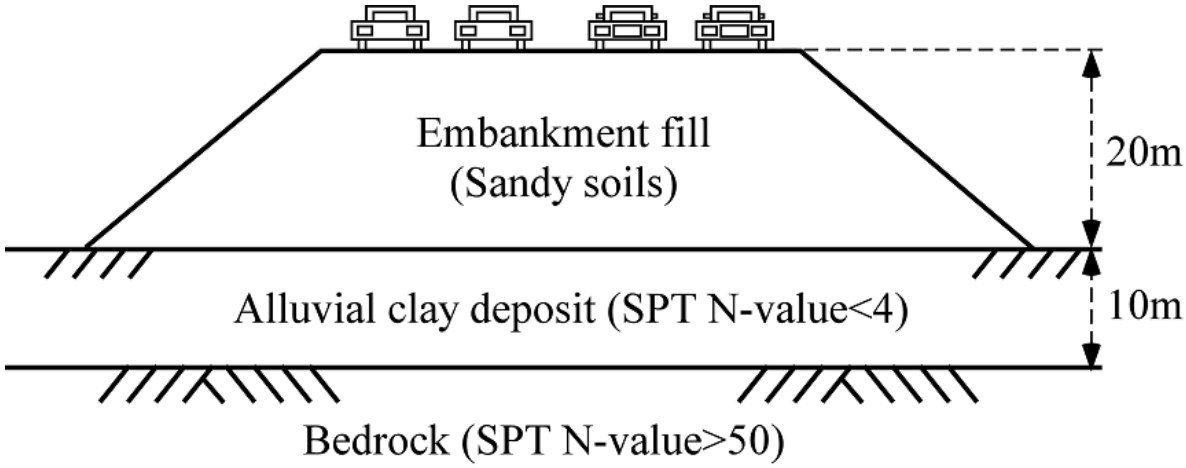

(b) Traverse cross section of a site considered

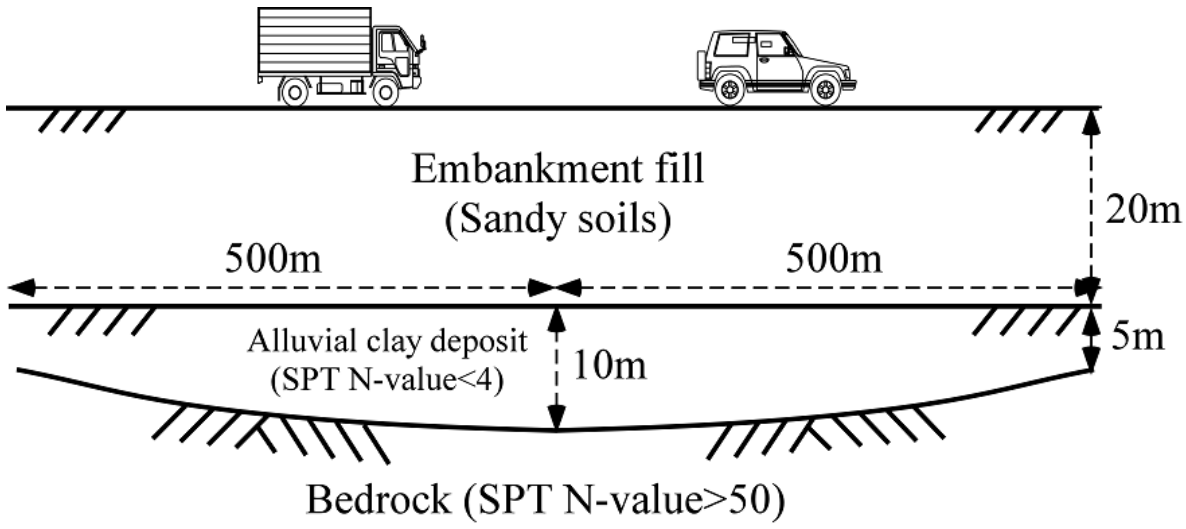

(c) Site and design conditions

There is a soft alluvial clay deposit with 10 metres deep in maximum. The SPT N-values along the depth of this deposit are consistently less than 4. A highway road with 2 lanes for each direction is planned to pass through. The construction of a road embankment with 20 metres high and 1 km long is envisaged. The fill materials of the road embankment are sandy soils.

(1) Describe the performance requirements that need to be satisfied.

<Current design specification>

The design specifications stipulated for normal road embankments and highway road embankments are different. Herein, The design specification for highway road embankments is concerned.

The current design specification is not based on a performance-based design principle, but can be characterized as what might be called a “regulation”-based design method. In the design manual stipulated by Japan Highway administration, (Design manual No.1 / Construction works, May 1998), there is no description on “seismic stability”. It is at the time when the design & construction guideline, (“2nd Toumei JH guideline”), was introduced on high road embankments and large-scale embankments for 2nd Toumei (Tokyo – Nagoya) Highway that the distinction was made on the levels of earthquake loading, i.e. small to medium-scale seismic loading (Level 1) and large-scale seismic loading (Level 2), in evaluating the seismic stability of road embankments. It is regulated in principle that the stability analyses would be employed through the use of a seismic coefficient assuming a circular slip surface, and the minimum factor of safety would be over 1 for design purposes. With the types of grounds characterized into type- , and , the design values of the seismic coefficient are stipulated as 0.16 for ground type- , 0.2 for ground type- and 0.24 for ground type- .

Introducing the following requirements is now under consideration for the revised design guideline incorporating a performance-based design principle.

<Requirements for seismic performance of highway road embankments>

(1) To secure the safety of road users and to prevent casualties of third parties.

(2) To conduct quick restoration for fostering the recovery of traffic function in case of disaster occurrence.

It is considered that the well-balanced combination of aseismic structural measures (hardware measures) and disaster-prevention as well as risk management (software measures) would lead to a more efficient aseismic system.

The requirements for seismic performance at each seismic level would be given as follows :

(1) Level 1 earthquakes : The occurrence of small-scale cracks on the structure would be permissible, as far as the easy repair work and quick functional restoration are possible after earthquakes.

(2) Level 2 earthquakes : The occurrence of the limited amount of irrecoverable deformation needs to be permitted during earthquakes. However, the traffic function needs to be recovered soon after

earthquakes.

The repair work of an embankment is relatively easy compared with other structures such as bridges, and its functions would easily be restored soon after earthquakes, as long as large-scale collapses and settlements could be prevented. On the other hand, it is virtually impossible to employ aseismic measures all through the long-distance structure such as embankments. Therefore, localized countermeasures are preferred at such locations where heavy damages are most probably incurred. In this respect, the requirements for seismic performance of road embankments are defined with respect to the difficulty in restoration and in securing traffic function.

In case of Level 1 earthquakes, the requirements for seismic performance are defined in such a manner that its function could be promptly recovered with only minor repair works after earthquakes. Easily recoverable minor damages such as cracks on pavements and bumps are specifically considered based on the experiences during past earthquakes.

In case of Level 2 earthquakes, the requirements for seismic performance are defined in such a manner that the occurrence of the limited amount of irrecoverable deformation needs to be permitted during earthquakes, as far as the quick restoration is possible in order to minimize the social influence.

(2) Specify the gradient of the side slopes. Make a sketch of a shape of the road embankment that ensures the safety of the structure. Indicate the sizes of the structure in detail. When a series of steps along the side slopes are preferred, include them into the sketch with their sizes.

According to “2nd Toumei JH guideline”, in case of usual fill materials, the gradient of the side slopes is determined as 1 : 1.8 in principle. In addition, in case of embankments with more than 15 metres in height, small steps with 1.5 metres wide need to be installed along the side slopes with the interval of 7 metres in height. Larger steps with 3 metres wide need to be installed with the interval of 21 metres in height.

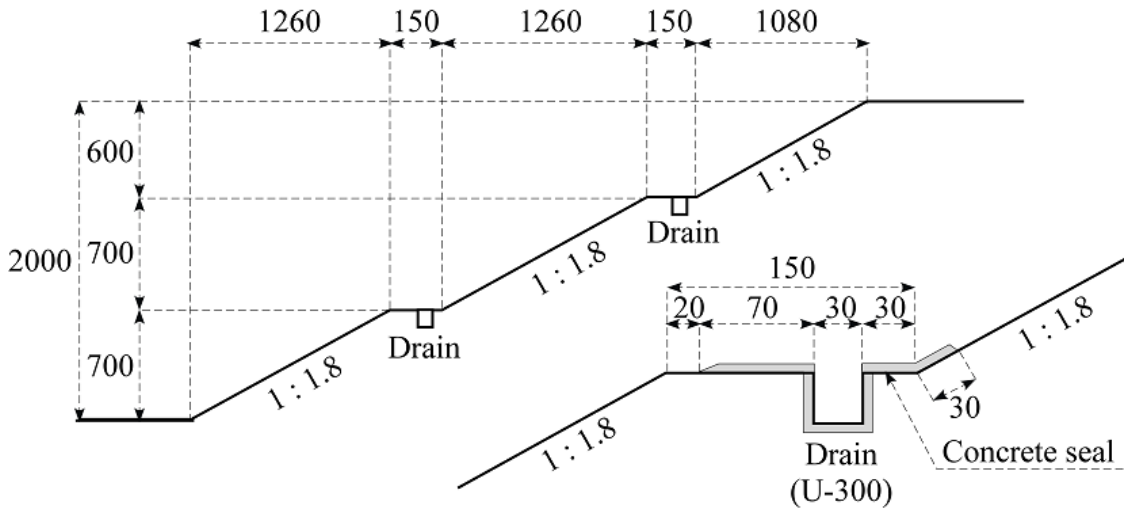

(3) Specify the design calculation methods for you to ensure that performance requirements are satisfied. Indicate the references (manuals), if any.

<Current design specification>

The current design specification is not based on a performance-based design principle, but can be characterized as what might be called a “regulation”-based design method. In the design manual stipulated by Japan Highway administration, it is regulated in principle that the stability analyses would be employed through the use of a seismic coefficient assuming a circular slip surface. In “2nd Toumei JH guideline”, the design values of the seismic coefficient are stipulated as 0.16 for ground type- , 0.2 for ground type- and 0.24 for ground type- , and the minimum factor of safety would be over 1 for design purposes. The minimum value of the factor of safety is 1 in case of Level 1 as well as Level 2 earthquakes. However, the strain level at which the failure states are determined in cyclic triaxial tests is 5% in case of Level 1 earthquakes, while the corresponding strain level is 10 or 15% in case of Level 2 earthquakes. Thus, the criteria of the determination of cyclic strength are given different depending upon the level of earthquakes.

Introducing the following requirements is now under consideration for the revised design guideline incorporating a performance-based design principle.

<Requirements for seismic performance of highway road embankments>

Based on the past experiences of the damages on the highway road embankments during Level 1 earthquakes, it is known that there have been only minor damages such as cracks and bumps along the boundary between cutting and filling and those behind the structures, and there have been no such cases where the irrecoverable deformation was observed. Hence, it is considered that the

embankments constructed by the current design specification are sufficiently seismic-resistant.

With respect to Level 2 earthquakes, it needs to be evaluated whether the deformation that occurs during earthquakes would stay within an allowable limit. Conventionally, it is most often that any seismic design has not been implemented. Instead, constructions have been carried out by using a typical gradient of side slopes, which was determined from the past experiences, and also by adopting the construction management on compaction. Even when the seismic design was implemented, the evaluation of the factor of safety against failure was conducted by using a seismic coefficient and a circular slip surface. However, in case of Level 2 earthquakes, there remain some problems associated with the determination of shear strength of soils and seismic level. In addition, the local soil failure would not necessarily result in the collapse of the whole embankment, and therefore, the conventional use of factor of safety might not be rationalized. On this vein, the Newmark method is adopted in evaluating the sliding displacement of the collapsing soil mass.

Reference : Japanese Geotechnical Society (2003) “Technical report on allowable displacements of soil structures and performance-based design”.

(4) In order to carry out the design and calculation as specified in the above (3), what kinds of geotechnical investigations are necessary? The geotechnical investigations include field testing (SPT, CPT, pressuremeter, etc.), undisturbed sampling and laboratory testing (unconfined compression tests, various triaxial tests, etc.). Indicate the type of testing, position and depth of testing in the cross sections across and traverse, shown in the above (a) and (b).

Geotechnical site investigations are comprised of a series of investigations. Those are the preliminary investigation, rough investigation, detailed investigations (1st & 2nd), investigation during construction and investigation during maintenance. The layout of the following investigations corresponds to the 1st detailed investigation, which would be employed after preliminary and on-site investigations. This investigation leads to the decisions on the route of a road and the type of road structures. It is to be noted here that there are no differences in the accuracy required for the determination of shear strength of soils and also in the aerial precisions, regardless of whether the stability analyses in the current design method are employed or the Newmark method in evaluating the residual deformation is implemented.

The geotechnical investigations for high embankments are conducted from the following points.

(1) Bearing capacity and settlement of the foundations on which embankments sit.
(2) Stability and settlement of embankments sitting on soft soil foundations
(3) Stability of embankments sitting on unstable slopes
(4) Possibility of occurrence of soil liquefaction in foundation soils

(5) Application of countermeasures

The methods of investigations are as follows.

(1) Understanding the topographical features of a site

(2) On-site inspection on geographical and geological features of a site

(3) Geophysical investigations

(4) Boring and soil sampling from bore-holes

The bore-hole investigations as listed in the above (4) can be planned as follows.

<Plan of bore-hole investigations>

(1) Cross section across a site considered

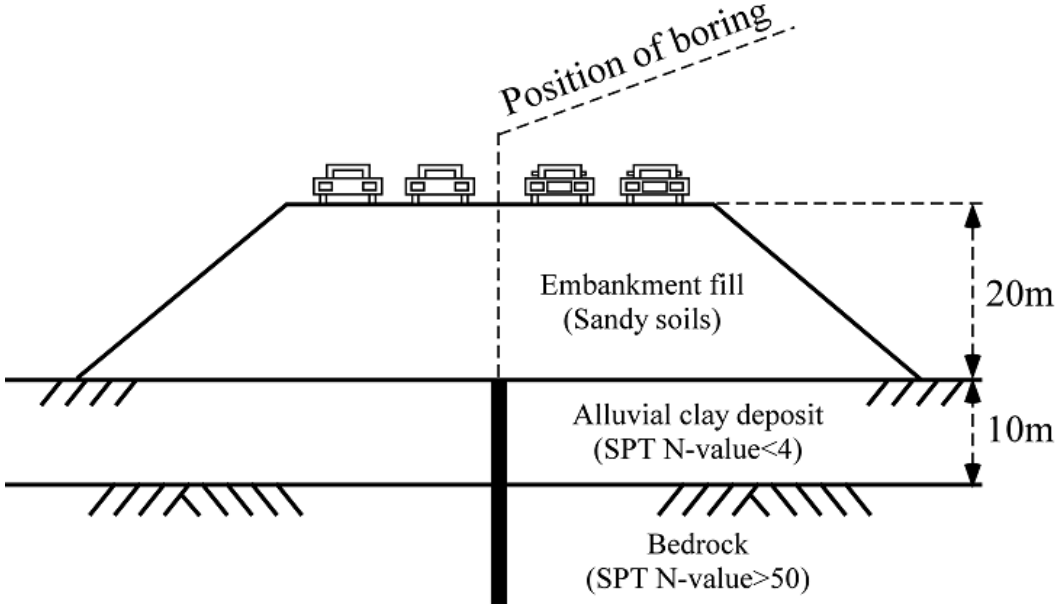

(2) Traverse cross section of a site considered

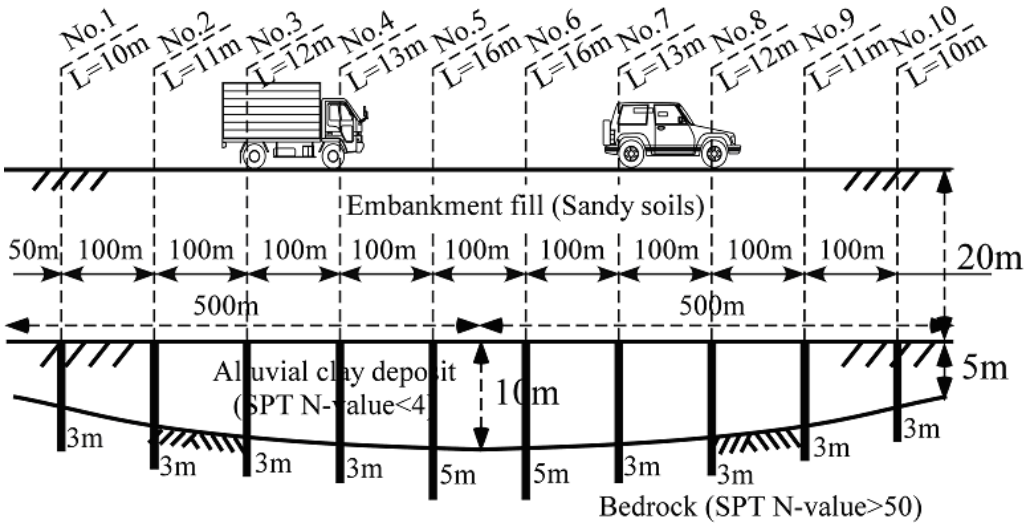

(3) Plan view

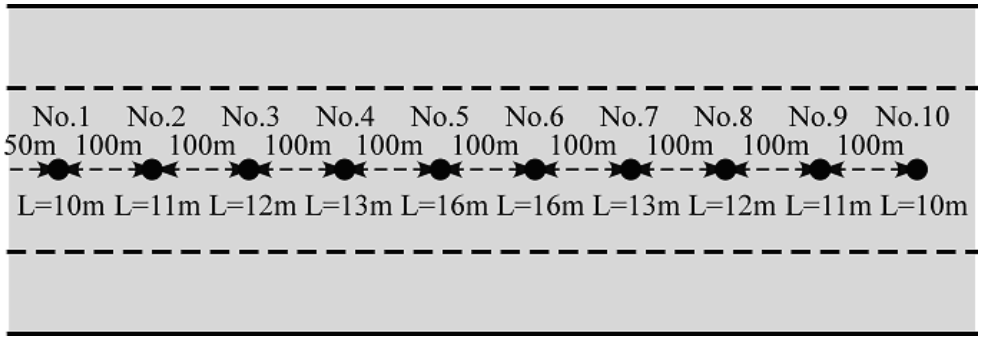

(4) Layout of bore-hole investigations

	Position along the bore-hole (No.)										
	1	2	3	4	5	6	7	8	9	10	Total
Distance of bore-hole drilling (m)											
ϕ 66mm drill Clay deposit	6	7	0	9	0	1	9	0	7	6	45
ϕ 66mm drill Rock	4	4	4	4	0	6	4	4	4	4	38
ϕ 86mm drill Clay deposit	0	0	8	0	10	9	0	8	0	0	35
ϕ 86mm drill Rock	0	0	0	0	6	0	0	0	0	0	6
Standard penetration tests (SPT)											
Clay deposit	6	7	5	9	10	7	9	5	7	6	71
Rock	4	4	4	4	6	6	4	4	4	4	44
Velocity (PS) logging tests	0	0	0	0	16	0	0		0	0	16
Thin-wall sampling	0	0	3	0	0	3	0	3	0	0	9
Particle size (sieve) analyses	2	2	3	3	3	3	3	3	2	2	26
Specific gravity (ρ_s)	2	2	3	3	3	3	3	3	2	2	26
Water content (w)	2	2	3	3	3	3	3	3	2	2	26
Liquid limit & plastic limit (w_L, w_P)	2	2	3	3	3	3	3	3	2	2	26
Wet density (ρ_t)	0	0	3	0	0	3	0	3	0	0	9
Oedometer tests	0	0	3	0	0	3	0	3	0	0	9
Triaxial tests (CU)	0	0	3	0	0	3	0	3	0	0	9
Cyclic triaxial tests (shear modulus & damping ratio against shear strain)	0	0	3	0	0	3	0	3	0	0	9

(5) Details of investigations at Boring No.1 & No.10

	Depth (m)										
0	5						10				Total
Soil type	Clay						Rock				
SPT N-value & Groundwater level		N<4					N>50				
Distance of bore-hole drilling (m)											
ϕ 66mm drill Clay deposit	═══	═══	═══	═══	═══	═══					6
ϕ 66mm drill Rock							═══	═══	═══	═══	4
ϕ 86mm drill Clay deposit											0
ϕ 86mm drill Rock											0
Standard penetration tests (SPT)											
Clay deposit											6
Rock											4
Velocity (PS) logging tests											0
Thin-wall sampling											0
Particle size (sieve) analyses											2
Specific gravity (ρ_s)											2
Water content (w)											2
Liquid limit & plastic limit (w_L, w_P)											2
Wet density (ρ_t)											0
Oedometer tests											0
Triaxial tests (CU)											0
Cyclic triaxial tests (shear modulus & damping ratio against shear strain)											0

(6) Details of investigations at Boring No.2 & No.9

	Depth (m)											
0	5							10				Total
Soil type	Clay							Rock				
SPT N-value & Groundwater level		N<4						N>50				
Distance of bore-hole drilling (m)												
ϕ 66mm drill Clay deposit	═══	═══	═══	═══	═══	═══	═══					7
ϕ 66mm drill Rock								═══	═══	═══	═══	4
ϕ 86mm drill Clay deposit												0
ϕ 86mm drill Rock												0
Standard penetration tests (SPT)												
Clay deposit												7
Rock												4
Velocity (PS) logging tests												0
Thin-wall sampling												0
Particle size (sieve) analyses												2
Specific gravity (ρ_s)												2
Water content (w)												2
Liquid limit & plastic limit (w_L, w_P)												2
Wet density (ρ_t)												0
Oedometer tests												0
Triaxial tests (CU)												0
Cyclic triaxial tests (shear modulus & damping ratio against shear strain)												0

(7) Details of investigations at Boring No.3 & No.8

	Depth (m)													
0	5							10						Total
Soil type	Clay							Rock						
SPT N-value & Groundwater level	N<4							N>50						
Distance of bore-hole drilling (m)														
ϕ 66mm drill Clay deposit														0
ϕ 66mm drill Rock								═══	═══	═══	═══			4
ϕ 86mm drill Clay deposit	═══	═══	═══	═══	═══	═══	═══							8
ϕ 86mm drill Rock														0
Standard penetration tests (SPT)														
Clay deposit														5
Rock														4
Velocity (PS) logging tests														0
Thin-wall sampling														3
Particle size (sieve) analyses														3
Specific gravity (ρ_s)														3
Water content (w)														3
Liquid limit & plastic limit (w_L, w_P)														3
Wet density (ρ_t)														3
Oedometer tests														3
Triaxial tests (CU)														3
Cyclic triaxial tests (shear modulus & damping ratio against shear strain)														3

(8) Details of investigations at Boring No.4 & No.7

	Depth (m)															
0	5								10							Total
Soil type	Clay									Rock						
SPT N-value & Groundwater level		N<4								N>50						
Distance of bore-hole drilling (m)																
ϕ 66mm drill Clay deposit	═══	═══	═══	═══	═══	═══	═══	═══	═══							9
ϕ 66mm drill Rock										═══	═══	═══	═══			4
ϕ 86mm drill Clay deposit																0
ϕ 86mm drill Rock																0
Standard penetration tests (SPT)																
Clay deposit																9
Rock																4
Velocity (PS) logging tests																0
Thin-wall sampling																0
Particle size (sieve) analyses																3
Specific gravity (ρ_s)																3
Water content (w)																3
Liquid limit & plastic limit																3
Wet density (ρ_t)																3
Oedometer tests																3
Triaxial tests (CU)																3
Cyclic triaxial tests (shear modulus & damping ratio against shear strain)																3

(9) Details of investigations at Boring No.5

	Depth (m)																
0	5								10								Total
Soil type	Clay										Rock						
SPT N-value & Groundwater level		N<4									N>50						
Distance of bore-hole drilling (m)																	
ϕ 66mm drill Clay deposit																	0
ϕ 66mm drill Rock																	0
ϕ 86mm drill Clay deposit																	10
ϕ 86mm drill Rock																	6
Standard penetration tests (SPT)																	
Clay deposit																	10
Rock																	6
Velocity (PS) logging tests																	16
Thin-wall sampling																	0
Particle size (sieve) analyses																	3
Specific gravity (ρ_s)																	3
Water content (w)																	3
Liquid limit&plastic limit(w_L, w_P)																	3
Wet density (ρ_t)																	0
Oedometer tests																	0
Triaxial tests (CU)																	0
Cyclic triaxial tests (shear modulus & damping ratio against shear strain)																	0

(10) Details of investigations at Boring No.6

	Depth (m)															
0	5								10							Total
Soil type	Clay										Rock					
SPT N-value & Groundwater level		N<4									N>50					
Distance of bore-hole drilling (m)																
ϕ 66mm drill Clay deposit										■						1
ϕ 66mm drill Rock											■	■	■	■	■	6
ϕ 86mm drill Clay deposit	■	■	■	■	■	■	■	■	■							9
ϕ 86mm drill Rock																0
Standard penetration tests (SPT)																
Clay deposit																7
Rock																6
Velocity (PS) logging tests																0
Thin-wall sampling																3
Particle size (sieve) analyses																3
Specific gravity (ρ_s)																3
Water content (w)																3
Liquid limit&plastic limit(w_L, w_P)																3
Wet density (ρ_t)																3
Oedometer tests																3
Triaxial tests (CU)																3
Cyclic triaxial tests (shear modulus & damping ratio against shear strain)																3

The numbers of bore-holes and sounding tests are determined in such a manner that bore-holes are located at every 50 to 100 metres and sounding tests are conducted at 20 to 40 metres in the traverse cross section of a site of valley-shaped topography. The number of bore-holes and sounding tests across a site supposed to have a bedrock inclined beneath the foundation soils is typically 2 to 4 locations at every traverse cross section.

In the present investigation, since there is little inclination of the bedrock foundation, only one location for boring is planned across the site, and 10 locations are planned for boring in the traverse cross section at every 100 metres for 1 km distance. Except for SPT and soil sampling, the locations of the bore-holes for field testing are chosen at the positions where the thickness of the soft soil foundations is largest. At other locations, the standard penetration tests are only planned, which provide SPT N-value and other index properties of the soil retrieved by disturbed sampling.

(5) Indicate the required strength of the fill material. Specify the methods of investigation or testing methods for obtaining dynamic properties of the fill material. Describe the process of their evaluations.

The geotechnical investigations on the borrow pit of the fill material need to be planned. In addition to the geological features at the site of the borrow pit, the degree of weathering, strike and dip structures, and the distribution of cracks need to be carefully examined. Soil sampling needs to conform to the requirements given in the Table below.

Table

	Specific gravity	Water content	Particle size (sieve)	Liquid & plastic limits	Ignition loss	Compaction (Proctor density)	Cone index on compacted soil	California bearing ratio (CBR)	Permeability tests	Oedometer tests	Unconfined compression tests	UU triaxial tests	CU triaxial tests	CU triaxial tests	CD triaxial tests	Crushing tests (rock)	Slaking tests (Rock)	Frost heave tests	Unconfined compression tests on chemically stabilized soils
Soil classification																			
Base course																			
Stability of side slopes Gravel & sand Silt																			
Compressibility of embankment																			
Trafficability																			
Chemical stabilization																			
Utility as upper base course																			
Subgrade																			
Strength characteristics																			
Long-term effects of weathering & pulverizing																			
Chemical stabilization																			
Effects of frost heave																			
Placeing, spreading & filtering																			
Compaction management																			

The number of bore-holes at the borrow pit of the fill material is determined typically as 1 to 3 locations per 10,000 m^3. The depth of the bore-hole should be given so that it penetrates at least 3 metres deeper than the excavated surface.

In the present investigation, the total volume of the borrow-pit is about 1500,000 m^3. Hence, 150 locations for boring may be needed to guarantee at least one location per 10,000 m^3.

Reference : Japan Highway (1992) “Manual for geotechnical and geological investigations”.

(6) Describe in detail how to evaluate the stability of the structure based on the outcome of the field investigations and laboratory testing.

The physical properties of soils, and the deformation and strength properties of soils are basically evaluated from the results of field testing and laboratory testing on undisturbed samples.

The variations of such properties, such as those induced by disturbance on the bore-hole wall and stress relief during sampling, need to be calibrated properly. The heterogeneity of the soils also needs to be taken into consideration through the inspection on bored soil samples and SPT N-values, which can be correlated with the results of field testing and laboratory testing.

(7) Describe in detail how to conduct the construction management for this structure. When the observational method is required, describe what sort of measurement is necessary, and specify the period and interval of such measurements.

<Current design specification>

As far as the construction works involving embankments of over 30,000 m^3 are concerned, the compaction procedure needs to be controlled by introducing the radio isotrope (RI) device, (Japan Highway (1992) “Manual for geotechnical and geological investigations”).

In determining the quality of the works, it is stipulated that the measurements of the porosity with respect to air voids need to be conducted. In case where the measurements of such air porosity are found difficult, some designed values of density ratio are taken for compaction control.

In some cases, the observational methods are introduced to ensure the stability of embankments during construction. Typical measurements during the observational procedure are given as follows.

Table

Monitoring equipments	Data acquired
Surface settlement plate	Time history of ground surface settlement
Settlement gauges	Time history of relative (differential) settlements
Displacement-gauged pile	Time history of vertical & horizontal displacements
Landslide (wire) extensometer	Time history of movement of landslide
Bore-hole inclinometer	Time history of ground displacements
Pore water pressuremeter	Time history of pore water pressure

(8) Indicate round figures of the costs required for investigation and testing described in the above (4), and also for the construction management described in the above (7), respectively.

The estimated costs for the investigations listed in the above (4) are summarized in the Table below. The costs for numerical analyses and construction management are not included herein.

Table

		Unit	Unit cost (yen)	Number	Total cost (yen)
ϕ 66mm boring	Clay deposit	m	10,000	45	450,000
	Rock	m	20,000	38	760,000
ϕ 66mm boring	Clay deposit	m	11,000	35	385,000
	Rock	m	235,000	6	141,000
Standard penetration tests (SPT)					
	Clay deposit	m	5,500	71	390,500
	Rock	m	11,000	44	484,000
Velocity (PS) logging tests			22,000	16	352,000
Thin-wall sampling	Clay deposit	tube	21,500	9	193,500
Soil properties					
Particle size (sieve) analyses		sample	13,300	26	345,800
Specific gravity (ρ_s)		sample	6,000	26	156,000
Water content (w)		sample	1,500	26	39,000
Liquid limit		sample	8,000	26	208,000
Plastic limit		sample	4,000	26	104,000
Wet density (ρ_t)		sample	3,500	9	31,500
Laboratory tests					
Oedometer tests		sample	54,000	9	486,000
Triaxial tests (CU)		sample	101,000	9	909,000
Cyclic triaxial tests (shear modulus & damping ratio)		sample	104,000	9	936,000
Carriage fee		location	30,000	10	300,000
Temporary scaffolds		location	55,000	10	550,000
Preparation		set	200,000	1	200,000
Transportation fee		set	100,000	1	100,000
Total					7,521,300
Overheads					2,478,700
Grand Total					10,000,000

4.3 State of Art and Future Problems in Geotechnical Field Investigation

4.3.1 Remarks on Current Field Investigation

The collected answers are interpreted and the results are described in what follows. All the answers state that SPT (Fig. 4.1) is their first priority, with which the initial investigation schedule is planned. CPT (Fig. 4.2) is the second choice, which has many variations / developments so that pore water pressure or S wave velocity are measured in the course of penetration. The main reason for the preference for SPT seems to be the availability of many empirical formulae by which many soil parameters can be determined from SPT-N values. The other reason is the fact that many design codes specify the use of SPT-N based formulae.

The above situation does not mean that SPT is very reliable. For SPT procedure, only fundamental issues, such as borehole drilling methods, free height of a hammer, and the amount of penetration, as specified (Table 4.1) and, however, the working details are left free for boring site engineers. This situation is considered to make SPT data less reliable. This point is in good contrast with CPT.

Table 4.1 National and international specifications for SPT procedure

Items	**JIS A-1219 (1967)**	**ASTM D-1586-67 (1974)**	**BS 1377 test 19 (1975)**	**ISSMGE (1988)**
Rod < 15m	JIS M 1409 OD	A rod	AW rod	OD 40.5, 50, 60
		OD 41.2 ID 28.5	OD 41.3 5.7kg/m	>10.03kg/m(OD
60mm) > 15m	-----	Use more rigid rod	BW equiv rod	is not allowed
			or stabilizer	
			at every 3m	
Sampler				
Outer diam.	51mm	50.8mm	50mm	51mm+-1mm
Inner diam.	35mm	34.9mm	35mm	35mm+-1mm
Length	810mm	685.8mm	680mm	680mm
Tip angle	19-47’	18-25’	17-25’	18-37’
Tip thickness	---	1.6mm	1.6mm	1.6mm
Drain.hole	4 holes	φ12.7*4	φ13.0*4	Sufficient size*4
Hammer				
Weight	63.5kg	63.5kg	65kg	63.5+-0.5kg
Free fall	75cm	76cm	76cm	76cm
Method of fall	Not specified	Not specified	Care of friction	Minimum energy loss

Although CPT appears to be more reliable than SPT, CPT itself has problems as well. The most important one of them is its penetration capacity in granular soils. Since the most important problem in geotechnical earthquake engineering is the subsoil liquefaction of sand, the difficulty in penetration in sandy and gravelly soil is a significant problem. To cope with this, new kind of investigation technology with more automated and powerful operation is desired.

4.3.2 Field Investigation Suitable for Performance-Based Design

Field investigation is expected in geotechnical engineering to help determine design input parameters with a reasonable reliability. Fig. 4.3 illustrates the procedure for this activity with reference to the JGS4001-2004 specification. In this procedure, the primary data obtained by field investigation or laboratory tests are called measured data and cannot directly be employed for design purposes. The measured data is treated by considering existing theories, knowledge, and others to be called interpreted data. Thereinafter, further consideration is made of limitation of method, data scattering, and statistics, and the processed data is called assessed data. Their representative value is then called representative data which is relevant for soil characterization. Finally, further design consideration such as partial factors is made and the design soil parameter is obtained.

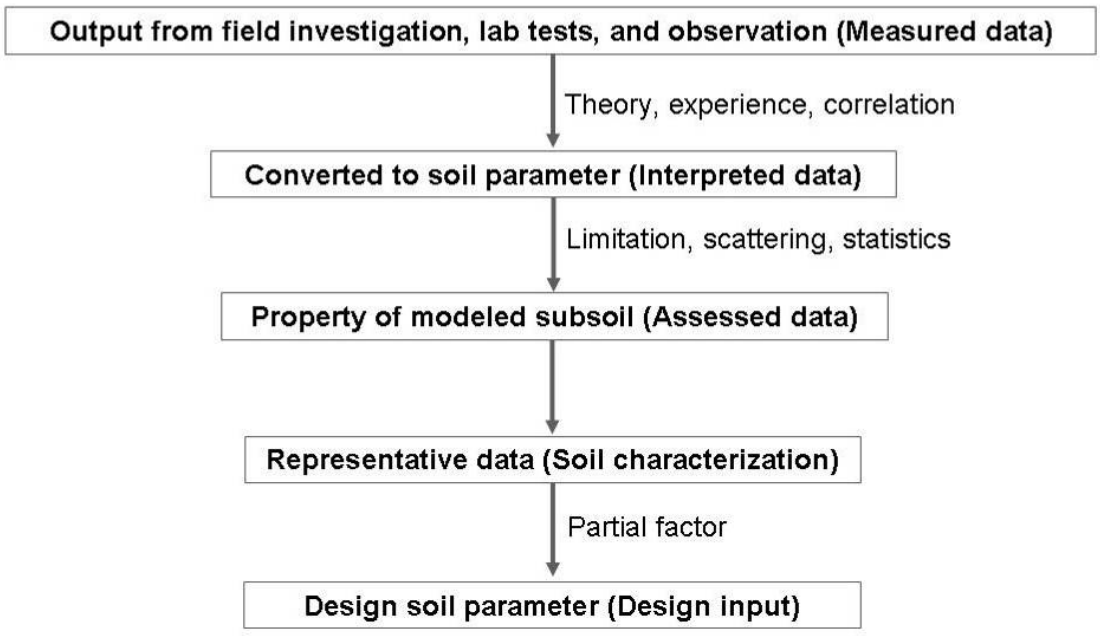

Fig. 4.3 Flow from field investigation to final decision of design input data (JGS 4001-2004)

To achieve relevant reliability in the subsoil data, it is necessary to understand the following

three factors, which are namely uncertainty (scattering), spatial nonuniformity, and discrepancy between design soil model and behavior of real soil. In this regard, the field investigation technology has to measure soil properties at a very short interval so that the density of data population may be increased. It is evident then that CPT, which can measure soil behavior continuously during penetration, is more adequate than SPT that measures the penetration resistance, N_{SPT}, at every one meter. The advantage of continuous measurement (N_d by dynamic drive cone) over SPT is illustrated in Fig. 4.4.

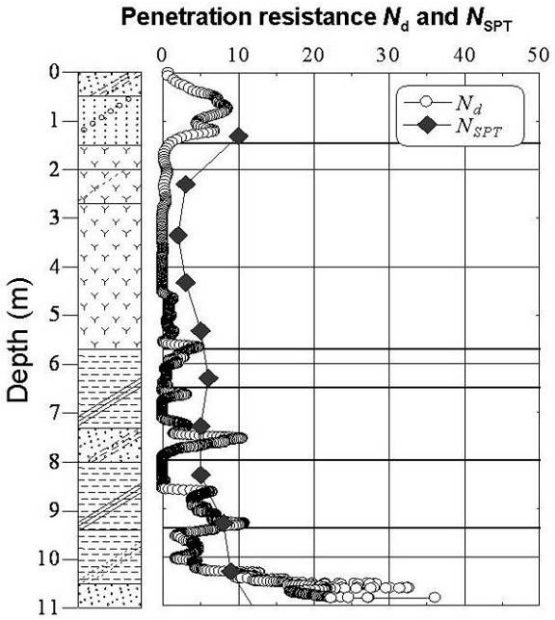

Fig. 4.4 Comparison of dynamic CPT and SPT

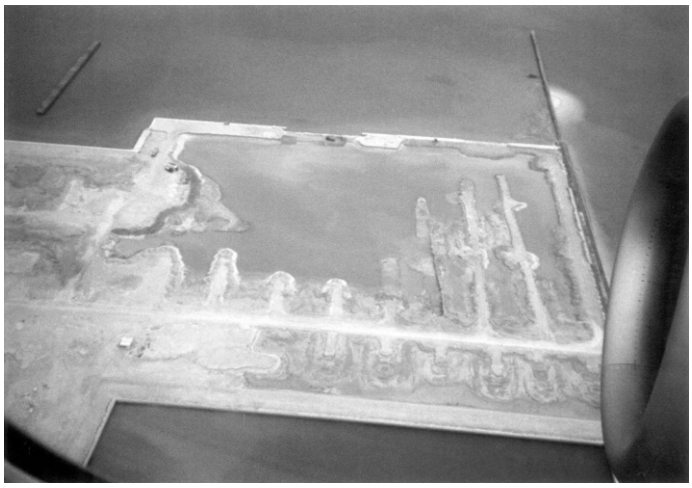

Fig. 4.5 Progress of land reclamation project

An example of the nonuniform nature of subsoil is demonstrated in Fig. 4.5 in which land

reclamation project is ongoing. Since subsurface ground is produced in a complicated order, its nonuniformity cannot be enhanced by a limited number of soil investigations. Thus, it is essential to interpolate the interval of elaborate investigations by further conducting simplified investigations. Although many people considers CPT a useful tool, it should be borne in mind that dynamic cone penetration becomes more useful than CPT when subsoil includes gravels that makes static pushing of CPT probe very difficult.

4.3.3 For Improvement of SPT Procedure

Although problems of SPT were pointed out in the previous sections, it is still true that SPT is a useful tool. This is not only because SPT-N value is related with many soil parameters in terms of empirical formulae but because SPT can supply soil specimens. Although disturbed, soil samples thus collected make it possible to determine physical soil properties such as grain size distribution, fines content, and Atterberg limits, which are very useful in, for example, determination of liquefaction potential of subsoil. In this respect, improvement of SPT is proposed in what follows.

(1) Importance of energy correction

It is often the case that SPT practice does not follow the internationally specified method. Although the specification has no legal effect because it is nothing more than a recommendation, site engineers should pay more attention to it. This is mainly because the design soil parameters are determined by using empirical formula which was obtained in a limited number of nations where the detailed procedure of SPT has been inspected more carefully. It should be noted, however, that this statement does not mean the SPT practice in those developed countries is good in general. In Japan, for example, SPT procedure is reliable only in a small number of reliable consulting firms. In this sense, each firm should evaluate the quality of its SPT practice qualitatively and quantitatively. The correction of SPT-N, to $N_{1,60}$ for example, is a good idea. Many empirical formulae which do not consider the energy correction should be revised.

(2) Maintenance of equipment

Another source of unreliable SPT practice lies in the shoe. It is possible that the shoe is not maintained in a sharp condition. This situation makes penetration more difficult and increases the N value. Since the overestimated N value increases the rigidity and liquefaction resistance of sand in design procedure, the risk of unexpected seismic disaster is increased. In this regard, the maintenance of equipment deserves more attention.

(3) Procedure of bore hole drilling procedure

Cleaning of the bottom of bore hole is frequently recommended. Its detail is beyond the scope of the present study.

5. Conclusions

The present study aimed to show the state of art of the performance-based design for geotechnical structures undergoing earthquake actions, and to demonstrate the advantage that is achieved by introducing the concept of life cycle cost. To achieve this goal, it was thought that prediction of seismic performance has to be reliable to a reasonable extent and that the methodology of life-cycle-cost calculation has to be established. Moreover, the products of the studies had to be shown to the international engineering community. On the basis of these ideas, a variety of activities were conducted. They can be summarized now as what follows.

- Shaking model tests under 1-G gravity or centrifugal environments were conducted in order to show the capability of numerical analyses
- The structures concerned in model tests and numerical analyses were pile foundation, embankment, quay wall in harbor, and earth dam.
- Numerical analyses have a reasonable, although not perfect, capability to reproduce the real seismic performance of geotechnical structures.
- Very advanced numerical analyses require expensive computation time and cost as well as determination of advanced soil parameters.
- To save the computation load, a method of regression analyses as combined with EXCEL calculation was proposed.
- Methodologies for calculation of life cycle cost which considers specific nature of geotechnical structures were constructed and practiced.
- International workshops were held at five cities in the world for familiarization of the importance of performance-based design and life-cycle-cost concepts.
- The seismic performance-based design and life cycle cost principle are the direction of future design of geotechnical structures in seismic countries because they help avoid unnecessarily conservatism and achieve the optimum choice of design.
- It is very important for engineers to improve the quality of field soil investigation by paying attention to details of procedures and maintenance of equipments.

6. Acknowledgment

The present study was financially supported by NEDO. This aid is deeply appreciated by the research group.

7.References

Annaka, T. and Nozawa, Y. (1988) A probabilistic model for seismic hazard estimation in the Kanto district, Proc. 9th Word Conf. Earthquake Engineering, Vol. II, pp. 107-112.

Annaka, T. and Yashiro, H. (2000) Uncertainties in a probabilistic model for seismic hazard analysis in Japan, Proceedings of 2nd Int. Conf. Computer Simulation in Risk Analysis and Hazard Mitigation, pp. 369-378.

Australian/New Zealand (2004) Risk Assessment, AS/NZS 4360, Third Edition.

Celik, O.C. and Ellingwood, B.R. (2007) Uncertainty analysis in fragility assessment of reinforced concrete frames designed for regions of low-to-moderate seismicity, Applications of Statistics and Probability in Civil Engineering, Proceedings of ICASP10

Furuta, H. and Frangopol, D.M. (2005) Life-cycle cost analysis of reinforced concrete bridge piers considering seismic performance, Proc. 8th Int. Conf. Structural Safety and Reliability, pp.1377-1384

Higashijima, M., Fujita, I., Ichii, K., Iai, S., Sugano, T. and Kitamura, M. (2006) Development of a simple seismic performance evaluation technique for coastal structures, 2006 Ocean Development Symposium.

Iai, S., Ichii, K., Liu, H. and Morita, T. (1998) Effective stress analyses of port structures, Soils and Foundations, Special Issue on Geotechnical Aspects of the January 17 1995 Hyogoken-Nambu Earthquake, No.2, pp. 97-114.

Iai, S. (1998) Seismic analysis and performance of retaining structures, Geotechnical Earthquake Engineering and Soil Dynamics III, Geotechnical Special Publication No.75, ASCE, pp. 1020-1044

Iai, S., Ichii, K., Sato, Y. and Liu, H. (1999) Residual displacement of gravity quaywalls - parameter study through effective stress analysis, 7th U.S.-Japan Workshop on Earthquake Resistant Design of Lifeline Facilities and Countermeasures against Soil Liquefaction, Seattle, Vol. NCEER-99-0019, pp. 549-563.

Iai, S. (2005) International standard (ISO) on seismic actions for designing geotechnical works - An overview, Soil Dynamics and Earthquake Engineering, Vol. 25, pp. 605-615.

Ichii, K. (2002) A seismic risk assessment procedure for gravity type quay walls, Journal of Structural Mechanics and Earthquake Engineering, JSCE, Vol. 19, No. 2, pp. 131-140.

Ichii, K., Iai, S., Sato, Y. and Liu, H. (2002) Seismic performance evaluation charts for gravity type quay walls, Journal of Structural Mechanics and Earthquake Engineering, JSCE, Vol. 9, No. 1, pp. 21-31.

ISO/IEC, Guide 73 (2002) Risk management – Vocabulary – Guidance for use in standards.

ISO TC 98/SC3/WG10, ISO23469. (2004) Basis for design of structures - Seismic actions for designing geotechnical works.

Japan Road Association (1999) Road earth work, slope protection, slope stabilization guideline (in Japanese).

JGS4001-2004 (2006) Principles of design for foundation structures on the basis of performance-based design concept.

Jones-Lee, M.W., Hammerton, M., and Philipps, P.R. (1985). The value of safety: Results of a NationalSample Survey. Economic Journal, Vol.95, No.377, pp.49-72.

Kramer, S. L., Mayfield, R.T. and Anderson, D.G. (2006) Performance-based liquefaction hazard evaluation: implications for codes and standards, 8th U.S. National Conference on Earthquake Engineering, San Francisco, Paper No.888.

Lee, K. L. (1974) Seismic permanent deformation in earth dams, Report to NSF, No. GI38521.

Newmark, N. M. (1965) Effects of earthquakes on dams and embankments, Geotechnique, Vol. 5, No. 2, pp. 137-160.

Public Works Research Institute (2004) Manual for risk analysis and management of road slope failures (draft), Report No. 3926 (in Japanese).

Rackwitz, R. (2002) Optimization and risk acceptability based on the life quality index, Structural Safety, Vol. 24, pp. 297-331.

Rackwitz, R. (2004) Life quality index revisited, Structural Safety 26, pp. 443–451.
Railway Technical Research Institute (2003) Design Standards for Railway Structures and Commentary (Seismic Design) (in Japanese).
Research Committee on Assessment of Investment on Road (1998) Guideline, p.68 (in Japanese).
Sawada, S. (2003). A new look at Level 1 earthquake motions for performance-based design of civil engineering structures: Japan Society of Civil Engineers, http://www.jsce.or.jp/committee/eec2/taishin/index.html.
Shi, L.P., Towhata, I. and Wieland, M. (1989) Prediction of seismically induced deformation of Liyutan Dam, Taiwan, by means of cyclic triaxial testing and finite element analysis, Computers and Geotechnics, Vol.7, No.3, 205-222.
Stewart, M.G. and Melchers, R.E. (1997) Probabilistic risk assessment of engineering systems, Chapman & Hall, Melcher and Stewart, Risk Management.
Takahashi, Y., Kiureghian, A.D., and Ang, H-S. A. (2004) Life-cycle cost analysis based on a renewal model of earthquake occurrences, Earthquake Engineering and Structural Dynamics, Vol. 33, pp. 859-880.
Towhata, I., Orense, R.P. and Toyota, H. (1999) Mathematical principles in prediction of lateral ground displacement induced by seismic liquefaction, Soils and Foundations, Vol.39, No.2, pp.1-19.
Yoshida, I. (2005) Fragility analysis and life cycle cost assessment considering risk, Proc. 8th Int. Conf. Structural Safety and Reliability, pp.1459-1464.